

Australian Labradoodle Dystrophinopathy:
A Novel Canine Model for the Study of Duchenne Muscular Dystrophy Cardiomyopathy

by

Stephanie M. Shrader, DVM, DACVP

A dissertation submitted to the Graduate Faculty of
Auburn University
in partial fulfillment of the
requirements for the Degree of
Doctor of Philosophy

Auburn, Alabama
May 2, 2020

Key Words: Duchenne, Cardiomyopathy, Transcriptome, Dystrophin, Labradoodle

Copyright 2020 by Stephanie M. Shrader

Approved by

Bruce F. Smith VMD, PhD, Chair, Professor of Pathobiology, Director of AURIC
Russell C. Cattley, VMD, PhD, DACVP, FIATP, Head of Department of Pathobiology
Richard C. Bird, PhD, Professor of Molecular Biology and Cancer Genetics

Abstract

Duchenne muscular dystrophy (DMD) is an X-linked recessive disorder that results in progressive damage to both skeletal and cardiac myocytes. As a result of improved ventilatory care, mortality in affected patients is increasingly attributed to cardiomyopathy. We have identified a novel dystrophin mutation in exon 21 in Australian Labradoodles. Affected dogs have poor weight gain and weight loss with gait abnormalities, exercise intolerance, skeletal muscle atrophy, macroglossa, ptyalism, dysphagia, kyphosis, and a plantigrade stance developing by 6 months of age. Concurrent echocardiographic and electrocardiographic abnormalities include hyperechoic foci in the left ventricular papillary muscles, septal hypokinesis, decreased left ventricular systolic and diastolic volume and internal diameter, and atrioventricular (AV) block. Skeletal muscle pathology in affected dogs is similar to what has been described in people with DMD and includes myocyte degeneration, necrosis, and regeneration, fibrofatty infiltration, lymphohistiocytic inflammation, and mineralization. Histopathologic findings in the heart were observed in the dog with the AV block and consisted of a focal area of mineralization adjacent to the sinoatrial node. Cardiac transcriptome sequencing on left ventricular myocardial samples found 29,740 genes expressed and 1267 differentially expressed genes. Expression patterns from affected dogs were generally distinct from controls and there was a high correlation between samples. The ten gene transcripts with

the greatest up regulation (in descending order of fold change) included BDNF, MYL4, PENK, BSPRY, PRR32, NPPA, LOC490471, LYZF2, CDH10, and FGF6. We also found that the most down-regulated transcripts (in ascending order of fold change) included LOC612108, ST8SIA2, FOXR1, P2RX6, LOC610380, DAO, CNR2, SDC1, LRRC55, and TMEM171). The majority of the above-mentioned genes have known roles in cardiac compensatory changes secondary to dystrophinopathic-associated damage, including survival, remodeling, contractility, conduction, and immunoregulation. Differential expression of genes was also observed in pathways associated with cardiac oxidative stress, apoptosis, and contractility. These findings are significant because they support the use of the Australian Labradoodle as a novel animal model for the study of DMD cardiomyopathy, they elucidate pathways and differential gene expression involved in Labradoodle dystrophinopathic cardiomyopathy, and they may aid in the development of therapeutic targets to treat dystrophinopathy-associated cardiac disease.

Acknowledgments

The completion of this work was made possible by the assistance of many people whose names may not all be enumerated. The contributions and support that I have received from the faculty, staff, and students at the Auburn University College of Veterinary Medicine and the Scott Ritchey Research Center have been sincerely appreciated and are gratefully acknowledged.

There are a few people, however, that deserve special mention:

My husband - for his constant support, understanding, and encouragement throughout veterinary school, residency, and my doctoral research.

Mr. Stephen Waters – for his high standard of animal care, devotion to animal welfare, and his willingness to assist with innumerable technical procedures.

The Labradoodles – for giving the ultimate sacrifice to aid in the understanding and treatment of DMD.

Table of Contents

Abstract.....	ii
Acknowledgments	iv
List of Tables	vii
List of Figures.....	viii
List of Abbreviations	ix
Chapter 1: Literature Review.....	1
DMD Epidemiology	2
DMD Clinical Findings.....	3
Therapeutic Strategies.....	11
Dystrophin and the Dystrophin Associated Protein Complex	13
DMD Animal Models.....	21
Labradoodle History.....	26
Transcriptomics.....	27
Chapter 2: Characterization of Australian Labradoodle Dystrophinopathy	31
Chapter 3: Cardiac transcriptome analysis identifies differentially expressed genes in Australian Labradoodle dystrophinopathy	43
Chapter 4: Conclusions.....	82
References.....	86

Appendix I: Supportive Photographs and Figures 107

List of Tables

Table 1. Dystrophin Isoforms	19
Table 2. Comparison of GRMD and DMD cardiac abnormalities	24

List of Figures

Figure 1. Photographs of dystrophin-deficient Labradoodles.....	107
Figure 2. Comparison of weight gains between dystrophin-deficient and control dogs	108
Figure 3. ³¹ P MR spectra.....	109
Figure 4. Echocardiographic image of tricuspid valve regurgitation	110
Figure 5. Gross photograph of the diaphragm from an affected dog.....	111

List of Abbreviations

ACE	Angiotensin Converting Enzyme
ADHD	Attention-Deficit/Hyperactivity Disorder
AKC	American Kennel Club
ALT	Alanine transaminase
AST	Aspartate aminotransferase
AV	Atrioventricular
ATP	Adenosine triphosphate
BMD	Becker Muscular Dystrophy
CBC	Complete blood count
cGMP	Cyclic guanosine monophosphate
Chem	Chemistry
CK	Creatine kinase
DAPC	Dystrophin-Associated Protein Complex
DMD	Duchenne Muscular Dystrophy
ECG	Electrocardiogram
FS	Fractional shortening
GRMD	Golden Retriever Muscular Dystrophy

IQ	Intelligence quotient
LGMD	Limb-Girdle Muscular Dystrophy
LMD	Labrador Retriever Muscular Dystrophy
LVEF	Left Ventricular Ejection Fraction
MAPK	Mitogen-Activated Protein Kinase
MD STARnet	Muscular Dystrophy Surveillance Tracking and Research Network
MR	Magnetic resonance
MRI	Magnetic Resonance Imaging
MRS	Magnetic Resonance Spectroscopy
NOS	Nitric Oxide Synthase
ORF	Open reading frame
RNA	Ribonucleic acid
RT-PCR	Reverse transcriptase polymerase chain reaction
SA	Sinoatrial
SRRC	Scott Ritchey Research Center
TTE	Transthoracic Echocardiography
XLDCM	X-Linked Dilated Cardiomyopathy

Chapter 1: Literature Review

Duchenne muscular dystrophy (DMD) is an X-linked recessive disorder that is caused by mutations in the dystrophin gene. The result is a lack of functional dystrophin, or less commonly, a truncated, partially functional N-terminal dystrophin fragment. It inevitably causes progressive, degenerative changes in skeletal and cardiac muscle and also alters the functionality of other cell types within the body, such as cerebral and cerebellar neurons, depending on the mutation involved and isoform(s) affected (Table 1) (Hoffman et al., 1987). Boys with this disorder are often diagnosed when young (less than five-years-old), and generally become non-ambulatory by the age of ten. Wheelchair bound, these patients typically develop various medical problems associated with skeletal and respiratory muscle weakness (such as difficulty rising from a seated position, frequent falls, delayed motor-skill development, gait abnormalities, and respiratory infections), in addition to cardiomyopathy. Death often occurs in the second or third decades of life, historically attributed primarily to respiratory failure (Spurney et al., 2008). Complications of respiratory muscle weakness resulting in failure include progressive restrictive ventilatory defects, chronic hypoventilation, and various pulmonary infections (Wagner et al., 2007). According to a recent longitudinal study evaluating the cause of death in DMD patients over the last 50 years, mean age at death before initiation of mechanical ventilation (January 1977 - July 1984) was 18.9 ± 4.1 years. Following the use of mechanical ventilation, the mean age of death improved each decade to 31.1 ± 5.4 years (January 2004 to December 2010). Prior to use of

mechanical ventilation, more than half of all deaths in DMD patients were due to respiratory failure. Based on the cohort of patients included in this longitudinal analysis, no DMD patients have died from respiratory failure since 2000 (Matsumara et al., 2011).

In the last few decades, treatment of skeletal muscle and respiratory complications has improved, and as a result, mortality in DMD patients is increasingly attributed to cardiac-related disease. Between 1985 and 1989, greater than 30% of reported DMD deaths in Japan resulted from cardiac failure (Moriuchi et al., 1993). Similarly, a separate study conducted at the Naples Centre of Cardiomyology and Medical Genetics reviewed the records from 835 DMD patients who were examined between 1961 and 2006. Similar to the study published by Matsumara and colleagues, their findings also indicated that the major cause of death until the 1980's was due to respiratory illness and that there has been a significant decade on decade improvement in the survival rate (the mean age of death in the 1960's was 14.4 years, while the mean age of death for those ventilated since 1990 was 25.3 years). The same study found that cardiomyopathy significantly decreased life expectancy from a mean age of 19 years to 16.9 years (Passamano et al., 2012).

DMD Epidemiology

Duchenne muscular dystrophy is an X-linked recessive disorder caused by various types of mutations in the dystrophin gene, all of which result in the lack of a functional dystrophin protein product. As such, DMD is classified as a type of dystrophinopathy (literally meaning a disorder of dystrophin). Although the disease phenotypes vary, other forms of muscular dystrophies categorized as dystrophinopathies include: Becker muscular dystrophy (BMD), isolated quadriceps myopathy, muscle cramps with myoglobinuria, and X-linked dilated

cardiomyopathy (XLDCM) (Beggs, 1997; Sunohara et al., 1990; Wicklund, 2013). With Becker muscular dystrophy, partial functionality of dystrophin is maintained, and the disease phenotype can vary widely. With progression, the clinical course can resemble DMD; however, the severity of skeletal muscle weakness can vary substantially, with milder respiratory dysfunction and variable cardiac involvement compared to patients with DMD (Wicklund, 2013).

According to the CDC, in 2007, 349 out of 2.37 million males between the ages of 5-24 had either DMD or BMD in the United States. This means that 15 out of every 100,000 males aged 5-24 years were affected that survey year. Similar survey results were reported from Northern England in 2009: 233 out of 1.49 million males were reported to have DMD or BMD, equating to roughly 16 out of every 100,000 males (CDC, 2009; Norwood et al., 2009). In the United States, the prevalence of DMD and BMD is currently estimated to be 1 in every 7,250 males aged 5-24 years with DMD being 3x more common than BMD (Romitti et al., 2015).

DMD Clinical Findings

Based on data compiled by the Muscular Dystrophy Surveillance, Tracking, and Research Network (MD STARnet), a definitive diagnosis of DMD typically does not occur until 2.5 years after the parents first noticed physical developmental delays in their child (Ciafaloni et al., 2009). Because of this delay, boys with DMD are typically presented to the pediatrician between 3 and 5 years of age with difficulties rising from a seated position, frequent falls, and delayed milestones in motor-skill development. Physical examination findings often include (pseudo)hypertrophy of the calves (seen in about 2/3 of patients), variably severe lumbar lordosis, waddling gait, macroglossa (seen in about 1/3 of patients) and a distinctive way of rising from the floor (known as Gowers' maneuver). Because of weakened leg muscles, boys

with DMD rise from the floor by first getting on hands and knees, then elevating the posterior, followed by “walking” their hands up the legs to raise the upper body (Gozal, 2000; MDA, 2014). Muscle weakness becomes progressive over time, eventually resulting in wheelchair dependence at an early age (usually by 10-years-old). By convention, pediatricians consider boys with dystrophinopathies to have DMD if the ability to walk ceases before 12-years of age. Boys who are able to walk beyond their 16th birthday are considered to have BMD (Wicklund, 2013).

Skeletal muscle biopsy samples from patients with DMD are characterized by necrotic and/or degenerating myocytes with foci of mineralization, myofiber size variability, and myofibers with centralized nuclei (evidence of regeneration from myoblasts). Necrotic myocytes/myofibers are often surrounded and/or infiltrated by macrophages and CD4+ T-lymphocytes. As the regenerative capacity of the affected muscle wanes, there is gradual replacement of the tissue by fibrosis and infiltrating adipose tissue (Klinger et al., 2012). Because of dystrophin’s role in myocyte structural integrity (to be discussed at length in the section entitled “Dystrophin and the Dystrophin Associated Protein Complex”), it has been proposed that the occurrence of muscular necrosis is resultant from recurrent contraction-associated mechanical damage. Others have proposed that altered myocyte calcium homeostasis is to blame for the presence of myocyte necrosis (Deconinck & Bernard, 2007). This second hypothesis seems short-sighted and lacks experimental evidence to support it. Mechanical cellular damage can and will cause altered sarcolemmal integrity, secondary calcium influx, and resultant cell death. Because inherently altered calcium channels have not been documented in dystrophin-deficient myofibers, calcium-associated muscular necrosis is likely secondary to contraction-related myocyte damage. Vascular anomalies, aberrant glycosylation of dystrophin-associated proteins, and gene regulatory anomalies have also been proposed as potential causes

for the observed muscular necrosis; however, they lack supportive experimental data (Deconinck & Bernard, 2007).

Another interesting finding in >50% of patients with DMD is the presence of rare “revertant fibers,” myofibers that have strong, seemingly counterintuitive, dystrophin immunolabeling (Nicholson et al., 1989). Studies have shown that although these revertant fibers produce a dystrophin protein that lacks the region encoded by the deleted exons, they do have a normal C-terminus, consistent with a restored reading frame (Hoffman et al., 1990; Klein et al., 1992). The prevalence of somatic mutations resulting in reading frame restoration is unknown. It has been hypothesized that many somatic mosaic males for DMD exist, and indeed there are numerous case reports describing somatic mosaicism in individual patients; however, most are likely not detected clinically because of genetic normalization (Klein et al., 1992). By utilizing exon-specific monoclonal antibodies against dystrophin, Le Thiet Thanh and colleagues demonstrated that somatic mutations in revertant-fiber nuclei result in the removal of additional exons from dystrophin mRNA, confirming the previous supposition that the reading frame was restored (Thanh et al., 1995). The clinical implications of revertant fibers continue to be explored. For example, in a recent phase I clinical trial (that sought to deliver a transgene that encoded a miniaturized version of human dystrophin), dystrophin-specific T-cell responses were unexpectedly detected in two patients prior to gene therapy delivery. Interestingly, the epitopes were mapped to myofibers with revertant dystrophin expression. It has been postulated that revertant dystrophin expression may participate in the poorly understood mechanisms behind DMD-related myositis (Campbell et al., 2010).

Additional physical examination findings in DMD patients often include fatigue, joint contractures, decreased cardiopulmonary functionality, and cognitive impairment. Joint

contractures typically develop in the hips and knees, owing to the time spent in a wheelchair as the disease progresses. Abnormal seating postures (i.e. kyphosis, lordosis, and scoliosis) are reported in 68-90% of ambulatory and non-ambulatory DMD patients. In non-ambulant patients, there is a much higher risk for scoliosis development, which can be rapidly progressive without aggressive orthotic measures and/or surgical interventions (Oda et al., 1993; Yamashita et al., 2001). Respiratory complications are typically attributed to decreased thoracic compliance resulting from diaphragmatic, intercostal, and accessory respiratory muscle dysfunction and weakness. Ventilatory failure inevitably develops over time, necessitating the use of non-invasive and invasive ventilation techniques (Boland et al., 1996; Gozal, 2000; Wicklund, 2013). DMD patients should remain up-to-date on vaccines in order to prevent pneumonia and they may require manual or mechanically assisted support to stimulate coughing when pulmonary infections do occur (CDC, 2016). The ability to better manage DMD-associated respiratory complications has resulted in prolongation of life, but it has also unmasked concurrent cardiac dysfunction in these patients (Bach, 1994).

Currently, most if not all patients with DMD that survive into their thirties will be diagnosed with cardiomyopathy at some point. Traditionally, recognition was often delayed due to a general lack of physical activity; however, in more recent years, clinicians are using more sophisticated screening techniques at earlier ages, regardless of outward symptomology (McNally, 2007). A study published in 2013 found that cardiac problems typically begin by 14 years of age, and that for every year corticosteroids were taken by the patient (see “Therapeutic Strategies” below for more information on corticosteroid usage in DMD), the chance of developing heart problems decreased by 4% (Barber et al., 2013). Cardiac involvement in

patients with DMD can be associated with various cardiac alterations and therefore variable phenotypes.

In 2008, the recommended cardiac screening protocol for boys with DMD included an electrocardiogram (ECG) and transthoracic echocardiography (TTE) every two years until the age of ten, and then once a year thereafter (Bouhouch et al., 2008). In 2010, the DMD Care Considerations were published; these too addressed cardiac care recommendations based on minimal surveillance standards. Similar to Bouhouch and colleagues, the working group recommended that minimum assessment include an ECG at least once every two years until the age of ten and then once a year thereafter. If ventricular functional abnormalities are noted, cardiac functionality should be evaluated at least every six months, and pharmacological interventions should be initiated immediately (Bushby et al., 2010). Most commonly, children with the most severe manifestations of DMD will have persistent sinus tachycardia, an increased R-S ratio in the right precordial leads, deep Q waves in the lateral leads, and conduction abnormalities (i.e. alterations in the progression of electrical impulses through the heart). In addition to persistent sinus tachycardia, other common arrhythmias in DMD patients include sinus bradycardia, atrial premature beats (usually isolated), and ventricular premature beats (also typically isolated). Often, patients with ventricular premature beats are in advanced stages of disease (Yanagisawa et al., 1992). In one study, cardiac conduction abnormalities were reported in 24 of the 50 patients examined (48%). Of the 24 patients, 23 had intra-atrial conduction abnormalities, five had infranodal conduction abnormalities, and one patient had prolongation of atrioventricular (AV) conduction. Of those with infranodal conduction defects, one patient had a right bundle branch block and three patients had a left anterior fascicular block (Sanyal &

Johnson, 1982). First- and second-degree AV blocks have also been documented in DMD patients (Perloff, 1984; Sanyal & Johnson, 1982; Yanagisawa et al., 1992).

Heart blocks occur when the electrical signal is slowed or disrupted as it moves through the heart. In order of least to most severe, the three types of heart block are first-degree, second-degree, and third-degree. With a first-degree block, the heart's electrical signals are slowed as they progress from the atria to the ventricles. Electrocardiographically, this is represented by a longer, flatter line between the P and the R waves. Second-degree heart blocks are characterized by atrioventricular electrical signals that are slowed to a large degree; as a result, a QRS wave doesn't always follow each P wave as it should. Second-degree heart blocks can be further categorized as either a Mobitz type I or Mobitz type II block. In a Mobitz type I block, electrical conduction is progressively delayed with each heartbeat, until the heart skips a beat. When viewed using an ECG, the delay is shown as a PR interval that gets longer with each heartbeat until the QRS waves don't follow the subsequent P wave. Mobitz type II blocks are less common than type I and are generally more severe. With this type of block, some of the electrical signals fail to reach the ventricles, making the pattern less regular than that which is seen with Mobitz type I. Electrocardiographically, the QRS wave follows the P wave at a normal speed; however, when it is blocked, the QRS wave is missing. A third-degree block (also known as a complete heart block or complete AV block) is characterized by complete failure of the electrical signals to reach the ventricles. When this occurs, independent accessory pacemaker signals will attempt to activate the ventricles (known as an escape rhythm). The resultant ECG pattern is characterized by P waves that occur at a faster rate and aren't coordinated with the QRS waves. This type of conduction anomaly can result in bradycardia, hypotension, sudden cardiac arrest, and death (NIH, 2012).

Histologically, myocardial changes consist of multifocal areas of fibrosis (most prominent in the inferolateral wall), myocyte vacuolation (consistent with degeneration), myocyte necrosis, myofiber size variation, and fatty infiltration. Specific areas of the conduction system that have been reported to be affected include the sinoatrial (SA) and AV nodes, AV bundle, left bundle branch, and right bundle branch. It has been postulated that the myocardial lesions result from mechanical stresses imposed on a metabolically and structurally abnormal heart; however, it remains to be determined why a segmental, rather than diffuse, pattern of myocardial injury occurs. Although other factors are likely at play, these microscopic changes presumably play a role in the development of the before mentioned conduction anomalies, arrhythmias (both subclinical and fatal), and compensatory changes (such as dilated cardiomyopathy (DCM)) (Sanyal & Johnson, 1982; Verhaert et al., 2011; Yanagisawa et al., 1992).

Recently, cardiac magnetic resonance imaging (MRI) has also been proposed as a useful (and perhaps better) diagnostic tool to identify early myocardial remodeling changes (Verhaert et al., 2011). Both echocardiography and MRI are able to identify abnormal left ventricular fractional shortening (FS), left ventricular hypokinesia, and left ventricular dilation; however, research shows that the majority of echocardiographic studies have suboptimal scanning windows and significantly over- or underestimated left-ventricular function compared to cardiac MRI. As an example, Brunklaus and colleagues performed a retrospective analysis of case records from 35 boys with DMD underwent cardiac evaluation for surgical procedures between 2010 and 2013. They reported ECG found a median left ventricular FS of 29%. 37% of boys (13/35) had abnormal FS <25%, 66% (23/35) had evidence of hypokinesia, and 26% (9/35) had left ventricular dilatation. Cardiac MRI revealed a median left ventricular ejection fraction

(LVEF) of 52%. 57% of boys (20/35) had abnormal LVEF <55%, 71% (25/35) had left ventricular hypokinesia, and 82% had late gadolinium enhancement. Data also showed that extensive late gadolinium enhancement is associated with reduced LVEF (48% vs 58%), consistent with more severe cardiac pathology (Brunklaus et al., 2015). In addition to cardiac MRI, cardiac magnetic resonance spectroscopy (MRS) is also being utilized to better evaluate cardiac functionality in patients with DMD and BMD. One of the benefits is that MRS can be used to noninvasively analyze the cardiac phosphocreatine to adenosine triphosphate ratio (PCr/ATP), a useful measure of cardiac energy metabolism. In a recent publication, 13 men with BMD, 10 female carriers, and 23 control patients were studied using phosphorus-31 MRS and conventional echocardiography. Results indicated that the PCr/ATP was significantly reduced in BMD patients (1.55 ± 0.37) and carriers (1.37 ± 0.25) when compared to controls (2.44 ± 0.33 ; $p < 0.0001$). Interestingly, the PCr/ATP did not correlate with LVEF or mass index. Because the reduced PCr/ATP lacked correlation with indices of left ventricular functionality, it has been posited that there may be a direct link between altered dystrophin expression and the development of cardiomyopathy (Grilley et al., 2000).

Cognitive impairment is also a common manifestation in patients with Duchenne muscular dystrophy, and although it was first noted by Duchenne in his original description of the disease (Duchenne, 1868), it hasn't been until much more recently that the underlying mechanisms involved in this process have been elucidated. Recent data suggests that 45% of the oldest males affected with DMD or BMD has at least one of the following mental health concerns: behavior anomalies, depression, or attention-deficit/hyperactivity disorder (ADHD) (Caspers et al., 2015). Behavioral studies have shown that roughly 30% of boys with DMD are intellectually disabled with an average IQ around 85 (one standard deviation below the mean).

Verbal IQ is reportedly more affected than performance IQ and developmental language delays are common. DMD patients also have an increased prevalence of obsessive compulsive disorder (5%) and autism spectrum disorder (3% to 6%) (Anderson et al., 2002; Bresolin et al., 1994; Hendriksen & Vles, 2008; Leibowitz & Dubowitz, 1981). Recently, in a sample of 80 boys with DMD, it was found that regardless of IQ, the patients displayed a specific cognitive profile, characterized by poor performance in digit span, story recall, and comprehension. The authors found that the degree of cognitive impairment did vary between patients (similar to variances seen in DMD-related skeletal and cardiac pathologies), which they surmised was due to variations in dystrophin gene mutations in the sampled patient population (Hinton et al., 2000).

Therapeutic Strategies

Currently, there is no cure for Duchenne muscular dystrophy and treatment is generally only palliative. One of the current mainstays of treatment is prolonged glucocorticosteroid use, which improves quality of life by increasing the potential years of ambulation, and likely plays a role in increased survival (Wagner et al., 2007). Clinical studies with glucocorticoids have demonstrated a prolongation of ambulatory abilities by approximately 2 years (Manzur et al., 2008). These clinical effects likely result from the ability of glucocorticoids to up-regulate anti-inflammatory mediators and inhibit pro-inflammatory molecules, including various cytokines, chemokines, arachidonic acid metabolites, and adhesion molecules (Velden, 1998). There are numerous documented side effects associated with glucocorticosteroid administration, such as weight gain, hirsutism, behavioral abnormalities, hyperglycemia, hypertension, shortened stature, cataracts, Cushing's syndrome (hyperadrenalcortisolism), and osteoporosis. Unfortunately, these negative side effects are not infrequent; the most common reason for DMD patients to

discontinue corticosteroid use (specifically prednisone) is due to weight gain (Wagner et al., 2007).

Other available therapies are mainly supportive, such as:

- Physiotherapy – Focusing on stretching the upper extremity musculature to decrease contractures. This daily routine of stretching often focuses on forearm pronators, elbow flexors, wrist flexors, and long finger flexors (Bushby et al., 2010; Collins & Morgan, 2003). Stretching of the distal extremities, even when non-ambulatory, is also beneficial.
- Implantable cardio-defibrillators - For those patients with an increased risk of fatal ventricular arrhythmias.
- Cardiac medications – There are a wide range of clinical presentations associated with cardiomyopathy and heart failure. Based on the individual, several different medications may be prescribed, such as ACE inhibitors, spironolactone, loop diuretics, and digoxin (Bushby et al., 2010).
- Wheelchair and other mechanical support (braces).
- Scoliosis surgery – Often surgery is performed when DMD patients are adolescents in order to decrease respiratory compromise, pain and deformity.
- Assisted ventilation – This includes noninvasive positive pressure ventilators, tracheostomy, and mechanical insufflation-exsufflation (Bushby et al., 2010; Passamano et al., 2012).
- Treatment of respiratory infections.

Although beneficial, none of these therapeutic measures impact the fundamental cause of DMD, the lack of dystrophin expression in skeletal and cardiac musculature.

Dystrophin and the Dystrophin Associated Protein Complex

The dystrophin gene, the largest gene currently known in nature, measures 2.4-megabases at locus Xp21 (NCBI, 2020). It was isolated by Louis Kunkel and his colleagues in 1985 (Kunkel et al., 1985), 117-years after Duchenne first described the phenotype associated with the disease that now bears his name (Duchenne, 1868). This gene encodes the protein dystrophin, which is a large, 427-kD sub-membrane protein that links cytoskeletal F-actin to the extracellular matrix protein laminin via the transmembrane protein α/β -dystroglycan complex. Dystrophin is a member of the β -spectrin/ α -actinin protein family; together, it and its associated sarcolemmal proteins form the dystrophin-associated protein complex (DAPC) (Fine et al., 2011; Holland et al., 2013; Koenig & Kunkel, 1990; Spurney et al., 2008).

The overall role of the DAPC is to mediate signaling between the intracellular cytoskeleton and the extracellular matrix. As it pertains to muscular function, the role of this complex is to protect myocytes and myofibers from injury associated with contractile forces. When membrane degradation occurs (such is the case with dystrophinopathies), the histomorphologic changes include edema, inflammation, necrosis, and muscle fibrosis, resulting in the well-known physical manifestations of the disease (Frankel & Rosser, 1976).

Dystrophin is composed of four, well-described functional domains. The N-terminal domain (composed of two calponin homology [CH] molecules) binds F-actin within the cytoplasm (Winder et al., 1995). The adjacent central rod domain is composed of greater than 2800 amino acids that build 24 spectrin-like triple helical repeats with four intervening non-helical segments (known as “hinge” regions) that are thought to result in protein flexibility (Ervasti & Campbell, 1993; Koenig & Kunkel, 1990; Sunada et al., 1994; Suzuki et al., 1994;

Sweeney & Barton, 2000; Yang, Jung, Rafael, et al., 1995). The third domain, the WW region, is a β -sheet motif involved in intracellular signaling via recognition of proline-rich or phosphorylated linear peptides. This domain recognizes a PPxY motif and plays a role in the β -dystroglycan interaction.(Bork & Sudol, 1994) Adjacent to the WW domain is a cysteine-rich region composed of two ER-hand motifs (Koenig et al., 1988) and two ZZ modules (Ponting et al., 1996) that bind calmodulin. Studies later showed that this binding takes place in a calcium-dependent manner (Anderson et al., 1996).

The COOH terminal domain is composed of two regions that form α -helical coiled coils, which make up the binding site for dystrobrevin (Blake et al., 1995). This region also associates with syntrophin (alpha and beta subunits) and neuronal nitric oxide synthase (nNOS) indirectly, binding to dystroglycan within the transmembrane portion of the DAPC. Dystrophin, along with the syntrophins and dystrobrevin, form the subsarcolemma subcomplex. The dystrophin subcomplex is stabilized the sarcoglycan-sarcospan subcomplex, which is composed of alpha, beta, gamma and delta subunits of sarcoglycan, and sarcospan (Kobayashi & Campbell, 2012).

Dystroglycan, a ubiquitously expressed protein, consists of an alpha and beta subunit (Ibraghimov-Beskrovnaya et al., 1992). The alpha subunit consists of a mucin domain and a C-terminal domain, which has been shown to bind to laminin-2 (also known as merosin) with high affinity in a calcium-dependent manner (Ervasti & Campbell, 1991; Ibraghimov-Beskrovnaya et al., 1992). In addition, α -dystroglycan serves as an agrin receptor in muscle, regulating agrin-induced acetylcholine receptor clustering at the neuromuscular junction. Related to this function, it has been shown that dystroglycan can cluster within the sarcolemma in response to rapsyn (a receptor-associated synapse protein), thus playing a pivotal role in neuromuscular junction formation and activity (Campanelli et al., 1994). Recently, it has been shown that neither

dystrophin nor utrophin are required for the expression of the DAPC in cardiac musculature; however, α -dystroglycan is differentially glycosylated in *mdx* and dystrophin/utrophin double knock-out mouse hearts with aberrant sarcolemmal localization. Of note is that these alterations do not affect laminin binding, and the implications of these changes are as of yet, unknown (Sharpe et al., 2013).

Beta-dystroglycan is composed of a single transmembrane domain that spans the sarcolemma and an extracellular amino-terminal domain that binds the carboxy-terminal globular domain of the alpha subunit (Boffi et al., 2001; Di et al., 1999). The cytoplasmic COOH terminus has multiple proline residues necessary for dystrophin binding; it binds directly to the WW modules and the cysteine-rich domain that have the EF and ZZ regions (Ishikawa-Sakurai et al., 2004; Renschler et al., 1999; Suzuki et al., 1992). A separate study found that the WW-like domain within caveolin-3 recognizes the C-terminal end of β -dystroglycan which has a PPXY motif (Sotgia et al., 2000). Based on these findings, it was surmised that the interaction of caveolin-3 with β -dystroglycan may be able to competitively regulate dystrophin recruitment to the complex.

In addition to the role of anchoring dystrophin to the sarcolemma, β -dystroglycan has also been shown to participate in MAPK (mitogen-activated protein kinase) signaling. Interaction with laminin results in recruitment of a Grb2 (Growth factor receptor-bound protein 2) - Sos1 (Son of sevenless homolog 1) complex to dystroglycan (Oak et al., 2003). Within dystroglycan, the proline-rich motif then interacts directly with Grb2, an adaptor protein involved in signal transduction, cell communication and cytoskeletal organization (Yang, Jung, Motto, et al., 1995). The dystroglycan-Grb2 interaction results in activation of Rac1 which in turn activates JNK via the Cdc42-Race effector PAK1 (p21 activated kinase 1). The β -

dystroglycan interaction with MEK and ERK may indicate the dystroglycan acts as a signaling scaffold (Spence et al., 2004).

Interestingly, and contradictory to earlier research, a recent study indicates that most of the dystroglycan complexes at the sarcolemma do not in fact interact with dystrophin or utrophin in wild-type muscles. Evidence also suggests that a subset of dystroglycan that does not directly bind to dystrophin is also destabilized in the absence of dystrophin. Although much more work needs to be done to further characterize the potential differences in dystroglycan, this research seems to indicate that additional disease mechanisms may be involved in the variable disease phenotypes associated with dystrophinopathies and dystroglycanopathies (Johnson et al., 2013).

As mentioned, the sarcoglycan complex is composed of α -, β -, γ - and δ -sarcoglycan subunits and sarcospan, and like other portions of the DAPC, this complex and its components can be secondarily disrupted and destabilized when dystrophin is mutated. The sarcoglycans are single transmembrane glycoproteins with N-terminal domains oriented extracellularly (α -sarcoglycan) and intracellularly (β -, γ - and δ -sarcoglycans) (Lim et al., 1995; Noguchi et al., 1995; Roberds et al., 1993). Sarcospan is composed of four transmembrane-spanning portions, homologous to the tetraspanin family (Crosbie et al., 1999). The sarcoglycan complex appears to function by strengthening the interaction between β -dystroglycan, α -dystroglycan and dystrophin (Ozawa et al., 2005).

Unlike dystroglycan, which has been shown to be expressed in various cell types, the sarcoglycans have a much narrower tissue range and appear to only be expressed in skeletal and cardiac myocytes (Roberds et al., 1993; Roberds et al., 1994). In addition to being disrupted by dystrophin mutations, autosomal recessive mutations in any of the four main sarcoglycan isoforms result in autosomal recessive limb-girdle muscular dystrophy (LGMD-2C-2 F). When

δ -sarcoglycan is lacking, as seen with LGMD-2 F, the remaining three sarcoglycan members are unable to assemble and are thus degraded before transport from the Golgi (Draviam et al., 2006; Shi et al., 2004).

Recently, additional sarcoglycans have been identified. Epsilon-sarcoglycan was discovered and found to be highly similar to α -sarcoglycan. Like the other four sarcoglycans, epsilon can also be found in cardiac and skeletal musculature; however, analysis has shown that it is not part of the sarcoglycan complex (Durbeej et al., 2000). Epsilon-sarcoglycan has been found to be highly expressed in the central and peripheral nervous systems and loss-of-function mutations in its associated gene result in myoclonus-dystonia syndrome in people (Zimprich et al., 2001). Zeta-sarcoglycan, which shows the most sequence similarity to γ - and δ -sarcoglycan isoforms, has also been discovered (Wheeler et al., 2002).

Together with the sarcoglycan subunits, sarcospan helps form the link between the subsarcolemmal cytoskeleton and the extracellular matrix. As seen with sarcoglycans, sarcospan localization to the membrane is dependent on proper dystrophin expression; therefore, its expression is markedly decreased in patients with DMD. Interestingly, the gene encoding sarcospan maps to human chromosome 12p11.2, part of the locus for an autosomal dominant muscular dystrophy known as congenital fibrosis of the extraocular muscle (Crosbie et al., 1997; Crosbie et al., 2000).

Not only does the DAPC play a role in protecting the myocytes from contraction-associated damage, it also serves in scaffolding signaling molecules like nNOS. Sarcolemmal nNOS is lacking when dystrophin levels are low or absent due to deletions in critical regions of the rod domain. This results in deficiency in the normal contraction-induced cGMP-dependent attenuation of local vasculature leading to post-exercise vasoconstriction within muscles

(Kobayashi & Campbell, 2012; Torelli et al., 2004). The degree and extent of vasoconstriction can lead to muscle ischemia, as reported in DMD patients (Sander et al., 2000), in addition to exaggerated fatigue and intramuscular edema (Kobayashi & Campbell, 2012).

The dystrophin gene produces a variety of different transcripts encoding various dystrophin isoforms (proteins of varying lengths that have different segments of the basic dystrophin sequence). Transcription of this gene is controlled by three different promoters whose names reflect the general tissue distribution of dystrophin expression: brain (B), skeletal and cardiac muscle (M) and purkinje (P) (Blake et al., 2002). The dystrophin gene also has four internal promoters that result in shorter transcripts encoding for several isoforms (Retinal [R], Brain 3 [B3], Schwann cells [S], and General [G]) (Constantin, 2014). The different isoforms, generated via splicing at a unique first exon, function in various tissue types and their functions are summarized in Table 1 (below):

Table 1. Dystrophin Isoforms

Isoform	Synonyms and Subtypes	Tissue of Expression
Dp427	Dp427l (L-Dystrophin)	Lymphoblastoid (Nishio et al., 1994; Wheway & Roberts, 2003)
	Dp427c (Brain or C-Dystrophin)	Brain (hypothalamus and cortex) (Bovolenta et al., 2012; Muntoni et al., 2003; Nudel et al., 1989; Tokarz et al., 1998)
	Dp427m (M-Dystrophin)	Skeletal and cardiac muscle (Bovolenta et al., 2012; Holland et al., 2013; Muntoni et al., 2003; Tokarz et al., 1998)
	Dp427p (P-Dystrophin)	Purkinje cerebellar neurons (Bovolenta et al., 2012; Gorecki et al., 1992; Muntoni et al., 2003)
		Expression in other tissues: Fetal tissues (Feener et al., 1989; Muntoni et al., 2003), eye, intestine, kidney, liver, lung, spleen, stomach, testis, thymus, and uterus (Tokarz et al., 1998)
Dp260		Retina (D'Souza et al., 1995), brain, cardiac muscle, intestine, kidney, liver, lung, skeletal muscle, spleen, stomach, testis, thymus, and uterus (Tokarz et al., 1998)
Dp140	Dp140b	Kidney (Tokarz et al., 1998)
	Dp140ab	Cerebellum and kidney (Lidov et al., 1990; Lidov et al., 1995)
	Dp140c	Cerebellum (Lidov et al., 1990; Lidov et al., 1995)
	Dp140bc	Cerebellum and kidney (Lidov et al., 1990; Lidov et al., 1995)
		Expression in other tissues: Other portions of brain, cardiac muscle, eye, intestine, liver, lung, skeletal muscle, spleen, stomach, testis, thymus, and uterus (Tokarz et al., 1998)
Dp71	apo-dystrophin 1 (Liver or G-Dystrophin)	Expressed in all tissues (Tadayoni et al., 2012), including: kidney (Austin et al., 1995; Haenggi et al., 2005; Tokarz et al., 1998), CNS (numerous cell types) (Austin et al., 1995; Benabdesselam et al., 2012; Schofield et al., 1994; Tokarz et al., 1998), liver (deLeon et al., 2006; Tokarz et al., 1998), skeletal muscle, heart, lung, testis (Austin et al., 1995; Tokarz et al., 1998), eye, intestine,

		spleen, stomach, thymus, and uterus (Tokarz et al., 1998)
Dp116	apo-dystrophin 2 (S-Dystrophin)	Typically described in Schwann cells (Byers et al., 1993) and brain (Schofield et al., 1994); however, RT-PCR has revealed expression in multiple other organs: cardiac muscle, eye, intestine, kidney, lung, skeletal muscle, spleen, stomach, testis, thymus, and uterus (Tokarz et al., 1998)
Dp40		Brain (synaptic vesicles in neurons) (Tinsley et al., 1993; Tozawa et al., 2012)

Various types of dystrophin mutations have been documented (in both people and animal models). The majority of these mutations are deletions, accounting for nearly 43% -65% of all *DMD* mutations, depending on cohort evaluated (Dent et al., 2005; Flanigan et al., 2009). Two-thirds of *DMD* patients inherit the mutation from a carrier mother and the remaining one-third of patients have de novo *DMD* mutations. These de novo mutations are believed to occur via the following situations:

1. De novo mutations arise in meiosis either in the grand-parental generation or in the mother
2. Mitotic de novo mutations arise during spermatogenesis of the grandfather, during oogenesis of the grandmother, or during oogenesis of the mother (Grimm et al., 2012)

Several studies have reviewed the relative probabilities of de novo mutations per mutation type and have found that large deletions arise predominantly during oogenesis while point mutations and duplications more commonly result from errors during spermatogenesis (Grimm et al., 1994; Kawamura et al., 1997). Spontaneous *DMD* mutations have been reported in dogs (see *DMD*

Animal Models below); however, the prevalence of de novo *DMD* mutations in canine dystrophinopathies has not been reported.

Roughly two-thirds of *DMD* deletions are reportedly greater than one exon and are typically found in the central rod domain around exons 44-53 and to a lesser extent, the 5' terminus (Beggs et al., 1990; Dent et al., 2005; Johnson et al., 2012). In the *mdx* mouse, and in people with DMD, loss of the dystrophin C-terminal domain results in loss of the entire DAPC (Ohlendieck & Campbell, 1991). In addition to deletions, duplications and point mutations have also been identified in DMD patients. For example, in a study by Flanigan and colleagues, point mutations accounted for 46% of all mutations in the cohort evaluated. In that study, there were no point mutation hotspots; the mutations were evenly distributed across the exons of the *DMD* gene (Flanigan et al., 2009).

Additional cardiac-specific, dystrophin-associated proteins (Cypher, Ahnak1, Cavin-1 and CRYAB) have been identified in humans and mice (Johnson et al., 2012), and recently decreased Claudin-5 (a cell junction protein) was demonstrated in the cardiac tissue of dystrophin deficient mice (Delfin et al., 2012). It has been posited that variability in cardiac disease progression and severity may be due to differences in expression of these dystrophin associated proteins.

DMD Animal Models

Although the clinical course, disease severity, and microscopic lesions don't completely recapitulate DMD-associated skeletal and cardiac disease, rodent models are frequently utilized to study DMD because they are convenient, reproduce quickly, have a short life-span, and are relatively inexpensive to maintain (compared to other laboratory animals). The *mdx* mouse, first

described in 1977 in mice from a C57BL/10ScSn background, is one of the conventional animal models of DMD. This model is genetically similar to DMD patients with a deletion in the Xp21.1 locus; it results from a T to C substitution at position 3185. The substitution creates a stop codon in exon 23 with the remainder of the protein being produced in frame (Sicinski et al., 1989; Spurney et al., 2008). Although these spontaneous *Dmd*^{mdx} mutant mice do not express dystrophin, the disease phenotype is generally milder than what is seen in people with DMD. Mechanical function and muscular changes are less severe, which result in an almost normal lifespan for these mice (Collins & Morgan, 2003). In the young *mdx* mouse, the resultant phenotype includes stunted growth and muscle atrophy. In aged mice, skeletal muscle atrophy, weakness, and extensive compensatory hypertrophy are typically observed (Lefaucheur et al., 1995). Although not a consistent finding, prominent cardiac dysfunction has been reported as early as 9-10 months of age. Cardiac imaging in these mice shows decreased fractional shortening (Spurney et al., 2008). Over time, fibrosis occurs (Quinlan et al., 2004) as it does in humans, but it is much less severe. Histopathologic findings in *mdx* mice typically include skeletal myofiber degeneration, myonecrosis, chronic-active inflammation, numerous centralized nuclei, and increased numbers of satellite cells. With the notable exception of the diaphragm, *mdx* mice do not typically develop fibro-fatty muscular replacement, a frequent finding in people with DMD (Stedman et al., 1991). They do, however, develop “revertant fibers” within skeletal muscles and the myocardium (Danko et al., 1992).

Another mouse model that initially held great promise for DMD therapeutic development is the double knockout (dko) model. This mouse model is deficient in both dystrophin and a dystrophin homologue known as utrophin. Utrophin is normally localized to the neuromuscular junction; however, it is also capable of sarcolemmal redistribution. At the neuromuscular

junction, utrophin co-localizes with the acetylcholine receptors and is thought to play a role in synaptic cytoskeletal stabilization. Because these two proteins have reciprocal roles in muscle function and development, it was initially theorized that utrophin could compensate for the lack of dystrophin. Although the dko mice have aided in the understanding of utrophin-dystrophin interactions and premature musculoskeletal aging, they develop a disease phenotype that resembles that which is seen in DMD, indicating that utrophin therapy is not the therapeutic breakthrough for which researchers and patients were hoping (Blake et al., 1996; Deconinck et al., 1997).

Dystrophin-deficiency has also been discovered in various dog breeds; several of these have subsequently been studied as potential DMD animal models. Compared to other animal models, such as the *mdx* mouse, the disease phenotype that is noted in dogs is much more comparable to the disease manifestations characterized in humans. In Golden Retriever muscular dystrophy (GRMD), the most well-documented of the canine dystrophinopathies, a point mutation in intron 6 disrupts normal splicing, resulting in elimination of exon 7 and a premature stop codon (Cooper et al., 1988; Sharp et al., 1991). The effect of this mutation is stunted growth, altered gait, skeletal muscle atrophy, a plantigrade stance secondary to hyperextension of the carpal joints and flexion of the tibiotarsal joints, marked ptyalism, and lumbar kyphosis that can progress to lordosis. Paradoxical muscular hypertrophy, as well as cardiac failure associated with cardiomyopathy, can also occur in GRMD dogs just as in humans (Kornegay et al., 2012). Cardiac dysfunction is similar in presentation in both GRMD and DMD, but in both diseases, signs/symptoms can vary widely in severity, and may include a combination of findings. Table 2 compares typical cardiac abnormalities in both GRMD and DMD (Kornegay et al., 2012; Mazur et al., 2012; Verhaert et al., 2011):

Table 2. Comparison of GRMD and DMD cardiac abnormalities

Cardiac Findings/Diagnoses	GRMD	DMD
Dilated cardiomyopathy	✓	✓
Congestive heart failure	✓	✓
Left ventricular dilation	✓	✓
Left atrial enlargement	✓	
Left ventricular enlargement	✓	✓
Decreased left ventricular fractional shortening	✓	✓
Decreased left ventricular ejection fraction	✓	✓
Mitral regurgitation	✓	✓
Variable heart murmurs	✓	✓
Ventricular arrhythmias	✓	✓
Myocardial fibrosis	✓	✓

Histopathologic changes in GRMD skeletal and cardiac myofibers include foci of degeneration, regeneration, mineralization, fibrosis, and fatty infiltration. Revertant fibers are also documented, resulting from alternative splicing out of exons 3-9 or 5-12 (Schatzberg et al., 1998).

Spontaneous dystrophinopathies have also been recognized and described in other dog breeds. For example, in Labrador retriever muscular dystrophy (LMD), disease results from an insertion in intron 19 (Smith et al., 2007). In the Pembroke Welsh Corgi model, a repetitive element-1 [LINE-1] insertion in intron 13 aborts dystrophin expression (Smith et al., 2011). In the Cavalier King Charles Spaniel, a missense mutation in the 5' donor splice site of exon 50 occurs, which results in the deletion of exon 50 in the mRNA transcripts (Walmsley et al., 2010).

Additional dog breeds with known dystrophin mutations are summarized below:

- Rottweilers - point mutation in exon 52 (Winand et al., 1994)
- German Shorthaired Pointers - deletion of entire dystrophin gene (Schatzberg et al., 1999)
- Tibetan Terriers - deletion of exons 8–29 (Kornegay et al., 2012)
- Beagle - Point mutation in intron 6 acceptor splice site (Shimatsu et al., 2003)
- Cocker Spaniel - Deletion in exon 65 (Kornegay et al., 2012)

- Japanese Spitz - Inversion disrupts dystrophin and RPGR genes (Jones et al., 2004)

Although individual mutations have not yet been characterized, based on clinicopathologic data, dystrophinopathies are suspected in the Alaskan Malamute, Old English Sheepdog, Grand Basset Griffon Vendéen, and Norfolk Terrier (Beltran et al., 2015; Ito et al., 2011; Klarenbeek et al., 2007; Wieczorek et al., 2006).

Several other lesser-known DMD animal models have been studied. For example, dystrophin deficiency in domestic short-haired cats results in hypertrophic feline muscular dystrophy. Periods of degeneration and regeneration of muscle occur, but debilitating fibrosis, which is characteristic of DMD and GRMD, does not develop. Post-mortem evaluation of affected cats finds substantial glossal and diaphragmatic hypertrophy. Microscopic skeletal muscle changes include myofiber hypertrophy (with resultant size variation), foci of mineralization, myofiber splitting, and nuclear centralization. Endomysial fibrosis is typically minimal (Blunden & Gower, 2011; Carpenter et al., 1989; Kohn et al., 1993). Although affected cats lack outward evidence of cardiac disease, gross findings, histopathologic evaluation, and imaging studies indicate that cats can develop myocardial hypertrophy (Gaschen et al., 1999).

Recently a large animal model of DMD was created via deletion of exon 52 in male pig cells. The resultant pigs exhibited absence of dystrophin in skeletal muscles, increased serum creatine kinase levels, progressive dysfunction of skeletal muscles, impaired mobility, muscular weakness and a maximum life span of 3-months resultant from respiratory impairment. Unlike human DMD patients, some dystrophin-deficient pigs in the study died shortly after birth (Klymiuk et al., 2013). Non-mammalian models of DMD, such as the Zebrafish and the nematode *Caenorhabditis elegans*, both express a dystrophin orthologue, resulting in their use in DMD-related gene analyses and drug discovery studies (Collins & Morgan, 2003).

Labradoodle History

Labradoodles were first created in 1988 by Wally Conron (of The Royal Guide Dog Association of Australia) by crossing a Labrador Retriever with a Standard Poodle. This purposeful breeding occurred after Mr. Cochran received a request from a client to produce a guide-dog with a low allergen coat for people with allergies. Today, the Australian Labradoodle is the result of breeding a Labradoodle with a Cocker Spaniel (American or English), while the true Labradoodle is only a cross between the Labrador Retriever and Standard Poodle. Although the Labradoodle is popular among pet owners, the American Kennel Club (AKC) does not currently recognize it, or the Australian Labradoodle, as one of the 175 pure breeds of dogs. In order to be considered an official pure breed by the AKC, the breed must have at least 300 Labradoodles within the U.S. and be distributed among at least 20 states, the dogs must have a national breed club demonstrating interest, and there must be at least a three generation pedigree. In addition, each recognized breed must also have predictable characteristics and fulfill a specific purpose (AKC, 2019; ALAA, 2018).

The dystrophin deficient Labradoodle colony housed at the Scott Ritchey Research Center (SRRC), at Auburn University, was established via a carrier dam named “Scout” that was donated to the research center in 2008. This dam resulted from breeding two Australian Labradoodles. Subsequent breeding of “Scout” resulted in the following familial lines:

- “Scout” x “Kodiak” (normal Australian Labradoodle) → Carrier female named “Bella”
 - “Bella” x “Yaz” (normal Labrador retriever) → 1 dystrophin deficient male
- “Scout” x “Tegan” (normal Australian Labradoodle) → 1 dystrophin deficient male
- “Scout” x “Rody” (normal Australian Labradoodle) → 4 dystrophin deficient males

Additional breeding of “Bella” and her carrier female offspring have resulted in continued selection for this novel Dystrophin mutation.

Transcriptomics

RNA sequencing provides an excellent way to characterize transcriptomic variations by measuring the expression of thousands of genes in a tissue type at the same time. This expanding technology allows for long read lengths, which enables accurate de-novo transcriptome assembly and high-confidence identification of transcripts and isoform variants, essential for interpreting the functional elements of the genome and understanding disease pathogenesis. The goals of transcriptome sequencing are to determine all transcript species (i.e. mRNAs, non-coding RNAs and small RNAs), the transcriptional structure of genes, and to evaluate differential gene expression (Wang et al., 2009).

The standard process of RNA sequencing can be broken down into a few main steps. Once RNA has been isolated and purified from the desired tissue sample, the process of sequencing begins by converting the RNA (total or fractionated) to a library of cDNA fragments. Library preparation involves generating the cDNA fragments, adding adapters, and amplifying the DNA for sequencing. The adapter sequences vary depending upon platform and contain various functional elements necessary for sequencing; regardless of the platform, adaptors must contain a terminal sequence (used for clonal amplification and attachment to the sequencing support) and sequencing reaction priming elements. Once the adapters have been added, generally via RT-PCR or ligation, the stranded cDNA libraries are prepared and checked for quality prior to sequencing. The cDNAs are then sequenced using the sequencing platform that

best matches the researcher's needs (multiple platforms are now available to choose from, including Ion Torrent, PacBio, and Illumina) ("RNA-seqlopedia,").

Transcriptome sequencing has been performed on tissue samples from DMD patients in order to detect mutations, understand aberrant splicing events and variants, evaluate allelic imbalances, and to analyze differential gene expression. RNA sequencing on skeletal muscle from patients with Duchenne muscular dystrophy has found that 30% of human genes were expressed and detectable in skeletal muscle, of which, 3% showed differential expression in dystrophic muscle compared to controls. 1,324 of the 1,882 dysregulated probe sets corresponded to characterized genes/proteins. As part of the evaluation, members of the insulin-like growth factor (IGF) pathway were preferentially investigated, as was the potential for cardiac gene expression in skeletal muscle and sex-specific transcripts. Results indicated that dystrophic skeletal muscle not only had up-regulation of IGF-I and IGF-II, but also upregulation of inhibitory IGF-binding proteins and regulators such as IGFBP-2, -4, -6 and -7 and IGFBP-5 protease. Evaluation of six genes predominantly expressed in cardiac tissues, including Actin alpha cardiac muscle 1 (ACTC1), Cardiac ankyrin repeat protein (CARP), Calsequestrin 2 (CASQ2), Troponin T2 cardiac-type (TNNT2), CUG triplet repeat RNA-binding protein 2 (CUGBP2), and Connexin 43 (CX43), found that CARP and CX43 were macrophage-associated and TNNT2 activated-myoblast-associated. ACTC1 and CUGBP2 up-regulation were not associated with muscle regeneration. They also found two Y-linked genes only expressed in male muscle (Ribosomal protein S4 Y-linked 1 [RPS4Y] and DEAD-box helicase 3 Y-linked [DDX3Y]) and two autosomal genes with increased expression in female muscle (C-X-C motif chemokine ligand 2 [CXCL2; also known as GRO2] and Zinc finger protein 91 [ZNF91]) (Bakay et al., 2002). Although endomyocardial biopsies have been performed on DMD patients

with clinical and cardiac MRI-confirmed cardiovascular compromise, the biopsies were utilized for DNA and RNA viral genome extraction rather than cardiac RNA sequencing (Mavrogeni et al., 2010).

RNA sequencing has also been performed in canine and murine models of DMD. In dogs, profiling in GRMD skeletal muscle has yielded differentially expressed genes associated with myogenesis/muscle regeneration, metabolism, and inflammation. Researchers also found up-regulation of Chitinase 3-like 1 (CHI3L1) in GRMD dogs with a more rapid clinical course, suggesting an association with disease progression in GRMD and potentially DMD.(Brinkmeyer-Langford et al., 2018) Though cardiac transcriptome sequencing has not previously been performed in a canine model of DMD, it has been utilized to study the consequences of obesity-related hypertension on cardiac gene regulation and end-stage heart failure (Gao et al., 2006; Philip-Couderc et al., 2003). To date, cardiac muscle RNA sequencing has only been performed in the Australian Labradoodle model. Transcriptome analysis of *mdx* mouse skeletal muscle has found significant differential expression of 3844 genes, of which 2695 were upregulated and 1149 downregulated. Enrichment pathway analysis using Ingenuity Pathway Analysis (IPA) software found enrichment genes associated with inflammation, fibrosis, adhesion, apoptosis, muscle cell structure and metabolism. Additionally, there was enrichment of canonical signaling pathways (e.g. NF-kB, Wnt, calcium signaling, etc.) (Yanay et al., 2017).

Because mortality in DMD patients is increasingly associated with cardiomyopathy and heart failure, it is imperative that we gain a better understanding of the possible pathways involved in the development of DMD-associated cardiac disease. We have identified a novel dystrophin mutation in Australian Labradoodles that develop early-onset cardiac disease in

addition to the typical clinical signs associated with skeletal myopathy. Based on these preliminary findings, we sought to study the Australian Labradoodle as a potential model for DMD cardiomyopathy.

The first research objective was to fully characterize the disease phenotype that occurs in the Australian Labradoodle model. To that end, we performed monthly echocardiography and trimonthly cardiac Magnetic Resonance Imaging (MRI) / Magnetic Resonance Spectroscopy (MRS). The results of these cardiac analyses were then correlated to the observed clinical signs, necropsy findings, and histopathology data to determine if dystrophin-deficient Australian Labradoodles are an appropriate model for the study of DMD-associated cardiomyopathy.

The second research objective was to compare the RNA profiles of normal and dystrophin-deficient Australian Labradoodle hearts via transcriptome sequencing. These transcriptomic comparisons allowed us to study how changes in the normal level of gene activity may reflect or contribute to the cardiac disease process. We hypothesized that cardiac transcriptome sequencing in the Australian Labradoodle model of DMD would reveal key genetic and epigenetic markers that may be associated with cardiomyopathy. Understanding the cardiac manifestation of DMD at the level of gene expression would potentially allow for future development of targeted therapeutics for both dystrophin-deficient dogs and Duchenne muscular dystrophy patients.

Chapter 2: Characterization of Australian Labradoodle Dystrophinopathy



Characterization of Australian Labradoodle dystrophinopathy

Stephanie M. Shrader^{a,*}, SeungWoo Jung^b, Thomas S. Denney^{c,d}, Bruce F. Smith^{a,e}

^aDepartment of Pathobiology, Auburn University College of Veterinary Medicine, Auburn, AL 36849, USA

^bDepartment of Clinical Sciences, Auburn University College of Veterinary Medicine, Auburn, AL 36849, USA

^cDepartment of Electrical and Computer Engineering, Auburn University, Auburn, AL 36849, USA

^dAuburn University MRI Research Center, Auburn, AL 36849, USA

^eScott-Ritchey Research Center, Auburn University College of Veterinary Medicine, Auburn, AL 36849, USA

Received 16 February 2018; received in revised form 5 August 2018; accepted 23 August 2018

Abstract

In humans, dystrophin mutations cause the X-linked recessive disorder known as Duchenne muscular dystrophy (DMD). These mutations result in skeletal and cardiac muscle damage with mortality increasingly associated with cardiomyopathy. We have identified a novel dystrophin mutation in exon 21 in a line of Australian Labradoodles; affected dogs develop progressive clinical signs including poor weight gain and weight loss, gait abnormalities, exercise intolerance, skeletal muscle atrophy, macroglossa, ptialism, dysphagia, kyphosis, and a plantigrade stance. Echocardiographic abnormalities include hyperechoic foci in the left ventricular papillary muscles, septal hypokinesis, and decreased left ventricular systolic and diastolic volume and internal diameter. Holter recordings found a Mobitz type II second-degree atrioventricular (AV) block in one affected dog. Analysis of phosphocreatine-to-ATP ratios (PCr/ATP) (obtained via cardiac magnetic resonance imaging and spectroscopy evaluation), found no statistically significant difference in the mean PCr/ATP between groups. Histopathologic skeletal muscle changes included fibrofatty infiltration, myocyte degeneration, necrosis, and regeneration, lymphohistiocytic inflammation, and mineralization; cardiac changes were limited to a focal area of mineralization adjacent to the sinoatrial node in the dog with a second-degree AV block. Due to rapidly progressive clinical signs, a severe phenotype, and potential for cardiac involvement, Australian Labradoodle dystrophinopathy may be a useful model to further study DMD pathogenesis.

© 2018 Elsevier B.V. All rights reserved.

Keywords: Labradoodle; Dystrophinopathy; Duchenne; Myopathy; Cardiomyopathy; MRI.

1. Introduction

Duchenne muscular dystrophy is an X-linked recessive disorder in humans caused by mutations in the largest known gene in nature, dystrophin. Dystrophin measures 2.4-megabases at locus Xp21 and encodes for a 427-kD sub-membrane protein that anchors cytoskeletal F-actin to the extracellular matrix protein laminin [1]. Mutations in the dystrophin gene result in a partially functional or completely non-functional protein product, causing affected individuals to develop progressive skeletal and cardiac myofiber damage with an early loss of ambulatory ability [2]. Historically, mortality in DMD patients has been attributed primarily to respiratory failure, most often associated with ventilatory

defects, chronic hypoventilation, and respiratory infections [3,4]. Over the past two decades, the treatment of skeletal muscle complications and respiratory disease has improved; however, these advances have unmasked DMD-associated cardiac disease in many patients. Recent retrospective studies indicate that death attributable to cardiac disease occurs in approximately 20–30% of DMD patients [5–7].

Early clinical findings in DMD patients include difficulties rising from a seated position, frequent falls, delayed motor-skill development, and learning disabilities. Physical examination findings often include (pseudo)hypertrophy of the calves, lumbar lordosis, waddling gait, macroglossa, and a distinctive way of rising from the floor (known as Gowers' maneuver). Progressive muscle weakness eventually results in wheel chair dependence, generally by ten years of age [8,9]. Histologically, skeletal muscle changes in DMD patients are characterized by necrotic and/or degenerating myocytes with foci of

* Corresponding author.

E-mail address: sms0059@tigermail.auburn.edu (S.M. Shrader).

mineralization, myofiber regeneration (characterized by myofiber basophilia, enlarged centralized nuclei with prominent nucleoli, and/or nuclear rowing), and resultant variation in myofiber cross-sectional diameter. Necrotic myofibers are often surrounded and/or infiltrated by macrophages and lymphocytes. As the regenerative capacity of the affected muscle declines over time, there is gradual replacement of the tissue by mature fibrous connective tissue and infiltrating adipose tissue (i.e. fibrofatty replacement). Individuals with cardiomyopathy may also have foci of degeneration, necrosis, inflammation, and fibrofatty replacement in the myocardium [10].

Cardiac pathology varies among DMD patients; however, findings can include dilated cardiomyopathy (DCM), congestive heart failure, left ventricular eccentric hypertrophy, decreased left ventricular systolic function assessed by fractional shortening (FS) and ejection fraction (EF), mitral regurgitation, tricuspid regurgitation, and myocardial fibrosis [11,12]. Affected individuals may also show persistent electrophysiologic abnormalities on ECG; sinus tachycardia, an increased R-S ratio in the right precordial leads, deep Q waves in the frontal leads, and conduction abnormalities. In addition to persistent sinus tachycardia, other common arrhythmias in DMD patients include sinus bradycardia, atrial premature beats, and ventricular premature beats. Conduction defects, including right bundle branch blocks, left anterior fascicular blocks, and first- and second-degree AV blocks have also been observed [13–15].

Recently, cardiac magnetic resonance imaging (MRI) has been proposed as a beneficial diagnostic tool to identify early myocardial remodeling changes [11]. Both echocardiography and MRI are able to identify abnormal left ventricular FS, left ventricular hypokinesia, and left ventricular dilation; however, research shows that the majority of echocardiographic studies have suboptimal scanning windows and significantly over- or under-estimate left-ventricular systolic function compared to cardiac MRI [16]. In addition to cardiac MRI, cardiac magnetic resonance spectroscopy (MRS) is also being utilized to accurately evaluate cardiac functionality in patients with DMD. The metabolic demands of the heart necessitate the need for high-energy phosphate being transferred from ATP (via oxidative phosphorylation in the mitochondria) to creatinine, generating phosphocreatine (PCr) and ADP. Phosphorus-31 is utilized for the detection of PCr, ATP, intracellular pH, and flux through the creatine kinase reaction. Analyzing these spectra via MRS is therefore beneficial because the PCr-to-ATP ratio (PCr/ATP) provides a useful measure of cardiac energy metabolism and functionality [17]. PCr/ATP has been shown to be significantly reduced in Becker Muscular Dystrophy (BMD) patients and carriers when compared to controls; this change did not, however, correlate with left ventricular EF or mass index, indicating that a direct association between altered dystrophin expression and the development of cardiomyopathy may be possible, and that MRS may be a useful diagnostic tool to detect early stage cardiomyopathy prior to echocardiographic identification of left ventricular systolic dysfunction [18].

Various animal models have been utilized in the study of DMD. The traditional model is the *mdx* mouse, which has a deletion in the Xp21.1 locus that results in a stop codon in exon 23 [19,20]. Compared to people with DMD, the disease phenotype in *mdx* mice is generally milder with an almost normal lifespan, stunted growth, skeletal muscle atrophy, and eventual compensatory hypertrophy [21,22]. Cardiac dysfunction is not a consistent finding in mice, but has been reported as early as 9–10 months of age; decreased FS values have been demonstrated via echocardiographic analyses [19,23,24]. Spontaneous dystrophin mutations have been reported in multiple dog breeds, though Golden Retriever muscular dystrophy (GRMD) continues to be the best documented of the canine dystrophinopathies. It results from a point mutation in intron 6 that disrupts normal splicing and creates a premature stop codon [25–27]. Cardiac dysfunction has been documented in GRMD; however, clinical signs can vary widely in incidence and severity. Reported clinical, echocardiographic, and electrocardiographic findings in the GRMD model include DCM, congestive heart failure, left atrial enlargement, left ventricular enlargement, decreased left ventricular FS, decreased left ventricular EF, mitral regurgitation, heart murmurs, ventricular arrhythmias, and myocardial fibrosis [28,29].

We have identified a novel dystrophin mutation in exon 21 in a line of Australian Labradoodles. The propositus of this pedigree died suddenly at six months of age with clinical signs suggestive of cardiac disease. Subsequent males in this line have consistently developed early clinical signs of skeletal muscle pathology similar to what has been reported in other dog breeds. We therefore hypothesized that dystrophin-deficient Labradoodles would show echocardiographic, electrocardiographic, and cardiac MRI/MRS abnormalities indicative of cardiomyopathy and that cardiac MRI/MRS may be more sensitive than the other two diagnostic modalities for detecting early cardiac dysfunction. In addition to identifying early manifestations of cardiac disease in this model, we aimed to correlate these findings with clinical signs and necropsy and histopathology data, and to determine whether Labradoodle dystrophinopathy is an appropriate model for studying DMD-associated cardiomyopathy.

2. Materials and methods

All animal experiments were approved by the Animal Care and Use Committee of Auburn University. A 3-month old male Australian Labradoodle presented to the Auburn University College of Veterinary Medicine for a suspected muscular dystrophy and genetic testing for the Labrador Retriever dystrophin mutation (intron 19 insertion) after showing signs of muscle atrophy and exercise intolerance. PCR amplification of intron 19 from whole blood showed no insertion. mRNA was obtained from skeletal muscle and sequenced, demonstrating a C to T transition at position 2668 of the dystrophin open reading frame. This nonsense mutation results in a CGA codon (arginine) becoming a stop codon (TGA), causing a

truncated protein. This dog was used to establish a breeding colony of carrier females that continues to be maintained at the Scott Ritchey Research Center (SRRC) at Auburn University; male offspring of the colony were used for the present study.

Experimental dogs were produced using the semen from a normal Labrador retriever, a normal Australian Labradoodle, or a dystrophin-deficient Australian Labradoodle (male donor selection based on availability) to vaginally inseminate a carrier Australian Labradoodle (several related females were utilized). Multiple breeding cycles produced seven dystrophin-deficient and five control (normal) male littermates.

For each dog in every litter produced during the course of the study, the dystrophin genotype was determined via DNA sequencing, performed on whole blood submitted to Eurofins Genomics (12701 Plantside Drive, Louisville, KY 40299, USA). Male offspring with a correct dystrophin gene sequence (and lacking clinical signs of a muscular dystrophy) were used as controls. Female offspring, regardless of their dystrophin status, were not included in this study.

The founder of this line died unexpectedly at 6-mos of age from a possible terminal arrhythmia or cardiac conduction anomaly; therefore, all study dogs had monthly echocardiographic and electrocardiographic evaluations, in addition to cardiac magnetic resonance imaging (MRI) and magnetic resonance spectroscopy (MRS) at three and six months of age. Echocardiographic examinations were performed by a board-certified veterinary cardiologist (SWJ) at monthly intervals starting at 1-month of age. Phased-array transducers between 5.0–8.5 MHz (Vivid E9, GE, Milwaukee, WI, USA) were used with a probe selection based on image optimization, gain, and filter settings that were required to reduce background noise and provide clear images of blood flow and tissue signals. Electrocardiogram (ECG) was simultaneously recorded during echocardiographic evaluation. Ventricular end-diastole was defined as the frame before mitral valve closure, and ventricular end-systole was defined as the frame before mitral valve opening. Echocardiographic analyses included evaluation of left ventricular internal diameter during diastole (LVIDd), left ventricular internal diameter during systole (LVIDs), left ventricular end diastolic volume (LVEDV), left ventricular end systolic volume (LVESV), ejection fraction (EF), epicardial velocity, endocardial velocity, left ventricular free wall thickness during diastole (LVFWd), and interventricular septum thickness during diastole (IVSd). FS% was calculated as $[(LVIDd-LVIDs)/LVIDd]*100$. Myocardial velocity gradient was calculated as the difference between endocardial velocity and epicardial velocity [31].

A 24 h ambulatory Holter recording was performed (Trillium 5000, Forest Medical Holter Analysis System, Syracuse, NY, USA) when ECG abnormalities were observed during echocardiographic evaluations. Manual adjustments and accuracy verification of the arrhythmias were performed by SWJ.

MRI/MRS evaluation was performed on eight of the study dogs (3 control, 5 affected) using a MAGNETOM 7 Tesla scanner (Siemens Healthineers, Malvern, PA) and a dual-tuned $1H$ - ^{31}P loop coil (RAPID Biomedical GmbH, Rimpar,

Germany) at the Auburn University MRI Research Center. Dogs were scanned using a 3-dimensional ultra-short echo time chemical shift imaging sequence [32] with $16 \times 16 \times 8$ matrix, $11.25 \text{ mm} \times 11.25 \text{ mm} \times 22.5 \text{ mm}$ voxel size, 2.3 ms echo time, 1640 ms repetition time, 12 averages, 6 kHz bandwidth, and 2048 vector size. ^{31}P MR spectra were analyzed using a custom implementation of AMARES [33] to obtain amplitudes of the PCr and gamma ATP resonances. PCr/gamma ATP amplitude ratios were computed from three voxels in the midventricular anterior and anteroseptal myocardium and averaged. For MRI/MRS evaluation, each study dog was premedicated with 0.2–1.0 mg/kg butorphanol (subcutaneous administration), and induced with 3–5 mg/kg of propofol (intravenous administration). General anesthesia was maintained with isoflurane and the dogs were placed in left lateral recumbency for imaging acquisition.

All dogs were euthanized at 6 months of age (or earlier if a humane endpoint was reached). This terminal endpoint was established based on the founding dog's sudden death at 6-mos of age and progressive clinical decline in other affected males from this line beginning at 4-mos of age (including diminished/absent ambulation, weakness, and dysphagia requiring a gruel-based diet and supplemental fluid administration).

At the time of death, each dog had a post-mortem examination performed by a board certified veterinary pathologist (SMS), which included collection of blood for serum biochemistry analyses (performed by the Auburn University Clinical Pathology Laboratory), organ weight evaluation (heart, liver, kidneys, lung, spleen, brain), and measurement of cardiac parameters (left ventricular free wall thickness, right ventricular free wall thickness, septal thickness, aortic circumference, base-apex length, heart circumference [at the widest point], and pulmonic valve circumference). A complete set of tissues was collected for histopathologic evaluation (to include at a minimum: entire heart, entire diaphragm, tongue, spleen, liver, kidneys, pancreas, stomach, esophagus, duodenum, jejunum, ileum, colon, urinary bladder, adrenal glands, lung, biceps femoris, gluteus medius, and triceps brachii). Additional tissue sites were collected if gross lesions were observed.

All tissues were fixed in 10% neutral buffered formalin, processed routinely, and embedded in paraffin wax. Sections were cut to 5- μm thickness and stained with hematoxylin and eosin (H&E). Histopathologic evaluation of H&E stained tissue sections was performed by a board certified veterinary pathologist (SMS). For each dog, sections of heart that were histologically evaluated included the aorta, right ventricular free wall (including papillary muscle), interventricular septum, and left ventricular free wall (including papillary muscle). Additional cardiac anatomic sites were evaluated based on individual animal clinical signs and cardiac imaging findings.

Serum biochemistry values, gross findings, organ weights, cardiac measurements, and histopathologic findings were entered into Microsoft® Excel. Group means, standard deviations, and statistical significance were calculated with a Student's *t*-test (SAS® version 9.4) for independent samples. The level of significance was set at $p < 0.05$.

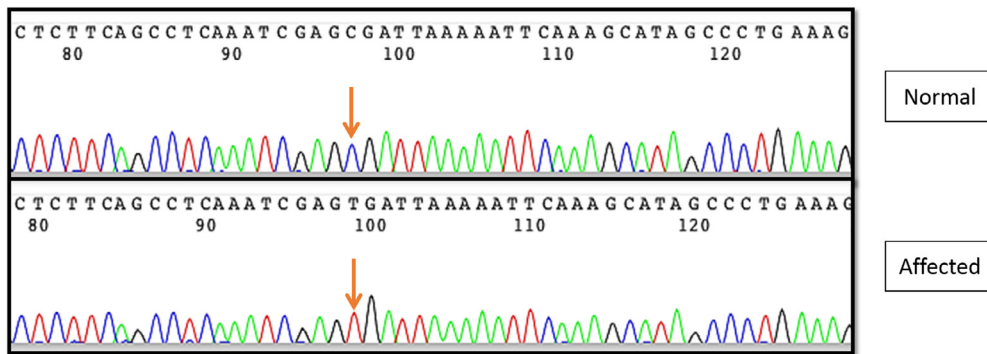


Fig. 1. Comparison of DNA sequences from exon 21 of the dystrophin gene from a normal male and affected male Labradoodle. Base pair 43 is indicated for each animal by an arrow; note the C to T transition in the affected dog.

3. Results

Seven dystrophin-deficient and five littermate control male Labradoodles were utilized for this study. Each affected Labradoodle had a C to T transition at base pair 43 in exon 21 of the dystrophin gene (Fig. 1). To the authors' knowledge, this is a novel spontaneous dystrophin mutation that has not been previously reported in dogs. Clinically, the dystrophin-deficient dogs had stunted growth, exercise intolerance, poor weight gains, and eventual weight loss (typically beginning at 4-months of age). There was a statistically significant decrease in the mean terminal body weight in the affected group (7.5-kg) compared to the control group (21.21-kg) ($p < 0.0001$). By 3-months of age, affected dogs developed a stiff gait that progressed to shuffling with slight carpal valgus and a pronounced plantigrade stance. At the time of study termination, all affected dogs had moderate to severe appendicular and axial skeletal muscle atrophy (most pronounced in the proximal limb musculature), temporalis atrophy, moderate to severe macroglossa, ptyalism, dysphagia, and kyphosis.

The dogs had monthly echocardiographic evaluations which included qualitative cardiac assessment and measurement of various parameters for cardiac functionality. In one of the affected dogs (14.3%), multifocal to coalescing, mild, hyperechoic foci in the left ventricular anterior and posterior papillary muscles were noted (Fig. 2). These changes became apparent at 2-months of age and remained static until study termination at 6-months of age. Trivial mitral valve regurgitation was observed in 1/7 affected dogs (14.3%) and 1/5 control dogs (20%), both at the 6-month time point. Mild tricuspid regurgitation was consistently present in 3/7 affected dogs (42.9%) throughout the study. Trivial to mild tricuspid regurgitation was also seen in 1/5 (20%) of control dogs throughout the study. Non-progressive, decreased dynamic septal motion, consistent with septal hypokinesis, was present in 3/7 (42.9%) of affected dogs as early as one month of age (Fig. 3). Two of the five control littermates, from related female carriers but different sires, also had a hypokinetic septal motion. Septal hypokinesis was non-progressive, minimal, and apparent at one-month of age in one of the control dogs; in the other

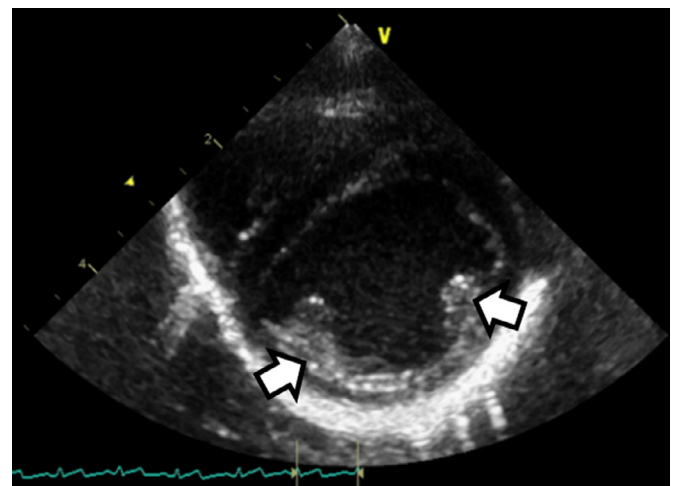


Fig. 2. Conventional echocardiographic image (right parasternal short axis view at the level of the papillary muscles) of one of the affected dogs showing multifocal hyperechoic foci in the left ventricular anterior and posterior papillary muscles (arrows).

dog, it was first noted at 4-months of age and progressed from mild to severe by study termination.

Quantitative echocardiographic parameters were evaluated at monthly intervals; a percent increase (%) of LVIDd, LVIDs, LVEDV, and LVESV from 3 month to 6 month was compared between control and affected dogs. The mean percent increase of LVIDs was significantly lower in affected dogs ($7.6\% \pm 5.2$, $p = 0.0045$) as compared to control dogs ($29.8\% \pm 2.1$) (Fig. 4). There was a trend that the mean percent increase of LVIDd was lower in affected dogs ($9.5\% \pm 6.6$, $p = 0.08$) as compared to control dogs ($25.3\% \pm 4.3$). The mean percent increase of LVESV was markedly diminished in affected dogs ($21.3\% \pm 12.3$) in comparison to control dogs ($98.1\% \pm 6.1$). A trend was noted in the mean percent increase of LVEDV that affected dogs had smaller diastolic filling volume ($26.3\% \pm 15.8$, $p = 0.075$) than control dogs ($69.2\% \pm 13.7$). These findings are consistent with a significant developmental growth defect of cardiac size and volume in dystrophin-deficient Labradoodle dogs.

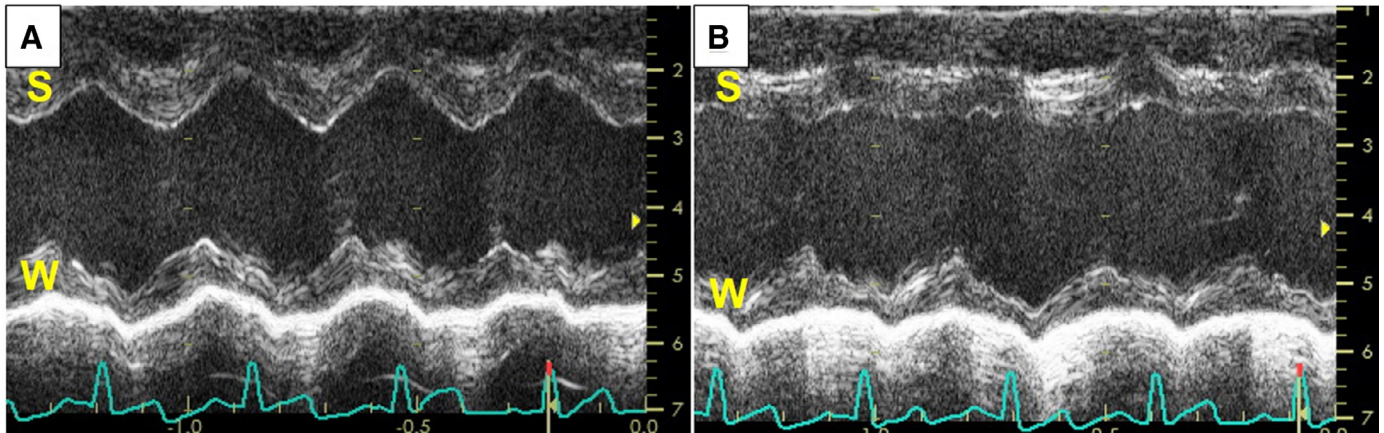


Fig. 3. Echocardiographic evaluation of the left ventricle on M-mode from a control dog (A) and an affected dog (B). (A) Normal dynamic motion of the left ventricular septum and free wall is seen in a control dog. (B) A marked hypokinetic motion of the interventricular septum is apparent in an affected dog. S: interventricular septum. W: left ventricular free wall.

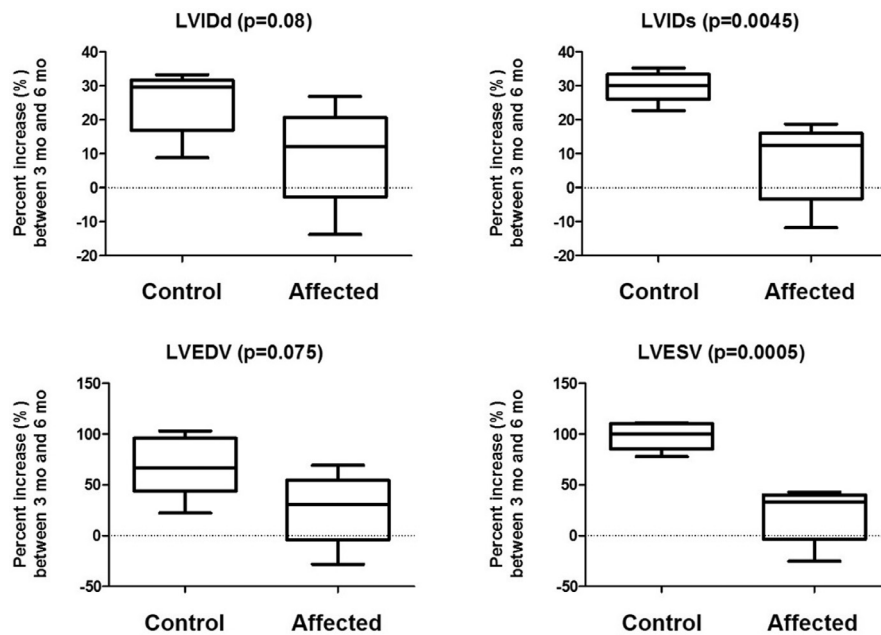


Fig. 4. Comparison of a percent increase (%) between control and affected dogs of echocardiographic dimensional parameters (LVIDd, LVIDs, LVEDV, and LVESV) from 3 month to 6 month.

At the 3-month time point, affected dogs had a statistically significant decrease in mean LVIDd ($24.29 \text{ mm} \pm 2.69$; $p=0.0287$), LVIDs ($16.14 \text{ mm} \pm 1.46$; $p=0.0195$), LVEDV ($21.43 \text{ ml} \pm 6.13$; $p=0.0281$), and LVESV ($7.43 \text{ ml} \pm 1.81$; $p=0.0090$) when compared to the control dogs. At the 6-month time point, affected dogs had a statistically significant decrease in mean LVIDd ($27.20 \text{ mm} \pm 3.56$; $p=0.0054$), LVIDs ($17.80 \text{ mm} \pm 1.92$; $p=0.0007$), LVEDV ($28.40 \text{ ml} \pm 9.34$; $p=0.0028$), and LVESV ($9.60 \text{ ml} \pm 2.70$; $p=0.0011$) when compared to the control dogs. There were no statistically significant differences in the remainder of the examined parameters (FS%, EF%, epicardial velocity, endocardial velocity, MVG, LVFWd, or IVSd). While performing the 3-month echocardiographic evaluations, one of the affected dogs was noted to have marked arrhythmias. The dog

was subjected to a 24 h Holter monitor. Holter recordings revealed the presence of low amplitude R-waves and profound S-waves and also showed intermittent, non-conducted P-waves (without progressive prolongation of the PR interval) that typically occurred at a frequency of 1–2 events/min. The PR intervals of the conducted beats consistently remained within normal limits (less than 130 ms). Findings were consistent with a Mobitz type II 2nd degree atrioventricular (AV) block (Fig. 5).

MRI/MRS evaluation was performed on eight of the study dogs (3 control, 5 affected). Only two of the dogs were evaluated at both the 3- and 6-month time points due to scheduling limitations and early euthanasia of two of the affected dogs following the 3-month MRI/MRS evaluation (at 100 days and 113 days of age). Both dogs were euthanized due to

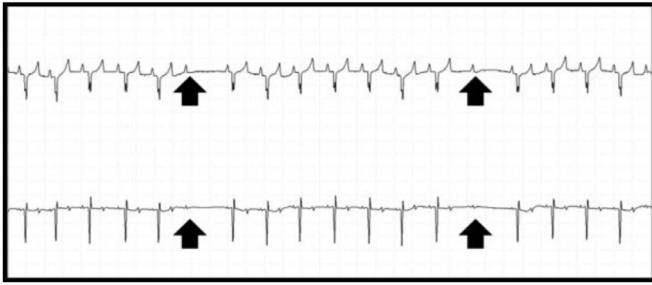


Fig. 5. Two channel Holter monitor data from an affected dog with a Mobitz type II 2nd degree AV block. The image shows non-conducted P waves (black arrows) and constant PR intervals in the conducted beats.

progressive dysphagia, dyspnea, inappetence, dehydration, lack of mobility, and weight loss. The relative amount of PCr was roughly 1.5x–2x that of ATP in the ^{31}P MR spectra of control dogs, resulting in a mean PCr/ATP of 1.55 and 1.57 at the 3- and 6-month time points respectively. Although the relative amount of PCr was decreased relative to ATP in the affected dogs, the ^{31}P MR spectra were highly variable and had low signal-to-noise ratios. The mean PCr/ATP was lower in the affected dogs in comparison to controls at the 3-month time point (1.08 ; $p=0.1138$); at the 6-month time point, mean PCr/ATP was similar to controls (1.55 ; $p=0.9218$).

Prior to euthanasia, each study dog had blood drawn for serum biochemistry analyses. Affected dogs had statistically significant increases in mean alanine aminotransferase (ALT) (492.83 ± 282.30 U/L; reference interval = 13–151 U/L) and aspartate aminotransferase (AST) ($1,096.33 \pm 1,186.68$ U/L; reference interval = 18–55 U/L). They also had a statistically significant increase in mean creatine kinase (CK) ($88,487.50 \pm 112,058.30$ U/L; reference interval = 53–337 U/L) (Fig. 6).

Gross necropsy findings in all affected dogs consisted of moderate to severe peripheral diaphragmatic hypertrophy (up to 2-cm in thickness) with thinning of the central tendinous portion, generalized appendicular and axial muscle atrophy, and macroglossa. In 2/7 (28.6%) of the affected dogs, macroglossa resultant from sublingual muscular hypertrophy was so severe that it resulted in oropharyngeal stenosis. The average body condition score of affected dogs was 1.7/9; the average body condition score of the control dogs was 7/9. One of the affected dogs (14.3%) had mild to moderate dilation of the cranial 2/3 of the esophagus. In 2/7 (28.6%) of the affected dogs, there was marked hypertrophy of the cranial aspect of the rectus abdominus and deep pectoral muscles. The left cranial lung lobe of one of the affected dogs (euthanized at 100 days of age, following the 3-month MRI/MRS evaluation) was mottled red and consolidated (consistent with aspiration pneumonia).

During the necropsy evaluation, organ weights were recorded for the heart, liver, kidneys, lung, spleen, and brain. Organ-to-body weight and organ-to-brain weight ratios are often used during toxicology studies to assess treatment effects [34]. Although this is not a toxicology study, overall organ weight assessment is a useful tool to characterize the

presence or absence of organ pathology in a novel animal model. Organ-to-body weight ratios resulted in statistically significant ($p < 0.05$) increases in liver-to-body weight, right kidney-to-body weight, and left kidney-to-body weight ratios within the affected group; however, these differences are thought to be due to the significant variation in body weights between the groups and are not resultant from organ pathology (confirmed histologically). Because the absolute weight of some organs (such as the brain) is relatively unaltered by modest changes in body weight [35], we also analyzed organ-to-brain weight ratios. Although there were statistically significant ($p < 0.05$) decreases in heart-to-brain weight, liver-to-brain weight, lung-to-brain weight, and spleen-to-brain weight ratios within the affected group, these results were interpreted with caution and again thought to be due to the significant variation in body weights between the groups.

To fully characterize the presence of dystrophinopathy-associated cardiac disease in the affected dogs, cardiac measurements were collected during each necropsy evaluation (Fig. 7). Compared to the control group, the affected group had statistically significant decreases ($p < 0.05$) in the mean measurements for left ventricular free wall (LVFW) thickness (7.60 ± 2.26 mm; control = 10.60 ± 1.95 mm), right ventricular free wall (RVFW) thickness (2.43 ± 0.53 mm; control = 3.90 ± 0.89 mm), base-apex length (5.04 ± 0.84 cm; 7.92 ± 1.34 cm), heart circumference (11.67 ± 3.00 cm; control = 17.48 ± 1.13 cm), and aortic valve circumference (3.37 ± 0.80 cm; 4.66 ± 0.67 cm). Similar to the organ weight changes previously described, group differences in the various cardiac measurements are likely resultant from the significantly smaller body size (and concomitant heart size) of the affected dogs.

Histopathologic findings in the skeletal muscles of affected dogs were consistent with the clinical findings and necropsy observations. In the sections of biceps femoris, triceps brachii, gluteus medius, peripheral aspects of the diaphragm, and tongue, all affected dogs had mild to marked, multifocal fibrofatty infiltration, myocyte degeneration (characterized by cellular swelling, pallor, and vacuolization) myocyte necrosis (characterized by cellular hypereosinophilia, loss of cross-striations, fragmentation, pyknosis, and karyorrhexis), regeneration (characterized by cellular basophilia and centralized nuclear rowing), lymphohistiocytic inflammation, and foci of mineralization (Fig. 8A–C). Similar histopathologic findings were present in the rectus abdominus and deep pectoral muscles of the two dogs that had marked, grossly evident hypertrophy of these muscles. In all affected dogs, the central, tendinous portion of the diaphragm was consistently < 1 -mm thick and composed of fibrous connective tissue that was occasionally mineralized. In the esophageal muscularis externa, 5/7 (71.4%) of affected dogs had mild to moderate, multifocal myocyte degeneration and necrosis, regeneration, foci of lymphohistiocytic inflammation, and rare mineralization. All examined skeletal muscle sections from the control dogs were histologically unremarkable.

Two of the study dogs (one affected and one control) had evidence of acute, suppurative, bronchopneumonia

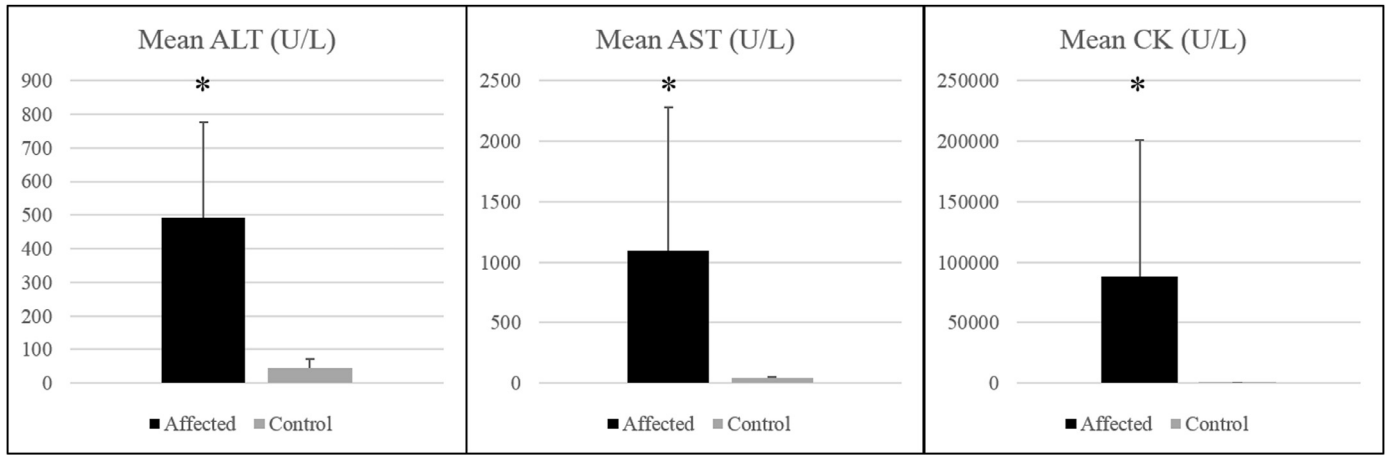


Fig. 6. Comparison of group mean terminal ALT, AST, and CK. The affected dogs had statistically significant increases in all three parameters (indicated by the asterisks; $p < 0.05$).

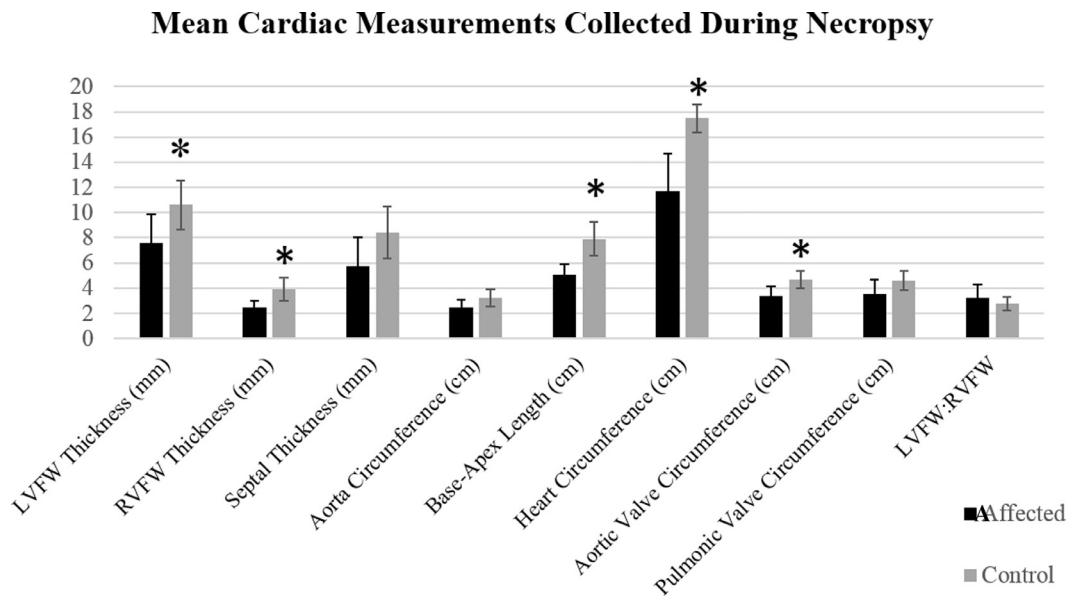


Fig. 7. Comparison of group mean cardiac measurements. The affected dogs had statistically significant decreases in LVFW thickness, RVFW thickness, base-apex length, heart circumference, and aortic valve circumference; $p < 0.05$.

(although it was only grossly appreciable in the affected dog that was euthanized at 100 days of age, following the 3-month MRI/MRS evaluation). In both dogs, the inflammatory infiltrate was limited to the cranial lung lobes, consistent with aspiration pneumonia.

For all study dogs, histopathologic evaluation of the right ventricular free wall (including papillary muscle), left ventricular free wall (including papillary muscle), interventricular septum, and aorta was unremarkable. However, in 1/7 (14.3%) of the affected dogs, there was a focal area of mineralization adjacent to the SA node in the right atrial epicardium and subjacent myocardium (Fig. 8D). This finding correlated with the clinical observation of a Mobitz type II second degree AV block.

With the exception of the above-mentioned changes in skeletal muscle, heart, and lung, all other microscopically

evaluated tissues/organs (as stated in the Materials and Methods) were histologically unremarkable.

4. Discussion

Spontaneous dystrophin-deficiency has been documented in various dog breeds. The resultant disease in dogs is known as canine X-linked muscular dystrophy or canine dystrophinopathy, to distinguish it from its human disease counterpart, Duchenne muscular dystrophy. Dog breeds with documented spontaneous dystrophin-deficiency include the Golden retriever (point mutation in intron 6) [36], Rottweiler (point mutation in exon 52) [37], Labrador retriever (insertion in intron 19) [30], miniature Poodle [38], Tibetan terrier (exon 8–29 deletion) [28], Pembroke Welsh corgi (repetitive element-1

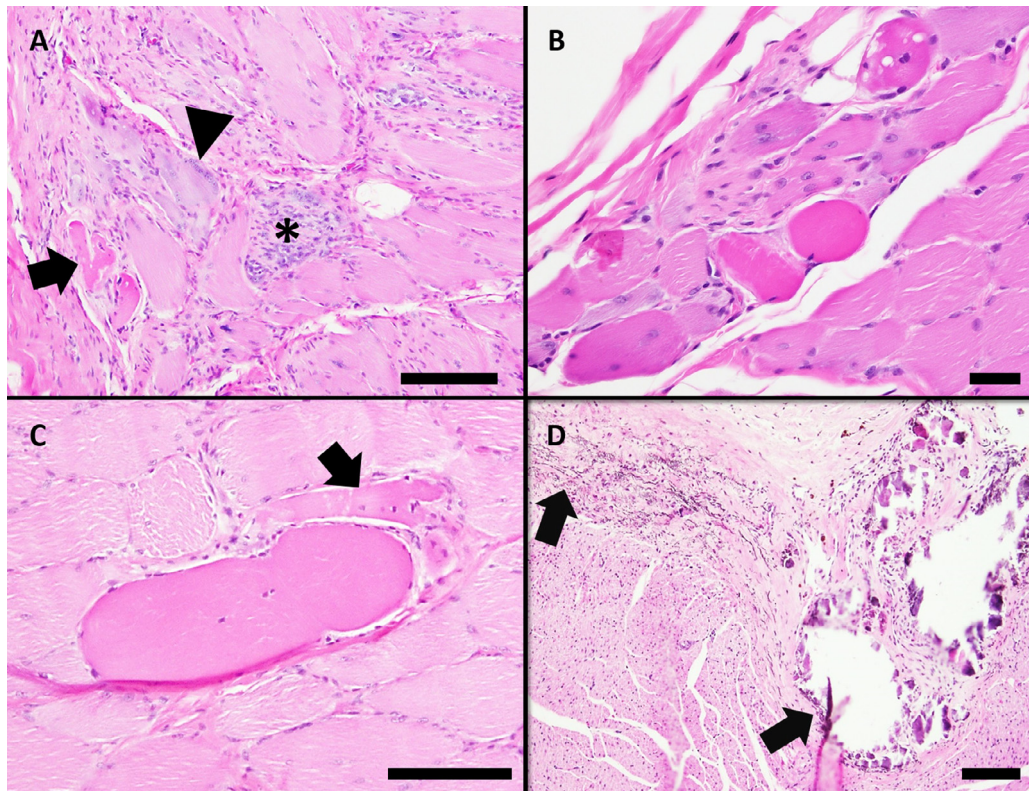


Fig. 8. A. Photomicrograph of a peripheral section of the diaphragm from an affected dog showing variation in myofiber size, myofiber regeneration (basophilia and nuclear rowing; arrowhead), lymphohistiocytic inflammation (asterisk), and necrosis (arrow). H&E. Bar=100 μ m. B. Photomicrograph of the biceps femoris from an affected dog showing variation in myofiber size and myofiber degeneration (hypereosinophilia and/or vacuolation). H&E. Bar=20 μ m. C. Photomicrograph of the triceps brachii from an affected dog showing myofiber degeneration (swelling and hypereosinophilia) and necrosis (arrow). H&E. Bar=100 μ m. D. Photomicrograph showing focal right atrial epicardial and myocardial mineralization (arrows) adjacent to the SA node in the affected dog with a Mobitz type II second degree AV block. H&E. Bar=100 μ m.

[LINE-1] insertion in intron 13) [39], and the Cocker spaniel (deletion in exon 65) [28].

Similar to what has been found in people, many of the reported canine dystrophin mutations are point mutations. In a recent study of DMD patients, point mutations accounted for 46% of all mutations in the studied cohort. The study also found that point mutations appeared to be randomly distributed across the dystrophin exons and were not found in hotspots [40].

Although mutations in exon 21 have not been previously reported in canine models of DMD, they have been noted in people with DMD. It is also interesting to note that in DMD patients, G: C > A: T transitions have been shown to be the most common stop mutation class, with the majority of these mutations being due to C > T transitions [40], similar to what we found in the Labradoodle model.

Dystrophin-deficiency in this line of Australian Labradoodles results in clinical signs that mimic those reported in other dystrophin-deficient dogs, including the well-studied Golden retriever model [28]. Like other dogs with dystrophin-deficiency, Labradoodles develop clinical signs shortly after birth, generally requiring extra care and nutritional management. In some instances, affected dogs die in the early post-natal period; often these that succumb extremely early

have already experienced stunted growth and are substantially smaller than their littermates. For all affected dogs used during the course of this study, stunted growth and weakness were evident by 4-weeks of age. Unlike what has been previously reported in other dystrophin-deficient dogs [28,41,42], the clinical course in the Labradoodle model is consistently very rapid, with weight loss, extensive skeletal muscular atrophy, difficulty ambulating, and moderate to severe dysphagia with ptyalism beginning by 4-months of age, necessitating study termination at 6-months of age. As mentioned, two of the affected dogs had such severe macroglossa that it resulted in oropharyngeal stenosis, making intubation during the MRI/MRS procedures extremely difficult.

Similar to what is seen in patients with DMD and other animal models of DMD, cardiac findings in the dystrophin-deficient Labradoodle vary between littermates and litters. Multifocal to coalescing, hyperechoic foci were observed in the left ventricular anterior and posterior papillary muscles in 1/7 affected dogs (14.3%). Differential diagnoses included areas of mineralization, fibrosis, and/or ischemia. There were no gross or histopathologic lesions correlating to these foci. Although hyperechoic foci in the left ventricular wall have been previously reported at later ages in both the GRMD and CXMD_J (Canine X-linked muscular dystrophy in Japan)

models, hyperechoic foci within the left ventricular papillary muscles have not been reported [43,44]. Similar hyperechoic papillary muscle foci, however, have been reported in the feline model of DMD by nine months of age [45]. In people with DMD, hyperechoic areas are most commonly seen in the posterior-basilar aspect of the left ventricle; however, they have not been reported exclusively within the left ventricular papillary muscles [46]. These findings likely indicate that early echocardiographic analyses in affected dogs are capable of detecting early ischemic damage of the papillary muscle that is not yet grossly or histologically evident.

Although LVIDd, LVIDs, LVEDV, and LVESV are often normalized to body weight to account for size variations between dog breeds, the presence of developmental cardiac defects, growth retardation in cardiac development, smaller overall cardiac size in the affected dogs, and extreme variations in growth rates observed between individual affected dogs and the affected dogs compared to the control dogs negated the use of quantitative normalization [29]. At the 3- and 6-month time points, affected dogs had significantly smaller mean values of LVIDd, LVIDs, LVEDV, and LVESV when compared to the control dogs. Volumetric indices of LVEDV and LVESV have also been reported to be significantly reduced in GRMD dogs at 6- and 12-months of age [47]. Interestingly, these two parameters are generally increased in patients with DMD [48] and greater LVESV has been associated with a greater risk of mortality [49]. In the present study, decreased values of LVIDd, LVIDs, LVEDV, and LVESV most likely resulted from significantly smaller hearts associated with developmental cardiac growth defects secondary to dystrophin-deficiency.

The presence of a Mobitz type II 2nd degree AV block in one of the affected dogs at 3-months of age is an intriguing finding in this animal model. Heart blocks occur when the electrical signal is slowed or disrupted as it moves through the heart. Second-degree heart blocks are characterized by atrioventricular electrical signals that are significantly slowed; as a result, the QRS complex doesn't always follow each P wave. Mobitz type II blocks are less common than type I, are generally more severe, and result from ischemic fibrosis in the AV node, causing a loss of electrical propagation to the ventricles [50]. In DMD patients, it is posited that fatty and fibrous tissue replacement of myocardium is the underlying cause of the AV block [51]. It is important to note that in the affected dog of the AV block, the right atrial myocardium subjacent to the SA node was infiltrated by multifocal areas of fibrous tissue with a focal area of mineralization. It is presumed that the disrupted AV electrical signals in this patient were resultant from this area of fibrosis.

Due to scheduling and early euthanasia (2 affected dogs; 100 and 113 days of age), only two study dogs had both the 3- and 6-month MRI/MRS evaluations (one control, one affected). In the normal human heart, the relative amount of PCr is nearly twice that of ATP in the ³¹P MR spectra, resembling the spectra of the control dogs in this study. In people with heart failure, the amount of PCr to ATP is greatly reduced due to decreased cardiac energy metabolism secondary

to altered myocardial high-energy phosphates [17,52]. In the current study, the diminished size of the affected dogs' hearts resulted in poor, highly variable MRS that had low signal-to-noise ratios. These spectra were therefore difficult to analyze, and although the diminished PCr peak relative to ATP resembled ³¹P MR spectra expected in people with heart failure [52], there were no statistically significant differences in PCr/ATP at either the 3-month or 6-month time points. The lack of statistically significant differences in PCr/ATP was likely resultant from the small sample size, genetic heterogeneity of study dogs, and possibly high coefficient of variation of MRS analysis. Further evaluation of PCr/ATP ratios in this animal model is warranted.

Significant elevations in ALT, AST, and CK are to be expected with any severe myopathy. Although ALT is a cytosolic enzyme that is considered to be fairly liver-specific in dogs, it has been noted to be elevated with various myopathies, including dystrophin-deficiency. AST, however, is present in most cell types, although muscle and liver are the major sources. Therefore, like ALT, AST is often elevated with severe muscular damage. CK is also a cytosolic enzyme that is present in multiple tissue types as different isozymes: nervous tissue and viscera (CK-BB), cardiac muscle (CK-MB), and skeletal and cardiac muscle (CK-MM). Because it is predominantly found in muscle, elevations in CK fairly reliably indicate muscular damage [53]. It is perhaps the most commonly analyzed serum enzyme in individuals with myopathies and has been shown to be dramatically elevated in other canine models of DMD [42,47] and in patients with DMD [54,55].

Gross and histopathologic findings were consistent with the clinical observations and were similar to findings reported in other dystrophin-deficient dog breeds including the Golden retriever [41,56], the Pembroke Welsh corgi [39], and CXMDJ beagles [42]. All affected Labradoodles had a grossly unremarkable heart and lacked microscopic cardiac changes as previously reported in dystrophin-deficient dogs (i.e. degeneration, necrosis, and fibrosis) [39,57–59]. The lack of these microscopic lesions does not preclude abnormal cardiac functionality in this model, but rather indicates that histologically discernable changes may have not yet occurred in such a young dog. We did, however, find a focal area of mineralization adjacent to the SA node in the affected dog with a Mobitz type II second degree AV block. In DMD patients, myocardial fibrosis and fatty infiltration are thought to cause AV blocks [51]; however, we posit that localized cardiac mineralization in this patient may have similarly disrupted myocardial conduction.

In summary, we have identified a novel mutation in exon 21 of dystrophin in a line of Australian Labradoodles. Affected Labradoodles rapidly develop clinical signs, have progressive clinical decline, and have gross lesions that resemble those reported in other dystrophin-deficient dog breeds. Histologically, skeletal muscle changes are similar to those observed in other dystrophin-deficient dog breeds and mirror those described in DMD patients. Although this animal model is difficult to maintain, with the majority of the dogs having

progressive clinical deterioration by 6-months of age, echocardiographic and electrocardiographic findings suggest that features of Labrador dystrophinopathy-related cardiomyopathy resemble DMD-related cardiomyopathy and warrant additional study.

Declarations of interest

None.

Acknowledgments

The authors would like to acknowledge Stephen Waters, Richard Rathbun, Ronald Beyers, Xiaoxia Zhang, and Atoska Gentry for their assistance throughout the course of the study.

Supplementary materials

Supplementary material associated with this article can be found, in the online version, at doi:10.1016/j.nmd.2018.08.008.

References

- Holland A, Carberry S, Ohlendieck K. Proteomics of the dystrophin-glycoprotein complex and dystrophinopathy. *Curr Protein Pept Sci* 2013;14(8):680–97.
- Hoffman E, Brown R, Kunkel L. Dystrophin: the protein product of the Duchenne muscular dystrophy locus. *Cell* 1987;51(6):919–28.
- Simonds A. Respiratory complications of the muscular dystrophies. *Semin Respir Crit Care Med* 2002;23(3):321–8.
- Wagner KR, Lechtzin N, Judge DP. Current treatment of adult Duchenne muscular dystrophy. *Biochim Biophys Acta* 2007;1772:229–37.
- Eagle M, Baudouin S, Chandler C, Giddings D, Bullock R, Bushby K. Survival in Duchenne muscular dystrophy: improvements in life expectancy since 1967 and the impact of home nocturnal ventilation. *Neuromuscul Disord* 2002;12(10):926–9.
- Moriuchi T, Kagawa N, Mukoyama M, Hizawa K. Autopsy analyses of the muscular dystrophies. *Tokushima J Exp Med* 1993;40(1–2):83–93.
- Passamano L, Taglia A, Palladino A, Viggiano E, D'Ambrosio P, Scutifero M, et al. Improvement of survival in Duchenne muscular dystrophy: retrospective analysis of 835 patients. *Acta Myol* 2012;XXXI:121–5.
- Ciafaloni E, Fox D, Pandya S, Westfield C, Puzhankara S, Romitti P, et al. Delayed diagnosis in Duchenne muscular dystrophy: data from the muscular dystrophy surveillance, tracking, and research network (MD STARnet). *J Pediatr* 2009;155:380–5.
- MDA Duchenne Muscular Dystrophy (DMD): muscular dystrophy association. Available from: <http://mda.org/disease/duchenne-muscular-dystrophy/signs-and-symptoms>; 2014.
- Deconinck N, Bernard D. Pathophysiology of Duchenne muscular dystrophy: current hypotheses. *Pediatr Neurol* 2007;36:1–7.
- Verhaert D, Richards K, Rafael-Fortney J, Raman S. Cardiac involvement in patients with muscular dystrophies: magnetic resonance imaging phenotype and genotypic considerations. *Circ Cardiovasc Imaging* 2011;4(1):67–76.
- Connuck D, Sleeper L, Colan S, Cox G, Jowbin J, Lowe A. Characteristics and outcomes of cardiomyopathy in children with Duchenne or becker muscular dystrophy: a comparative study from the pediatric cardiomyopathy registry. *Am Heart J* 2008;155:998–1005.
- Sanyal SK, Johnson WW. Cardiac conduction abnormalities in children with Duchenne's progressive muscular dystrophy: electrocardiographic features and morphologic correlates. *Circulation* 1982;66:853–63.
- Yanagisawa A, Miyagawa M, Yotsukura M, Tsuya T. The prevalence and prognostic significance of arrhythmias in Duchenne type muscular dystrophy. *Am Heart J* 1992;124:1244–50.
- Perloff J. Cardiac rhythm and conduction in Duchenne's muscular dystrophy: a prospective study of 20 patients. *J Am Coll Cardiol* 1984;3:1263–8.
- Brunklaus E, Parish E, Muntoni F, Scuplak S. The value of cardiac MRI versus echocardiography in the pre-operative assessment of patients with Duchenne muscular dystrophy. *Eur J Paediatr Neurol* 2015;19:395–401.
- Hove MT, Neubauer S. Evaluating metabolic changes in heart disease by magnetic resonance spectroscopy. *Heart Metab* 2006;32:18–21.
- Crilley J, Boehm E, Rajagopalan B, Blamire A, Styles P, Muntoni F. Magnetic resonance spectroscopy evidence of abnormal cardiac energetics in Xp21 muscular dystrophy. *J Am Coll Cardiol* 2000;36:1953–8.
- Spurney C, Knoblach S, Pistilli E, Nagaraju K, Martin G, Hoffman E. Dystrophin-deficient cardiomyopathy in mouse: expression of Nox4 and Lox are associated with fibrosis and altered functional parameter in the heart. *Neuromuscul Disord* 2008;18(5):371–81.
- Sicinski P, Geng Y, Ryder-Cook A, Barnard E, Darlison M, Barnard P. The molecular basis of muscular dystrophy in the mdx mouse: a point mutation. *Science* 1989;244(4912):1578–80.
- Collins C, Morgan J. Duchenne's muscular dystrophy: animal models used to investigate pathogenesis and develop therapeutic strategies. *Int J Exp Pathol* 2003;84(4):165–72.
- Lefaucheur J, Pastoret C, Sebillé A. Phenotype of dystrophinopathy in old mdx mice. *Anat Rec* 1995;242(1):70–6.
- Bostick B, Yue Y, Long C, Duan D. Prevention of Dystrophin-deficient cardiomyopathy in twenty-one-month-old carrier mice by mosaic dystrophin expression or complementary dystrophin/utrophin expression. *Circ Res* 2008;102(1):121–30.
- Bostick B, Yue Y, Duan D. Gender influences cardiac function in the mdx model of Duchenne cardiomyopathy. *Muscle Nerve* 2010;42(4):600–3.
- Cooper B, Winand N, Stedman H, Valentine B, Hoffman E, Kunkel L, et al. The homologue of the Duchenne locus is defective in X-linked muscular dystrophy of dogs. *Nature* 1988;334(6178):154–6.
- Sharp N, Kornegay J, Camp SV. An error in dystrophin mRNA processing in golden retriever muscular dystrophy, an animal homologue of Duchenne muscular dystrophy. *Genomics* 1991;13:115–21.
- Schatzberg S, Anderson L, Wilton S, Kornegay J, Mann C, Solomon G, et al. Alternative dystrophin gene transcripts in golden retriever muscular dystrophy. *Muscle Nerve* 1998;21(8):991–8.
- Kornegay J, Bogan J, Bogan D, Childers M, Li J, Nghiem P, et al. Canine models of Duchenne muscular dystrophy and their use in therapeutic strategies. *Mamm Genome* 2012;23(1–2):85–108.
- Mazur W, Hor KN, Germann JT, Fleck RJ, Al-Khalidi HR, Wansapura JP, et al. Patterns of left ventricular remodeling in patients with Duchenne muscular dystrophy: a cardiac MRI study of ventricular geometry, global function, and strain. *Int J Card Imaging* 2012;28:99–107.
- Smith B, Kornegay J, Duan D. Independent canine models of Duchenne muscular dystrophy due to intronic insertions of repetitive DNA. *Mol Ther* 2007;15(Suppl 1):S51.
- Boon J. *Veterinary echocardiography*. 2nd ed. West Sussex, UK: John Wiley & Sons; 2011.
- Rodgers C, Clarke W, Snyder C, Vaughan J, Neubauer S, Robson M. Human cardiac 31P magnetic resonance spectroscopy at 7 Tesla. *Magn Reson Med* 2014;72:304–15.
- Vanhamme L, Huffel SV, Hecke PV, Dv Ormondt. Time-domain quantification of series of biomedical magnetic resonance spectroscopy signals. *J Magn Reson* 1999;140(120-130).
- Piao Y, Liu Y, Xie X. Change trends of organ weight background data in Sprague Dawley rats at different ages. *J Toxicol Pathol* 2013;26(1):29–34.
- Frame S, Mann P. Principles of pathology for toxicology studies. In: Hayes A, editor. Principles and methods of toxicology. 5th ed. Boca Raton: CRC Press; 2008. p. 604.
- Sharp N, Kornegay J, Camp SV, Herbstreith M, Secore S, Kettle S, et al. An error in dystrophin mRNA processing in golden retriever mus-

- cular dystrophy, an animal homologue of Duchenne muscular dystrophy. *Genomics* 1992;13(1):115–21.
- [37] Winand N, Pradham D, Cooper B. Molecular characterization of severe Duchenne-type muscular dystrophy in a family of Rottweiler dogs. In: *Proceedings of the muscular dystrophin association: molecular mechanisms of neuromuscular disease*; 1994.
- [38] Sanchez L, Beltran E, deStefani A, Guo L, Shea A, Shelton G, et al. Clinical and genetic characterisation of dystrophin-deficient muscular dystrophy in a family of miniature poodle dogs. *Plos One* 2018;13(2):e0193372.
- [39] Smith B, Yue Y, Woods P, Kornegay J, Shin J, Williams R, et al. An intronic LINE-1 element insertion in the dystrophin gene aborts dystrophin expression and results in Duchenne-like muscular dystrophy in the Corgi breed. *Lab Invest* 2011;91(2):216–31.
- [40] Flanigan K, Dunn D, von Niederhausern A, Soltanzadeh P, Gappmaier E, Howard M, et al. Mutational spectrum of DMD mutations in dystrophinopathy patients: application of modern diagnostic techniques to a large cohort. *Hum Mutat* 2009;30(12):1657–66.
- [41] Valentine B, Cooper B, Lahunta Ad, O'Quinn R, Blue J. Canine X-linked muscular dystrophy. An animal model of Duchenne muscular dystrophy: clinical studies. *J Neurol Sci* 1988;88(1-3):69–81.
- [42] Shimatsu Y, Katagiri K, Furuta T, Nakura M, Tanioka Y, Yuasa K, et al. Canine X-linked muscular dystrophy in Japan (CXMDJ). *Exp Anim* 2003;52(2):93–7.
- [43] Yugeta N, Urasawa N, Fujii Y, Yoshimura M, Yuasa K, Wada M. Cardiac involvement in Beagle-based canine X-linked muscular dystrophy in Japan (CXMDJ): electrocardiographic, echocardiographic, and morphologic studies. *BMC Cardiovasc Disord* 2006;6:47.
- [44] Moise N, Valentine B, Brown C, Erb H, Beck K, Cooper B. Duchenne's cardiomyopathy in a canine model: electrocardiographic and echocardiographic studies. *J Am Coll Cardiol* 1991;17:812–20.
- [45] Gaschen L, Lang J, Lin S, Ade-Damilano M, Busato A, Lombard C, et al. Cardiomyopathy in dystrophin-deficient hypertrophic feline muscular dystrophy. *J Vet Intern Med* 1999;13(4):346–56.
- [46] Caplan L, Hurst J, Chimowitz M. Cardiac and cardiovascular findings in patients with nervous system diseases. *Clinical neurocardiology, fundamentals and clinical cardiology*. 1st ed. Boca Raton: CRC Press; 1999. p. 372.
- [47] Fine D, Shin J, Yue Y, Volkmann D, Leach S, Smith B, et al. Age-matched comparison reveals early electrocardiography and echocardiography changes in dystrophin-deficient dogs. *Neuromuscul Disord* 2011;21(7):453–61.
- [48] Mertens L, Ganame J, Claus P, Goemans N, Thijs D, Eyskens B. Early regional myocardial dysfunction in young patients with Duchenne muscular dystrophy. *J Am Soc Echocardiogr* 2008;21:1049–54.
- [49] Menon S, Ehteridge S, Liesemer K, Williams R, Bardsley T, Heywood M. Predictive value of myocardial delayed enhancement in Duchenne muscular dystrophy. *Pediatr Cardiol* 2014;35:1279–85.
- [50] Health NIo Types of heart block2012 February 12. Available from: <https://www.nhlbi.nih.gov/health/health-topics/topics/hb/types>; 2017.
- [51] Bies R, Friedman D, Roberts P, Perryman M, Caskey C. Expression and localization of the dystrophin in human cardiac Purkinje fibers. *Circulation* 1992;86:147–53.
- [52] Ingwall J, Weiss R. Is the failing heart energy starved? *Circ Res* 2004;95:135–45.
- [53] Hall R, Bender H. Muscle. In: Latimer K, editor. *Duncan & Prasse's veterinary laboratory medicine: clinical pathology*. 5th ed. Ames: Wiley-Blackwell; 2011. p. 283–7.
- [54] Burch PM, Pogoryelova O, Goldstein R, Bennett D, Guglieri M, Straub V, et al. Muscle-derived proteins as serum biomarkers for monitoring disease progression in three forms of muscular dystrophy. *J Neuromuscul Dis* 2015;2(3):241–55.
- [55] Sun S, Peng Y, He J. Changes of serum creatine kinase levels in children with Duchenne muscular dystrophy. *Zhongguo Dang Dai Er Ke Za Zhi* 2008;10(1):35–7.
- [56] Kornegay JN. The golden retriever model of Duchenne muscular dystrophy. *Skelet Muscle* 2017;7(9):1–22.
- [57] Valentine B, Cooper B, Cummings J, Ad Lahunta. Canine X-linked muscular dystrophy: morphologic lesions. *J Neurol Sci* 1990;97(1):1–23.
- [58] Valentine B, Cooper B, Cummings J, Lahunta Ad. A progressive muscular dystrophy in a golden retriever dog: light microscope and ultrastructural features at 4 and 8 months. *Acta Neuropathol* 1986;71:301–10.
- [59] Valentine B, Cummings J, Cooper B. Development of Duchenne-type cardiomyopathy. Morphologic studies in a canine model. *Am J Pathol* 1989;135:671–8.

Chapter 3: Cardiac transcriptome analysis identifies differentially expressed genes in Australian
Labradoodle dystrophinopathy

Cardiac Transcriptome Analysis Identifies Differentially Expressed Genes in Australian Labradoodle Dystrophinopathy

Submitted to Journal of Neuromuscular Diseases

Stephanie M. Shrader ^a, Nripesh Prasad ^b, Bruce F. Smith ^{a,c}

^a Department of Pathobiology, Auburn University College of Veterinary Medicine, Auburn, AL 36849, USA.

^b Genomic Services Laboratory, Hudson Alpha Institute for Biotechnology, Huntsville, AL 35806, USA.

^c Scott-Ritchey Research Center, Auburn University College of Veterinary Medicine, Auburn, AL 36849, USA.

Correspondence: Correspondence to Dr. Stephanie Shrader: Department of Pathobiology, Auburn University College of Veterinary Medicine, Auburn, AL 36849, USA. Phone: 334-844-4539. E-mail: sms0059@tigermail.auburn.edu.

Running Title: Dystrophinopathic Labradoodle Transcriptome

Abstract

Background: In people, Duchenne muscular dystrophy (DMD) is an X-linked recessive disorder caused by mutations in the *DMD* gene. The resultant disease phenotype is associated with progressive skeletal and cardiac muscle pathology and cardiomyopathy-associated mortality. We previously identified the dystrophin-deficient Australian Labradoodle as a novel animal model for the study of DMD-related cardiomyopathy. Objective: To evaluate the cardiac transcriptome in affected dogs in order to elucidate potential regulators of cardiomyopathy. Methods: Left ventricular myocardial samples from seven dystrophin-deficient and five control (normal) male littermates were included in the analyses, which were performed at the HudsonAlpha Genomic Services Laboratory. Results: Sequencing found 29,740 gene transcripts expressed in the ventricular myocardium samples; of these, there was a statistically significant difference ($p < 0.05$) and a \log_2 -fold change higher than 1.5 between affected and control dogs in 1267 transcripts. Differential expression patterns from affected dogs were generally distinct from controls, similar across affected vs. control dogs with a high correlation between samples, and suggestive of possible roles in processes such as cardiac oxidative stress, apoptosis, and contractility. Conclusions: These findings are significant because they could represent future therapeutic targets to aid in the treatment of Duchenne muscular dystrophy-associated cardiac disease.

Keywords: Dystrophin, Cardiomyopathies, Dogs, Transcriptome

1. Introduction

Duchenne muscular dystrophy, an X-linked recessive disorder, is recognized as the most common muscular dystrophy to arise in childhood with a birth prevalence ranging from 15.9 to 19.5 per 100,000 live births [1]. It is caused by mutations in the *DMD* gene and results in a well-documented spectrum of muscle pathology, clinical signs, and symptoms. Often, the first symptoms (e.g., difficulty rising from a seated position, delays in motor skill development, difficulty climbing stairs) are noted by 5 years of age with loss of ambulation and wheel chair dependence occurring by 12 years of age [2]. Death in affected individuals has traditionally been attributed to respiratory failure; however, improvements in ventilatory care over the last two decades has resulted in an increasingly high burden of cardiomyopathy in DMD patients. DMD-associated cardiomyopathy is characterized by ventricular dysfunction, attributable to cardiomyocyte hypertrophy, atrophy, and fibrosis; these changes ultimately result in chronic heart failure, arrhythmias, and conduction anomalies. Life expectancy now ranges from 30-40 years of age with intensive ventilatory support, heart medications, and advancements in cardiac monitoring [2, 3].

A recent retrospective study of 43 DMD patients found that all patients within the cohort developed a cardiomyopathy and most were being treated with angiotensin-converting enzyme (ACE) inhibitors and steroids. The study also found that poor prognostic factors for survival included lower body mass index (BMI), lower alanine aminotransferase (ALT) levels, decreased maximum inspiratory pressures, and elevated cardiac biomarkers (e.g., N-terminal pro-brain natriuretic peptide [NT-pro-BNP]) [4]. Because cardiac-related deaths are reported to occur in approximately 20-30% of DMD patients [5, 6], DMD-related cardiomyopathy is an active area

of research that includes evaluation and development of various animal models, therapeutic interventions, and cardiac diagnostic technologies.

We recently identified a novel dystrophinopathy in a line of Australian Labradoodles that results in skeletal and cardiac muscle changes similar to those observed in people with DMD [7]. The founding male of this line died suddenly at 6-months of age from presumptive cardiac disease and subsequent males in this lineage have consistently developed a rapidly progressive clinical course with weight loss, skeletal muscle atrophy, ambulatory difficulties, and dysphagia by 6-months of age. Echocardiographic abnormalities in affected dogs have included hyperechoic foci in the left ventricular papillary muscles, septal hypokinesis, and decreased left ventricular systolic and diastolic volume and internal diameter. One of the affected dogs also had a Mobitz type II second-degree atrioventricular (AV) block and mineralization associated with the sinoatrial (SA) node [7]. Because dystrophin-deficient Labradoodles have cardiac-related findings that resemble those observed in DMD-related cardiomyopathy, the purpose of this current study was to evaluate the cardiac transcriptome in affected dogs and their unaffected (normal) control male littermates in order to better understand the development of dystrophinopathy-associated cardiomyopathy. Over the last decade, cardiac transcriptome analysis has gained favor in human medicine and animal model research because of its potential to identify biomarkers of cardiac disease and to gain insights into the mechanisms and pathophysiology of heart diseases and heart failure [8-10].

We hypothesized that in addition to altered dystrophin expression, other cardiac genes would have altered expression profiles and that these may contribute to the cardiac disease phenotype in the Australian Labradoodle model of DMD. Cardiac transcriptome analysis found 29,740 gene transcripts expressed in the ventricular myocardial samples; of these, there was a

statistically significant difference ($p < 0.05$) and a \log_2 -fold change higher than 1.5 between affected and control dogs in 1267 transcripts. Many of the top ten most up-regulated and down-regulated genes from this cohort have important roles in cardiac stress response, tissue remodeling, and inflammation. Knowledge of such gene expression variations gives researchers greater insight into disease pathogenesis and progression and could help guide development of therapeutic interventions for DMD patients with cardiomyopathy.

2. Materials and Methods

All animal experiments were approved by the Institutional Animal Care and Use Committee of Auburn University. A 3-month old male Australian Labradoodle was referred to the Auburn University College of Veterinary Medicine due to skeletal muscle atrophy and exercise intolerance, consistent with a potential muscular dystrophy. Skeletal muscle mRNA sequencing found a novel C to T transition at position 2668 of the dystrophin open reading frame (nonsense mutation resulting in a TGA stop codon) [7]. This dog was then used to establish a breeding colony of carrier females at the Scott Ritchey Research Center (SRRC) at Auburn University. Several related carrier females were utilized during the course of the study; selected females were vaginally inseminated with semen from a normal Australian Labradoodle, a normal Labrador retriever, or a dystrophin-deficient Australian Labradoodle (selection of males was dependent upon availability). The resultant progeny included seven dystrophin-deficient and five control (normal) male littermates (female offspring were not included in study-related procedures/analyses). The dystrophin genotype was determined for each dog via DNA sequencing, performed on whole blood submitted to Eurofins Genomics (12701 Plantside Drive, Louisville, KY 40299, USA). All male offspring included in the study were humanely

euthanized at 6 months of age (or earlier if a humane endpoint was reached). The terminal endpoint was decided upon due to sudden death of the founding male at 6-mos of age (suspected to have been cardiac-related) and rapid clinical decline in other males of his lineage beginning at 4-mos of age (e.g., weakness, dysphagia, difficulty or inability to rise and/or ambulate). Clinical signs in the dystrophin-deficient cohort used for this study included poor weight gain and weight loss, gait abnormalities, exercise intolerance, skeletal muscle atrophy, macroglossa, ptyalism, dysphagia, kyphosis, and a plantigrade stance.

Due to the presence of echocardiographic, electrocardiographic, and histopathological cardiac abnormalities in the affected dogs (previously reported) [7], transcriptome sequencing was performed on left ventricular myocardium from each dog (sampled and snap frozen using liquid nitrogen during post-mortem examination). For each cardiac sample, total RNA was isolated by using TRIzol™ reagent (Invitrogen, Carlsbad, CA) following the manufacturer's protocol and submitted to the HudsonAlpha Genomic Services Laboratory (GSL; HudsonAlpha Institute for Biotechnology, Huntsville, AL) for library preparation, RNA sequencing, and descriptive analyses. The concentration and integrity of the extracted total RNA were estimated using the Qubit® 2.0 Fluorometer (Invitrogen) and Agilent 2100 Bioanalyzer (Applied Biosystems, Carlsbad, CA, USA), respectively. Five hundred nanograms of total RNA was required for downstream RNA-seq applications. Polyadenylated RNAs were isolated using NEBNext Magnetic Oligo d(T)25 Beads. The NEBNext mRNA Library Prep Reagent Set for Illumina (New England BioLabs Inc., Ipswich, MA, USA) was then used to prepare individually bar-coded next-generation sequencing expression libraries as per manufacturer's recommended protocol. Library quality was assessed using the Qubit 2.0 Fluorometer, and the library concentration was estimated by utilizing a DNA HS Chip on a Caliper Gx. Accurate

quantification for sequencing applications was determined using the qPCR-based KAPA Biosystems Library Quantification Kit (Kapa Biosystems, Inc., Woburn, MA, USA). Each library was diluted to a final concentration of 12.5 nM and pooled in an equimolar ratio prior to clustering. Paired-end sequencing (75bp, paired-end reads) was performed using an Illumina NextSeq 550 sequencer (Illumina, Inc., San Diego, CA, USA).

Post-processing of the sequencing reads from RNA-seq experiments for each sample was performed using HudsonAlpha's unique in-house RNA-seq data analysis pipeline. Briefly, quality control checks on raw sequence data for each sample were performed using FastQC (Babraham Bioinformatics, Cambridge, UK). Raw reads imported to the commercial data analysis platform AvadisNGS (Strand Scientifics, CA, USA) and were mapped to the reference canFam3. After quality inspection, the aligned reads were filtered on the basis of read quality metrics; reads with a base quality score of less than 30, alignment score of less than 95, and mapping quality of less than 40 were removed. Remaining reads were then filtered on the basis of their read statistics; missing mates, translocated, unaligned, and flipped reads were removed. The reads list was then filtered to remove duplicates. Samples were grouped and transcript abundance was quantified for this final read list using Trimmed Means of M-values (TMM) as the normalization method. Output data utilized for all subsequent comparisons were summarized as normalized signal values generated by AvadisNGS. Differential expression of genes was calculated on the basis of \log_2 -fold change (FC; using the default cut-off $\geq \pm 1.5$) observed in comparisons between defined conditions, and the p-value of the differentially expressed gene list was estimated by ANOVA using Benjamini Hochberg corrections of 0.05 for false-discovery rate.

3. Results

RNA sequencing found 29,740 genes expressed in the ventricular myocardial samples. Cardiac gene expression patterns from dystrophin-deficient male Australian Labradoodles were generally distinct from those seen in littermate controls, and similar across affected vs. control dogs, as observed in the principal component analysis (PCA; Figure 1) and Spearman correlation analysis (Figure 2). The correlation between all samples was very high (>0.95).

When using $p < 0.05$ and a \log_2 -fold change higher than 1.5 as cut-off, there were 1267 differentially expressed genes (DEGs; Figure 3). There was statistically significant down-regulation of the *DMD* gene transcript in the dystrophin-deficient dogs (-4.89 FC; p -value < 0.0001) but no statistically significant ($p < 0.05$) or remarkable (FC > 1.5) differences in expression of the other members of the dystrophin-associated glycoprotein complex; however, compared to controls, there was down-regulation in *AGRN* (-1.3 FC), *DAG1* (-1.1 FC), and *SGCA* (-1.5 FC). Due to their importance in cardiovascular disease, differential expression of genes associated with oxidative stress, apoptosis, and contractility were also evaluated (Figure 4). The top 10 up- and down-regulated gene transcripts are shown in Table 1 and discussed below.

4. Discussion

Top 10 up-regulated gene transcripts

The gene transcript with the greatest up-regulation was BDNF (Brain-derived neurotrophic factor) with 14.67 FC in expression in affected dogs compared to controls. Similar upregulation has been found in cardiac tissue from dogs with GRMD (Golden retriever muscular dystrophy). Additionally, circulating levels of BDNF in people with DMD has been shown to

inversely correlate with ventricular function and fibrosis [11]. BDNF has well-described roles in nervous system growth, survival, and regenerative responses, but more recent research has also shown that it has important roles in cardiovascular system development, angiogenesis, and cardiac contractility [12, 13]. Both BDNF and its receptor, TrkB, are expressed in coronary artery endothelial cells and are associated with capillary and cardiac endothelium development during late gestation [13, 14]. Studies of ischemic myocardial injury have shown that BDNF acts as a myocardial protectant, increasing factors that promote cardiomyocyte survival and stimulating angiogenesis to reduce cardiac remodeling [15]. These cardio-protective mechanisms involve survival signaling pathways that include vascular endothelial growth factor (VEGF) [15], protein kinase B (Akt) [16], transient receptor potential canonical (TRPC)3/6 channels, and macrophage activation [17]. In this study, elevated cardiac expression levels of *BDNF* in the affected dogs is considered secondary to dystrophinopathy-related cardiac damage as a compensatory response to stimulate cardiomyocyte viability and decrease fibrosis.

MYL4 (Myosin Light Chain 4; also known as Atrial Light Chain 1 [ALC1]) had the 2nd-highest level of transcript up-regulation at 14.23 FC above controls. *MYL4* encodes a myosin light chain that is usually expressed in the atria following birth; however, it can also be re-expressed in the ventricular myocardium in response to ventricular pathology [18]. This protein functions to regulate cross-bridge cycling kinetics which in turn regulates cardiac contractility [19, 20]. Because expression of *MYL4* improves contractility, its re-expression is thought to be part of the adaptive response that occurs during cardiac hypertrophy. It's re-expression in the affected dogs in this study is consistent with early subclinical dystrophinopathy-associated cardiac damage.

PENK (Proenkephalin) had the 3rd-highest level of transcript up-regulation at 10.72 FC above controls. *PENK* encodes a preproprotein that is proteolytically processed to generate multiple protein products known as enkephalins. Enkephalins are opioid peptides that are found in various tissues, with the highest levels of expression in tissues of the nervous and endocrine systems. These proteins activate G protein-coupled receptors (GPCRs) in the central and autonomic nervous system as a means to modulate thermoregulation, pain perception, respiratory rate, heart rate, and blood pressure. In the heart, myocardial expression of *PENK* results in a polypeptide precursor, which can undergo post-translational modifications to yield various protein products, including the pentapeptides Met- and Leu-enkephalin, the heptapeptide MEAP, the octapeptide Met-enkephalin-Arg⁶-Gly⁷-Leu⁸, the analogs amidorphin and metorphamide, and other larger peptides [21, 22]. Research has found that PENK expression levels are greater in the left vs. right ventricle and elevated PENK mRNA levels occur in the hearts of hamsters with hypertrophic cardiomyopathy [23-25]. Data from studies in various animal models suggest that enkephalin production and release from the heart is associated with cardioprotection and results from periods of ischemia and hemodynamic loads associated with cardiac hypertrophy [24, 26]. Elevated *PENK* expression levels in the hearts of dystrophin-deficient Labradoodles likely represent compensatory cardioprotection secondary to dystrophinopathy-induced cardiomyocyte injury.

BSPRY (B-Box and SPRY Domain Containing) had the 4th-highest level of transcript up-regulation at 10.05 FC above controls. The BSPRY protein is known to interact with TRPV5 (Transient receptor potential cation channel subfamily V member 5) and TRPV6 and is therefore suspected to play a role in epithelial calcium transport in the kidney and intestine [27]. It has also been found to have possible roles in immunoregulation. For example, BSPRY is up-regulated in

human T helper cell differentiation [28] and murine CD8⁺ tumor infiltrating lymphocytes in a transplantable colon carcinoma model [29]. In the normal human heart, there is little to no BSPRY RNA or protein expression [13, 30] and its role in cardiac disease has not been described. Based on these roles, upregulation in dystrophin-deficient Labradoodles may be resultant from immunoregulatory functions secondary to myocardial damage.

PRR32 (Proline Rich 32) had the 5th-highest level of transcript up-regulation at 10.00 FC above controls. The *PRR32* gene is known to be highly conserved across various species (including dogs, cows, mice, rats, chimpanzees, and Rhesus macaques); however, the function of the resultant protein product is not well understood. RNA sequencing of human tissues has found that the greatest expression of *PRR32* occurs in the heart, brain (cerebellum), and skeletal muscle (in order of descending expression levels) [26]. *PRR32* is one of 50 genes known to be overexpressed in patients with Amyotrophic Lateral Sclerosis (ALS; a progressive neurodegenerative disease). Though *PRR32*'s exact role in ALS disease progression is unknown, it is interesting to note that many ALS patients have subclinical cardiac deficits and cardiac-related death in later stages of disease. Affected patients have structural myocardial defects (discernible via cardiac magnetic resonance imaging) which may be attributable to sympathetic dysfunction [31]. *PRR32*'s potential role in the manifestation and progression of cardiac disease in dystrophin-deficient Labradoodles remains undetermined.

NPPA (Natriuretic Peptide A) had the 6th-highest level of transcript up-regulation at 9.93 FC above controls. *NPAA* encodes for an atrial natriuretic peptide (ANP), an endogenous peptide hormone. It is predominantly expressed by cardiomyocytes during embryo-fetal development and has greatly reduced expression in the ventricles following birth. However, following cardiac stress (i.e. ischemia and hypertrophy), *NPPA* is upregulated in the ventricular myocardium [32]

and plays a role in the maintenance of blood pressure homeostasis.[33] NPAA may be playing a similar role in dystrophin-deficient hearts.

LOC490471 (homolog of human SLC41A2; Solute Carrier Family 41 Member 2) had the 7th-highest level of transcript up-regulation at 9.75 FC above controls. Studies have indicated that in people, SLC41A2 acts as a Mg²⁺ transporter involved in magnesium homeostasis in renal epithelial cells [34]. Analysis has also found low levels of SLC41A2 RNA expression in the human heart [35]; however, it's functional role in this tissue has not been evaluated. Therefore, its role in Australian Labradoodle dystrophinopathy-associated cardiomyopathy remains undetermined.

LYZF2 (Lysozyme F2) had the 8th-highest level of transcript up-regulation at 8.88 FC above controls. Lysozyme is a conserved antimicrobial enzyme that plays a critical role in host defenses against Gram-positive and Gram-negative bacteria [36]. In mammals, lysozyme is found on mucosal surfaces, in the blood and liver, in various secretions (predominantly tears, urine, saliva, and milk), and in phagocytic cells (macrophages, neutrophils, and dendritic cells) [37]. Though lysozyme has been identified as a potential biomarker in patients with atheromatous cardiovascular disease (related to the presence of macrophages within atheromatous plaques) [38], its function in other, non-septic, cardiovascular diseases has not been established; therefore, its role in dystrophinopathy-associated cardiomyopathy is undetermined.

CDH10 (Cadherin 10) had the 9th-highest level of transcript up-regulation at 7.61 FC above controls. This gene encodes a type II classical cadherin. Alternative splicing results in multiple transcript variants that are integral membrane proteins with roles in calcium-dependent cell-cell adhesion, intracellular signaling, neural tube regionalization, neuronal migration, gray

matter differentiation, neural circuit formation, spine morphology, synapse formation, and synapse remodeling [30, 39, 40]. Diseases associated with alterations in *CDH10* expression include autism spectrum disorders, schizophrenia, bipolar disorder, major depressive disorder, and fetal ventricular septal defect associated with a familial 5p14.3-p14.1 deletion [40]. *CDH10*'s potential role in dystrophinopathy-associated cardiomyopathy is undetermined.

FGF6 (Fibroblast Growth Factor 6) had the 10th-highest level of transcript up-regulation at 6.72 FC above controls. Phylogenetic analyses has found that *FGF6* belongs to the *FGF4* subfamily, which is composed of secreted proteins with cleavable N-terminal signal peptides that regulate biological responses by binding to and activating FGF receptors (FGFR) [41, 42]. FGF6 is known to play an integral role in skeletal muscle development and regeneration [43, 44]. FGF6 knockout results in defective skeletal muscle regeneration [43] and a combined loss of FGF2, FGF6, and MDX results in severe dystrophic changes and reduced myotubule formation in regenerating skeletal muscle [44]. Overexpression of *FGF6* has been documented in human prostate cancer [45]. Its roles in cardiac disease in general, and dystrophin-deficiency-associated cardiomyopathy specifically, are unknown.

Top 10 down-regulated gene transcripts

LOC612108 had the highest level of transcript down-regulation at -23.83 FC compared to controls. This is an uncharacterized protein coding gene on the X-chromosome with base pair coordinates starting at 111,233,874 and stopping at 111,250,204. It has no known interactions with the *DMD* gene, which spans from base pair 26,290,903 to 28,444,635 [46]. LOC612108's potential role in Labradoodle dystrophinopathic cardiomyopathy remains undetermined.

ST8SIA2 (ST8 alpha-N-acetyl-neuraminide alpha-2,8-sialyltransferase 2) had the 2nd-highest level of transcript down-regulation at -15.94 FC compared to controls. The encoded protein product is a type II membrane protein that is believed to catalyze the transfer of sialic acid from CMP-sialic acid to N-linked oligosaccharides and glycoproteins [39]. A recent study in mice found that this gene is only expressed in neonatal atria. In that study, *ST8sia2*(*-/-*) mice had consistently altered atrial myocyte action potential waveforms and gating of less sialylated voltage-gated Na⁺ channels. The same study found that *ST8sia2* expression did not affect ventricular myocyte excitability, indicating that regulated and aberrant expression is sufficient to modulate cardiomyocyte excitability [47]. Because sodium ion flux plays a critical role in cardiac electrical activity, altered *ST8SIA2* expression in dystrophin-deficient hearts may represent altered cardiomyocyte excitability.

FOXR1 (Forkhead Box R1) had the 3rd-highest level of transcript down-regulation at -15.04 FC compared to controls. FOX transcription factors often play roles in determining early developmental cell fates in various tissues. Transcriptome analysis of 35 human fetal samples, collected between 10 and 20 weeks gestational time, found that the highest expression levels of *FOXR1* were in the heart at 10 weeks [48]. In adult humans, *FOXRI* expression has been shown to be limited to the testis [49]. To the authors' knowledge, altered *FOXRI* expression has no known association with cardiac disease in people and differential developmental and disease-associated expression patterns have not been evaluated in dogs.

P2RX6 (Purinergic Receptor P2X 6) had the 4th-highest level of transcript down-regulation at -14.61 FC compared to controls. Based on human tissue analyses, this gene is predominantly expressed in skeletal muscle and is regulated by p53. The encoded protein belongs to the family of P2X receptors (ATP-gated ion channels) which regulate cation

permeability [30, 50]. Copy number variants of *P2RX6* have been noted in cases of congenital heart disease in people (including atrial septal defect, ventricular septal defect, subaortic stenosis, double outlet right ventricle, and tetralogy of Fallot). However, the etiologic role of *P2RX6* in these developmental cardiac malformations remains undetermined. *P2RX6* has also been found to be up-regulated in people with chronic heart failure undergoing heart transplantation [51]; however, the relationship between receptor downregulation and cardiac disease etiopathogenesis remains undetermined.

LOC610380 (*CRHR1*; Corticotropin-Releasing Factor Receptor 1) had the 5th-highest level of transcript down-regulation at -14.52 FC compared to controls. Corticotropin-releasing hormone (CRH) is a neuropeptide that plays an important neuroendocrinological role in stress-associated responses involving the hypothalamic-pituitary-adrenal (HPA) axis and extra-hypothalamic circuits [52]. In addition to being expressed in the central nervous system, CRH is also expressed in peripheral tissues, including the heart and vasculature. CRH acts through two receptors, GPCRs, *CRHR1* and *CRHR2*. There are several known splice variants of *CRHR1*; however, a cardiac-specific role remains undetermined [53]. Glucocorticoid-mediated down-regulation of *CRHR2* is known to occur in rat hearts and aortic smooth muscle as part of a neuroendocrine stress response [54].

DAO (D-Amino Acid Oxidase) had the 6th-highest level of transcript down-regulation at -12.70 FC compared to controls. DAO is a flavoprotein that functions to degrade D-amino acids through oxidative deamination [55]. High levels of *DAO* expression and enzyme activity have been found in the mammalian liver, kidney, and brain; however, in human cardiac and skeletal muscles, DAO mRNA expression is limited and protein expression is lacking [55-57]. Research suggests that in people, DAO may play a minor or redundant role in D-serine regulation in the

brain and peripheral organs [58]. DAO does not yet have a defined role in normal or abnormal cardiac functionality; however, it is important to note that D-serine is a coagonist at the N-methyl D-aspartate receptor (NMDAR), and receptor activation is dependent on D-serine binding. NMDARs are expressed in the heart and are thought to play a role in autonomic heart rate regulation and cardiac conduction functionality [59].

CNR2 (Cannabinoid [CB] Receptor 2) had the 7th-highest level of transcript down-regulation at -11.48 FC compared to controls. Recent research indicates that the CNR2–endocannabinoid axis plays an important role in cardioprotection by preventing cardiomyocyte apoptosis and modulating the expression of antioxidative enzymes and contractile elements. This receptor also plays a regulatory role in the cardiac inflammatory response, macrophage activity following myocardial ischemia, and reparative responses via modulation of myofibroblasts and collagen production [60]. Based on these known functions, decreased expression of *CNR2* in dystrophin-deficient hearts likely plays a role in the perpetuation of cardiac damage via dysregulation of myocardial inflammation and fibrosis.

SDC1 (Syndecan 1) had the 8th-highest level of transcript down-regulation at -10.73 FC compared to controls. Syndecan-1 is the main component of the endothelial glycocalyx (eGC), a proteoglycan complex covering endothelial cells. The glycocalyx functions as a protective barrier to help maintain the endothelial surface, prevent unwanted extravasation of various molecules (water, salts, proteins), and inhibit unintended binding of cytokines and proteins on the endothelial surface [50]. Preclinical studies in mice have yielded varied results regarding the function of SDC1 in cardiac disease. One study found that loss of expression results in attenuated angiotensin II-induced cardiac dysfunction and fibrosis [61]. Others have found that loss of expression results in greater endothelial adhesion and extravasation of inflammatory cells,

enhanced adverse collagen matrix remodeling [62], and the development of greater neointimal hyperplasia and proliferation of vascular smooth muscle cells following vascular injury [63]. Based on these findings, down-regulation of *SDC1* in the present study likely reflects its role in cardiac injury and tissue remodeling.

LRRC55 (Leucine Rich Repeat Containing 55) had the 9th-highest level of transcript down-regulation at -10.45 FC compared to controls. LRRC55, and other LRRC proteins (including LRRC38, LRRC52 and LRRC26) have been identified as auxiliary proteins of BK (Big conductance of K⁺) channels. BK channels function to shift the conductance voltage curve of Slo1 channels, which in the heart, results in a mitochondrial BK channel cardioprotective role [64, 65]. Slo1 channels are Ca²⁺ activated potassium channels that are known to play a role in vascular fibrosis and remodeling [66]. Minimal LRRC55 RNA expression has been noted in human and mouse hearts; however, the exact role in normal and diseased cardiac tissue remains to be studied [30].

TMEM171 (Transmembrane Protein 171) had the 10th-highest level of transcript down-regulation at -10.11 FC compared to controls. RNA sequencing of normal adult and fetal human hearts has found minimal expression of TMEM171 [48, 49]. Its function in normal cardiac tissue and in cardiac disease is undetermined.

Though not all of the cardiac genes with altered expression profiles have known functions in normal or diseased cardiac tissue, many of the most up- or down-regulated genes have roles consistent with adaptive and/or compensatory cellular responses secondary to early dystrophinopathy-related cardiomyocyte damage. These findings are significant because they could represent future therapeutic targets to aid in the treatment of dystrophinopathy-associated cardiac disease.

Differential expression of genes associated with cardiac oxidative stress, apoptosis, and contractility

Oxidative Stress

Cardiac hypertrophy and decreased functionality occur in response to various stresses, including myocardial infarction, hypertension, coronary vascular disease, dilated hypertrophy, fibrosis, and contractile anomalies [67]. In patients with DMD, progressive weakening of the sarcolemma, resultant from a lack of functional dystrophin, results in degeneration of cardiac myocytes with eventual myocardial impairment that involves decreased left ventricular ejection fraction, left ventricular dilatation, fibrosis, increased cardiac workload, and altered heart rate and rhythm [68]. As part of this degenerative process, the affected cells have a build-up of intracellular calcium with subsequent leakage, activation of various proteases, and alteration of pathways involved in the production of reactive oxygen species (ROS) and nitrogen oxide (NO) [69].

The most up-regulated gene transcripts associated with oxidative stress were Glutathione Peroxidase 3 (GPX3; 2.18 FC), Carboxypeptidase A2 (CPA2; 2.01 FC), Carboxypeptidase A5 (CPA5; 2.04 FC), and Thioredoxin Interacting Protein (TXNIP; 2.06 FC). The initial defensive response to ROS-associated cardiac injury is mediated by several antioxidant enzymes, including various peroxidases. There are a number of glutathione peroxidase isozymes, each varying in tissue-specific functionality and substrate usage. These isozymes can be found in both the cytosol and in the mitochondrial matrix and have ability to utilize both hydrogen peroxide and lipid peroxides [70]. GPX3 is found abundantly in plasma and is known to be expressed in the kidney, lung, heart, liver, eyes, and white adipose tissue [71]. In people with heart failure and in

patients with DMD, GPX expression is known to be decreased; however, in dogs with congestive heart failure secondary to dilated cardiomyopathy (DCM), GPX expression has been found to be increased [57, 72, 73]. It is important to note that GPX measurements in these studies were obtained on plasma samples rather than tissue samples and GPX expression was not delineated based on isozymes involved. Though the exact role of GPX in the heart of dystrophin-deficient Labradoodles is unknown, results indicate that functionality of these antioxidant enzymes may be altered in affected dogs and that this altered enzyme activity may differ from what occurs in people with DMD.

Compared to controls, the dystrophin-deficient Labradoodles had up-regulation of CPA2 and CPA5. Carboxypeptidase A isoforms 1 and 2 (CPA1 and CPA2) have traditionally been referred to as pancreatic carboxypeptidases; however, gene transcripts for CPA1 and CPA2 have been detected in mesenteric vasculature and other extra-pancreatic tissues (suggestive of roles beyond digestion) [74]. In people, the highest levels of CPA5 expression are known to occur in the testes; however, low levels of expression are found in a variety of tissues, including the heart [75]. Recent research in rats indicates that CPA1 and CPA2 play a role in the renin-angiotensin system (RAS) by assisting in the reactions that convert Angiotensin I to Angiotensin II [76]. Though typically associated with kidney pathophysiology, a cardiac RAS has been described, with the principle enzymatic components being found in the atria, ventricles, valves, conduction system, vessels, fibroblasts, and cardiac myocytes [77]. Altered cardiac CPA2 expression has not been described in patients with DMD or other animal models for the disease; however, upregulation of CPA2 in the affected dogs in this study likely represents a compensatory alteration in cardiac RAS regulation secondary to myocardial damage. CPA5's role in normal

cardiac physiology and disease is uncertain; therefore, its role in dystrophinopathy-associated cardiomyopathy is undetermined.

The TXNIP gene encodes a thioredoxin-binding protein, which in addition to binding to and negatively regulating thioredoxin, also regulates cellular metabolism and endoplasmic reticulum stress. Thioredoxin is an oxidoreductase that participates in cellular protection from oxidative stress by regulating redox signaling in the heart, kidney, and vasculature [78-80]. In mice with cardiac TXNIP knock-out, researchers have found increased uptake in myocardial glucose, indicating that in the mouse heart, TXNIP plays a role in myocardial energy homeostasis rather than redox regulation [78]. TXNIP-KO mouse hearts have also been shown to have more robust cardiac recovery following ischemia-reperfusion injury as a result of enhanced anaerobic metabolism [81]. Though TXNIP's role in dystrophinopathy-associated cardiomyopathy has not been evaluated, blockade of myostatins/activins in *mdx* mouse skeletal muscle has been reported to result in increased protein expression levels of TXNIP in conjunction with up-regulation of unfolded protein response (UPR)/ER-pathway proteins [82]. These findings indicate that up-regulation in the dystrophin-deficient dogs in the current study may be associated with cardiomyocyte ER stress.

In affected dogs, the most down-regulated gene transcript associated with oxidative stress was NADPH oxidase 4 (NOX4; -2.61 FC). NOX4 expression is considered to be a source of oxidative stress in the failing heart, with up-regulation in aging cardiomyocytes and in response to hypertrophic stimuli and pressure overload [83]. Conversely, knock out of myocardial NOX4 in mice results in decreased levels of cardiac ROS, decreased mitochondrial swelling, decreased release of cytochrome c, and diminished cardiac hypertrophy and fibrosis following pressure overload [84]. In the *mdx* mouse heart, mRNA profiling has found up-regulation of NOX4,

considered to be associated with myocardial fibrosis [85]. Cardiac NOX4 expression has not been previously described in DMD patients or canine models of DMD. Based on what has been reported in *mdx* mice, down-regulation of the NOX4 transcript in the hearts of affected dogs in the current study is consistent with early cardiomyopathy and a lack of myocardial fibrosis in all but one animal. Decreased levels of NOX4 may also be indicative of a compensatory response attempting to limit generation of cardiac ROS.

Apoptosis

Oxidative stress and apoptotic cell death are interconnected processes. As discussed previously, cellular damage (in this instance mechanical damage resultant from diminished levels of dystrophin) causes increased intracellular calcium with a subsequent increase in ROS production, activation of Ca²⁺ dependent proteases, and activation of the caspase cascade. If left unchecked, these processes culminate in cell death, predominantly via apoptosis or necrosis [69, 86].

The most up-regulated gene transcript involved in the apoptotic signaling pathway was BCL2 Interacting Killer (BIK; 2.29 FC). BIK is a pro-apoptotic member of the BCL-2 family that has increased expression in response to oxidative stress, resulting in mitochondrial cristae reorganization and early release of Ca²⁺ from the ER [87]. It is expressed in various tissues including the liver, lung, heart, and kidneys and in hematopoietic cells including granulocytes, macrophages, and lymphocytes [88]. To the authors' knowledge, BIK expression has not been previously evaluated in cardiac tissue from DMD patients. It's up-regulation in the affected dogs in this study, in association with differential expression of other transcripts involved in cardiac

oxidative stress, suggest that apoptosis-mediated cell death pathways are involved in the pathogenesis of cardiomyopathy in dystrophin-deficient Labradoodles.

The most down-regulated apoptosis-associated gene transcripts were Apoptosis Inducing Factor 1 (AIF1; -2.58 FC), Caspase 10 (CASP10; -2.01 FC) and Caspase 12 (CASP12; -2.17 FC). AIF1 is a pro-apoptotic NADH-dependent oxidoreductase that is found in the mitochondrial intermembrane space. AIF1 plays an important role in the maintenance of mitochondrial morphology, energy metabolism, and oxidative phosphorylation and may also aid in the regulation of the respiratory chain [89]. Caspase 10 is an initiator caspase, involved in the initiation of apoptosis as the name suggests. Caspase 12 is an inflammatory caspase, traditionally believed to be involved in the innate immune response rather than apoptosis; however, recent research indicates that it can activate caspase 9 independent of Apaf-1, resulting in the activation of caspase 3 [90]. Compared to controls, the affected dogs in this study also had variable up- or down-regulation of other initiator caspases (2, 4, 8, and 9) and executioner caspases (3, 6, and 7). Because AIF1, CASP10, and CASP12 are the most down-regulated gene transcripts associated with apoptosis and because they are all involved in the initiation of apoptotic cell death, it is reasonable to propose that at least during the early stages of Labradoodle dystrophinopathic cardiomyopathy, cardiomyocyte apoptosis may be attenuated by decreased expression of pro-apoptotic genes such as AIF1, CASP10, and CASP12.

Cardiac contractility

In the dystrophin-deficient dogs, the most up-regulated gene transcripts associated with cardiac contractility (and indeed the most up-regulated of all transcripts evaluated) were BDNF (14.67 FC) and MYL4 (14.23 FC). As previously discussed, increased cardiac BDNF is likely

associated with a compensatory response to stimulate cardiomyocyte viability and decrease fibrosis while MYL4 improves cardiac contractility as part of an adaptive response to myocardial injury.

The greatest limitation of this study is the small sample size; this is expected given the clinical difficulties of maintaining this particular animal model and the general limitations of maintaining large animal models in research colonies. Additional analyses, such as a comparison to DMD patient ventricular myocardial transcriptional variation patterns and ingenuity pathway analysis, would provide further useful information to characterize the similarities and differences between cardiac changes seen in DMD patients and the dystrophin-deficient Australian Labradoodle. Regardless, the findings presented herein are significant because they elucidate potential pathways involved in Australian Labradoodle dystrophinopathic cardiomyopathy, shed light on how differential expression of genes in these pathways may vary between dystrophin-deficient humans and Australian Labradoodles, and represent potential future therapeutic targets to aid in the treatment of dystrophinopathy-associated cardiac disease.

Acknowledgements: The authors would like to thank Stephen Waters and Richard Rathbun for their assistance throughout the course of the study. This research received no specific grant from any funding agency in the public, commercial or not-for-profit sectors.

Conflict of Interest: The authors have no conflict of interest to report.

References

1. Ryder S, Leadley R, Armstron N, Westwood M, Kock Wd, Butt T, et al. The burden, epidemiology, costs and treatment for Duchenne muscular dystrophy: an evidence review. *Orphanet Journal of Rare Diseases*. 2017;12:2017.
2. Eagle M, Baudouin S, Chandler C, Giddings D, Bullock R, Bushby K. Survival in Duchenne muscular dystrophy: improvements in life expectancy since 1967 and the impact of home nocturnal ventilation. *Neuromuscul Disord*. 2002;12(10):926-9.
3. Bushby K, Finkel R, Birnkrant D, Case L. Diagnosis and management of Duchenne muscular dystrophy, part 2: implementation of multidisciplinary care. *Lancet Neurol*. 2010;9:177-89.
4. Cheeran D, Khan S, Khera R, Bhatt A, Garg S, Grodin J, et al. Predictors of Death in Adults With Duchenne Muscular Dystrophy-Associated Cardiomyopathy. *J Am Heart Assoc*. 2017;6(10):1-12.
5. Passamano L, Taglia A, Palladino A, Viggiano E, D'Ambrosio P, Scutifero M, et al. Improvement of survival in Duchenne Muscular Dystrophy: retrospective analysis of 835 patients. *Acta Myologica*. 2012;XXXI:121-5.
6. Connuck D, Sleeper L, Colan S, Cox G, JTJowbin J, Lowe A. Characteristics and Outcomes of Cardiomyopathy in Children with Duchenne or Becker Muscular Dystrophy: A Comparative Study from The Pediatric Cardiomyopathy Registry. *Am Heart J*. 2008;155:998-1005.
7. Shrader SM, Jung S, Denney TS, Smith BF. Characterization of Australian Labradoodle dystrophinopathy. *Neuromuscul Disord*. 2018;28(11):927-37.
8. Matkovich S. Transcriptome analysis in heart failure. *Curr Opin Cardiol*. 2016;31(3):242-8.
9. Ounzain S, Micheletti R, Beckmann T, Schroen B, Alexanian M, Pezzuto I, et al. Genome-wide profiling of the cardiac transcriptome after myocardial infarction identifies novel heart-specific long non-coding RNAs. *Eur Heart J*. 2015;36(6):353–68.

10. Isono T, Matsumoto T, Wada A, Suzaki M, Chano T. A Global Transcriptome Analysis of a Dog Model of Congestive Heart Failure With the Human Genome as a Reference. *J Card Fail.* 2012;18(11):872-8.
11. Galindo CL, Soslow JH, Brinkmeyer-Langford CL, Gupte M, Smith HM, Sensayadeth S, et al. Translating golden retriever muscular dystrophy microarray findings to novel biomarkers for cardiac/skeletal muscle function in Duchenne Muscular Dystrophy. *Pediatr Res.* 2016;79(4):629-36.
12. Fulgenzi G, Tomassoni-Ardori F, Babini L, Becker J, Barrick C, Puvarel S, et al. BDNF modulates heart contraction force and long-term homeostasis through truncated TrkB.T1 receptor activation. *J Cell Biol.* 2015;210(6):1003-12.
13. Pius-Sadowska E, Machalinski B. BDNF - A key player in cardiovascular system. *J Mol Cell Cardiol.* 2017;110:54-60.
14. Kermani P, Hempstead B. Brain-derived neurotrophic factor: a newly described mediator of angiogenesis. *Trends Cardiovasc Med.* 2007;17(4):140-3.
15. Halade G, Ma Y, Ramirez T, Zhang J, Dai Q, Hensler J. Reduced BDNF attenuates inflammation and angiogenesis to improve survival and cardiac function following myocardial infarction in mice. *Am J Physiol Heart Circ Physiol.* 2013;305(12):H1830-H42.
16. Katare R, Kakinuma Y, Arkawa M, Yamasaki F, Sato T. Chronic intermittent fasting improves the survival following large myocardial ischemia by activation of BDNF/VEGF/PI3K signaling pathway. *J Mol Cell Cardiol.* 2009;46(3):405-12.
17. Zhao R, Wang X, Wang H, Yu T, Wang Q, Yan X. Inhibition of long noncoding RNA BDNF-AS rescues cell death and apoptosis in hypoxia/reoxygenation damaged murine cardiomyocyte. *Biochimie.* 2017;138:43-9.
18. Hernandez O, Guzman J, Szczesna-Cordary D. Myosin essential light chain in health and disease. *Am J Physiol Heart Circ Physiol.* 2007;292:H1643-H54.

19. Morano I, Ritter O, Bonz A, Timek T, Vahl C, Michel G. Myosin light chain-actin interaction regulates cardiac contractility. *Circ Res.* 1995;76(5):720-5.
20. Morano M, Zacharzowski U, Maier M. Regulation of human heart contractility by essential myosin light chain isoforms. *J Clin Invest.* 1996;98(2):467-73.
21. Udenfriend S, Kilpatrick D. Biochemistry of the enkephalins and enkephalin-containing peptides. *Arch Biochem Biophys.* 1983;221:309-23.
22. Younes A, Pepe S, Barron B, Spurgeon H, Lakatta E, Caffrey J. Cardiac synthesis, processing, and coronary release of enkephalin-related peptides. *Am J Physiol Heart Circ Physiol.* 2000;279:H1989-98.
23. Oullette M, Brakia-Gingras L. Increase in the relative abundance of preprokephalin A messenger RNA in the ventricles of cardiomyopathic hamsters. *Biochem Biophys Res Commun.* 1988;155(1):449-54.
24. van den Brink O, Delbridge L, Rosenfeldt F, Penny D, Esmore DS, Quick D, et al. Endogenous Cardiac Opioids: Enkephalins in Adaptation and Protection of the Heart. *Heart, Lung and Circulation.* 2003;12(3):178-87.
25. Weil J, Eschenhagen T, Fleige G, Mittmann C, Orthey E, Scholz H. Localization of preproencephalin mRNA in rat heart: selective gene expression in left ventricular myocardium. *Am J Physiol.* 1998;275(2 Pt 2):H378-84.
26. Denning G, Ackermann L, Barna T, Armstrong J, Stoll L, Weintraub N, et al. Proenkephalin expression and enkephalin release are widely observed in non-neuronal tissues. *Peptides.* 2008;29(1):83-92.
27. van de Graff S, van der Kemp A, van den Berg D, van Oorschot M, Hoenderop J, Bindels R. Identification of BSPRY as a Novel Auxiliary Protein Inhibiting TRPV5 Activity. *J Am Soc Nephrol* 2006;17(1):26-30.
28. Aijo T, Edelman S, Lonner T, Larjo A, Kallionpää H, Tuomela S, et al. An integrative computational systems biology approach identifies differentially regulated dynamic transcriptome

- signatures which drive the initiation of human T helper cell differentiation. *BMC Genomics*. 2012;13:1-20.
29. Waugh K, Leach S, Moore B, Bruno T, Buhrman J, Slansky J. Molecular Profile of Tumor-Specific CD8+ T Cell Hypofunction in a Transplantable Murine Cancer Model. *J Immunol*. 2016:1-13.
30. Uhlen M, Fagerberg L, Hallstrom B, Lindskog C, Oksvold P, Mardinoglu A, et al. Tissue-based map of the human proteome. *Science*. 2015;347(6220).
31. Rosenbohm A, Schmid B, Buckert D, Rottbauer W, Kassubek J, Ludolph A, et al. Cardiac Findings in Amyotrophic Lateral Sclerosis: A Magnetic Resonance Imaging Study. *Front Neurol*. 2017;8:1-8.
32. Man J, Barnett P, Christoffels V. Structure and function of the Nppa–Nppb cluster locus during heart development and disease. *Cell Mol Life Sci*. 2018;75(8):1435-44.
33. Annilo T, Kepp K, Laan M. Natural antisense transcript of natriuretic peptide precursor A (NPPA): structural organization and modulation of NPPA expression. *BMC Mol Biol*. 2009;10:1-13.
34. Goytain A, Quamme GA. Functional characterization of the human solute carrier, SLC41A2. *Biochem Biophys Res Commun*. 2005;330(3):701-5.
35. Atlas THP. SLC41A2 [December 10, 2018]. Available from: <https://www.proteinatlas.org/ENSG00000136052-SLC41A2/tissue>.
36. UniProtKB - A0A077S9R2 (A0A077S9R2_CANLF) [Internet]. UniProt. 2014 [cited January 7, 2019]. Available from: <https://www.uniprot.org/uniprot/A0A077S9R2>.
37. Callewaert L, Michiels C. Lysozymes in the animal kingdom. *J Biosci*. 2010;35(1):127-60.
38. Abdul-Salam V, Ramrakha P, Krishnan U, Owen D, Shalhoub J, Davies A, et al. Identification and Assessment of Plasma Lysozyme as a Putative Biomarker of Atherosclerosis. *Arterioscler Thromb Vasc Biol*. 2010;30(5):1027-33.
39. ST8SIA2 ST8 alpha-N-acetyl-neuraminide alpha-2,8-sialyltransferase 2 [Homo sapiens (human)] [Internet]. [cited Nov. 30, 2018]. Available from: <https://www.ncbi.nlm.nih.gov/gene/8128>.

40. Chen C, Chang S, Lin C, Chern S, Wu P, Chen S, et al. Prenatal diagnosis of a familial 5p14.3-p14.1 deletion encompassing CDH18, CDH12, PMCHL1, PRDM9 and CDH10 in a fetus with congenital heart disease on prenatal ultrasound. *Taiwan J Obstet Gynecol.* 2018;57(5):734-8.
41. Itoh N, Ornitz D. Evolution of the Fgf and Fgfr gene families. *Trends Genet.* 2004;20(11):563-9.
42. Itoh N, Ornitz D. Fibroblast growth factors: from molecular evolution to roles in development, metabolism and disease. *J Biochem.* 2011;149(2):121-30.
43. Floss T, Arnold H, Braun T. A role for Fgf-6 in skeletal muscle regeneration. *Genes Dev.* 1997;11:2040-51.
44. Neuhaus P, Oustanina S, Loch T, Kruger M, Bober E, Dono R, et al. Reduced mobility of Fibroblast Growth Factor (FGF)-deficient myoblasts might contribute to dystrophic changes in the musculature of FGF2/FGF6/mdx triple-mutant mice. 2003; *Mol Cell Biol*(23).
45. Ropiquet F, Giri D, Kwabi-Addo B, Mansukhani A, Ittmann M. Increased expression of Fibroblast Growth Factor 6 in human prostatic intraepithelial neoplasia and prostate cancer. *Cancer Res.* 2000;60:4245-50.
46. The Rat Genome Database 2015: genomic, phenotypic and environmental variations and disease. [Internet]. 2015 [cited December 10, 2018]. Available from: <https://rgd.mcw.edu/rgdweb/search/genes.html?term=ENSRNOG00000033816&chr=X&start=&stop=&map=360&imapped=1&speciesType=6&obj=gene&sort=7>.
47. Montpetit ML, Stocker PJ, Schwetz TA, Harper JM, Noring SA, Schaffer L, et al. Regulated and aberrant glycosylation modulate cardiac electrical signaling. *PNAS.* 2009;106(38):16517-22.
48. Szabo L, Morey R, Palpant N, Wang P, Afari N, Jiang C, et al. Statistically based splicing detection reveals neural enrichment and tissue-specific induction of circular RNA during human fetal development. *Genome Biol.* 2015;16(126):1-26.

49. Fagerberg L, Hallstrom B, Oksvold P, Kampf C, Djureinovic D, Odeberg J, et al. Analysis of the human tissue-specific expression by genome-wide integration of transcriptomics and antibody-based proteomics. *Mol Cell Proteomics*. 2014;13(2):397-406.
50. Kim Y, Nijst P, Kiefer K, Wilson Tang W. Endothelial Glycocalyx as Biomarker for Cardiovascular Diseases: Mechanistic and Clinical Implications. *Curr Heart Fail Rep*. 2017;14(2):117-26.
51. Banfi C, Ferrario S, De Vincenti O, Ceruti S, Fumagalli M, Mazzola A, et al. P2 receptors in human heart: upregulation of P2X6 in patients undergoing heart transplantation, interaction with TNFalpha and potential role in myocardial cell death. *J Mol Cell Cardiol*. 2005;39(6):929-39.
52. Inda C, Armando N, dos Santos Claro P, Silberstein S. Endocrinology and the brain: corticotropin-releasing hormone signaling. *Endocr Connect*. 2017;6(6):R99-120.
53. Hauger R, Risbrough V, Brauns O, Dautzenberg F. Corticotropin releasing factor (CRF) receptor signaling in the central nervous system: new molecular targets. *CNS Neurol Disord Drug Targets*. 2006;5(4):453-79.
54. Tillinger A, Nostramo R, Kvetnansky R, Serova L, Sabban E. Stress-induced changes in gene expression of urocortin 2 and other CRH peptides in rat adrenal medulla: involvement of glucocorticoids. *J Neurochem*. 2013;125(2):185-92.
55. Smith S, Uslaner J, Hutson P. The therapeutic potential of D-Amino Acid Oxidase (DAAO) inhibitors. *Open Med Chem J*. 2010;4:3-9.
56. Tishkov V, Khoronenkova S. D-Amino acid oxidase: structure, catalytic mechanism, and practical application. *Biochemistry (Mosc)*. 2005;70(1):40-54.
57. Petrillo S, Pelosi L, Piemonte F, Travaglini L, Forcina L, Catteruccia M, et al. Oxidative stress in Duchenne muscular dystrophy: focus on the NRF2 redox pathway. *Hum Mol Genet*. 2017;26(14):2781-90.

58. Ohnuma T, Shibata N, Maeshima H, Baba H, Hatano T, Hanzawa R, et al. Association analysis of glycine- and serine-related genes in a Japanese population of patients with schizophrenia. *Prog Neuropsychopharmacol Biol Psychiatry*. 2009;33(3):511-8.
59. Makhro A, Tian Q, Kaestner L, Kosenkov D, Faggian G, Gassmann M, et al. Cardiac N-methyl D-aspartate Receptors as a Pharmacological Target. *J Cardiovasc Pharmacol*. 2016;68(5):356-73.
60. Dewald O, Duerr GD. The Role for the Endocannabinoid System in Cardioprotection and Myocardial Adaptation. In: Meccariello R, Chianese R, editors. *Cannabinoids in Health and Disease* 2016.
61. Schellings M, Vanhoutte D, van Almen G. Syndecan-1 amplifies angiotensin II-induced cardiac fibrosis. *Hypertension*. 2010;55(2):249-56.
62. Vanhoutte D, Schellings M, Gotte M. Increased expression of syndecan-1 protects against cardiac dilatation and dysfunction after myocardial infarction. *Circulation*. 2007;115(4):475-82.
63. Fukai N, Kenagy R, Chen L, Gao L, Daum G, Clowes A. Syndecan-1: an inhibitor of arterial smooth muscle cell growth and intimal hyperplasia. *Arterioscler Thromb Vasc Biol*. 2009;29(9):1356-62.
64. Yan J, Aldrich R. BK potassium channel modulation by leucine-rich repeat-containing proteins. *Proc Natl Acad Sci USA*. 2012;109:7917-22.
65. Singh H, Lu R, Bopassa J, Meredith A, Stefani E, Toro L. MitoBK(Ca) is encoded by the *Kcnma1* gene, and a splicing sequence defines its mitochondrial location. *Proc Natl Acad Sci USA*. 2013;110:10836-41.
66. Xu H, Garver H, Fernandes R, Phelps J, Harkema J. BK channel beta1-subunit deficiency exacerbates vascular fibrosis and remodelling but does not promote hypertension in high-fat fed obesity in mice. *J Hypertens*. 2015;33:1611-23.
67. Rababa'h A, Guillory A, Mustafa R, Hijjawi T. Oxidative Stress and Cardiac Remodeling: An Updated Edge. *Curr Cardiol Rev*. 2018;14(1):53-9.

68. Fayssoil A, Abasse S, Silverston K. Cardiac involvement classification and therapeutic management in patients with Duchenne muscular dystrophy. *J Neuromuscul Dis.* 2017;4(1):17-23.
69. Verhaert D, Richards K, Rafael-Fortney J, Raman S. Cardiac involvement in patients with muscular dystrophies: magnetic resonance imaging phenotype and genotypic considerations. *Circ Cardiovasc Imaging.* 2011;4(1):67-76.
70. Brigelius-Flohe R. Tissue-specific functions of individual glutathione peroxidases. *Free Radic Biol Med.* 1999;27:951-65.
71. Chu F, Esworthy R, Doroshov J, Doan K, Liu X. Expression of plasma glutathione peroxidase in human liver in addition to kidney, heart, lung, and breast in humans and rodents. *Blood.* 1992;79:3233-8.
72. Keith M, Geranmayegan A, Sole M, Kurian R, Robinson A, Omran A, et al. Increased oxidative stress in patients with congestive heart failure. *J Am Coll Cardiol.* 1998;31(6):1352-6.
73. Freeman L, Rush J, Milbury P, Blumberg J. Antioxidant Status and Biomarkers of Oxidative Stress in Dogs with Congestive Heart Failure. *J Vet Intern Med.* 2008;19(4):537-41.
74. Normant E, Gros C, Schwartz J. Carboxypeptidase A isoforms produced by distinct genes or alternative splicing in brain and other extrapancreatic tissues. *J Biol Chem.* 1995;270(35):20543-49.
75. Fricker L. Carboxypeptidase A5. 3 ed. Rawlings N, Salvesen G, editors. San Diego, CA: Academic Press; 2013.
76. Pereira H, Souza L, Costa-Neto C, Salgado M, Oliveira E. Carboxypeptidases A1 and A2 from the perfusate of rat mesenteric arterial bed differentially process angiotensin peptides. *Peptides.* 2012;33(1):67-76.
77. Paul M, Poyan M, Kreutz R. Physiology of local renin–angiotensin system. *Physiol Rev.* 2006;86(3):747-803.

78. Yoshioka J, Imahashi K, Gabel S, Chutkow W, Burds A, Gannon J, et al. Targeted Deletion of Thioredoxin-Interacting Protein Regulates Cardiac Dysfunction in Response to Pressure Overload. *Circ Res.* 2007;101:1328-38.
79. Forred B, Neuharth S, Kim D, Amolins M, Motamedchaboki K, Roux K, et al. Identification of Redox and Glucose-Dependent Txnip Protein Interactions. *Oxid Med Cell Longev.* 2016;2016:1-10.
80. Yamawaki H, Berk B. Thioredoxin: a multifunctional antioxidant enzyme in kidney, heart and vessels. *Curr Opin Nephrol Hypertens.* 2005;14(2):149-53.
81. Yoshioka J, Chutkow W, Lee W, Kim J, Yan J, Tian R, et al. Deletion of thioredoxin-interacting protein in mice impairs mitochondrial function but protects the myocardium from ischemia-reperfusion injury. *J Clin Invest.* 2012;122(1):267-79.
82. Hulmi J, Hentila J, DeRuisseau K, Oliveira B, Papaionnou K, Autio R, et al. Effects of muscular dystrophy, exercise and blocking activin receptor IIB ligands on the unfolded protein response and oxidative stress. *Free Radical Bio Med.* 2016;99:308-22.
83. Ago T, Kuroda J, Pain J, Fu C, Li H, Sadoshima J. Upregulation of Nox4 by hypertrophic stimuli promotes apoptosis and mitochondrial dysfunction in cardiac myocytes. *Circ Res.* 2010;106(7):1253-64.
84. Kuroda J, Ago T, Matsushima S, Zhai P, Scheider M, Sadoshima J. NADPH oxidase 4 (Nox4) is a major source of oxidative stress in the failing heart. *Proc Natl Acad Sci USA.* 2010;107(35):15565-70.
85. Spurney C, Knoblach S, Pistilli E, Nagaraju K, Martin G, Hoffman E. Dystrophin-deficient cardiomyopathy in mouse: Expression of Nox4 and Lox are associated with fibrosis and altered functional parameter in the heart. *Neuromuscul Disord.* 2008;18(5):371-81.
86. Shirokova N, Niggli E. Cardiac Phenotype of Duchenne Muscular Dystrophy: Insights from Cellular Studies. *J Mol Cell Cardiol.* 2013;58:217-24.

87. Dalal S, Zha Q, Singh M, Singh K. Osteopontin-stimulated apoptosis in cardiac myocytes involves oxidative stress and mitochondrial death pathway: role of a pro-apoptotic protein BIK. *Mol Cell Biochem.* 2016;418(1-2):1-11.
88. Coultas L, Bouillet P, Stanley E, Brodnicki T, Adams J, Strasser A. Proapoptotic BH3-only Bcl-2 family member Bik/Blk/Nbk is expressed in hemopoietic and endothelial cells but is redundant for their programmed death. *Mol Cell Biol.* 2004;24:1570-81.
89. Seviroukova I. Apoptosis-Inducing Factor: Structure, Function, and Redox Regulation. *Antioxid Redox Signal.* 2011;14(12):2545-79.
90. Shiraishi H, Okamoto H, Yoshimura A, Yoshida H. ER stress-induced apoptosis and caspase-12 activation occurs downstream of mitochondrial apoptosis involving Apaf-1. *J Cell Sci.* 2006;119(Pt 19):3958-66.
91. Gunning P, O'Neill G, Hardeman E. Tropomyosin-based regulation of the actin cytoskeleton in time and space. *Physiol Rev.* 2008;88:1-35.
92. Jiang H, Qiu G, Li-Ling J, Xin N, Sun K. Reduced ACTC1 Expression Might Play a Role in the Onset of Congenital Heart Disease by Inducing Cardiomyocyte Apoptosis. *Circ J.* 2010;74(24):10-8).
93. Rittoo D, Jones A, Lecky B, Neithercut D. Elevation of cardiac troponin T, but not cardiac troponin I, in patients with neuromuscular diseases: implications for the diagnosis of myocardial infarction. *J Am Coll Cardiol.* 2014;63:2411-20.

Tables

Up-regulated			Down-regulated		
Gene	FC	<i>p-value</i>	Gene	FC	<i>p-value</i>
BDNF	14.67	<0.0001	LOC612108	-23.83	<0.0001
MYL4	14.23	<0.0001	ST8SIA2	-15.94	<0.0001
PENK	10.72	<0.0001	FOXR1	-15.04	<0.0001
BSPRY	10.05	<0.0001	P2RX6	-14.61	<0.0001
PRR32	10.00	<0.0001	LOC610380	-14.52	<0.0001
NPPA	9.93	<0.0001	DAO	-12.70	<0.0001
LOC490471	9.75	<0.0001	CNR2	-11.48	<0.0001
LYZF2	8.88	<0.0001	SDC1	-10.73	<0.0001
CDH10	7.61	<0.0001	LRRC55	-10.45	<0.0001
FGF6	6.72	<0.0001	TMEM171	-10.11	<0.0001

Table 1. Top 10 up-regulated and down-regulated gene transcripts from dystrophin-deficient Australian Labradoodle ventricular myocardium.

Figures

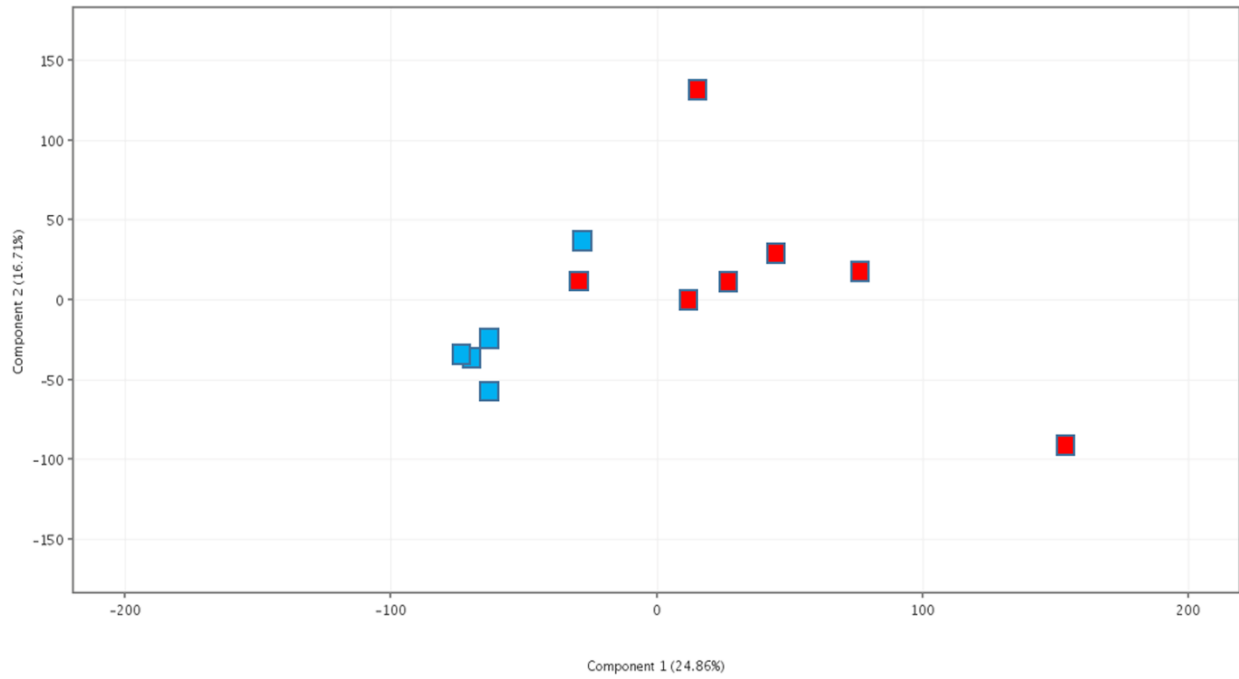


Figure 1. Principal component analysis of RNA sequencing read counts for individual cardiac transcriptomes. Axis percentages indicate variance contribution. Red dots represent dystrophin-deficient animals and blue dots represent littermate controls.

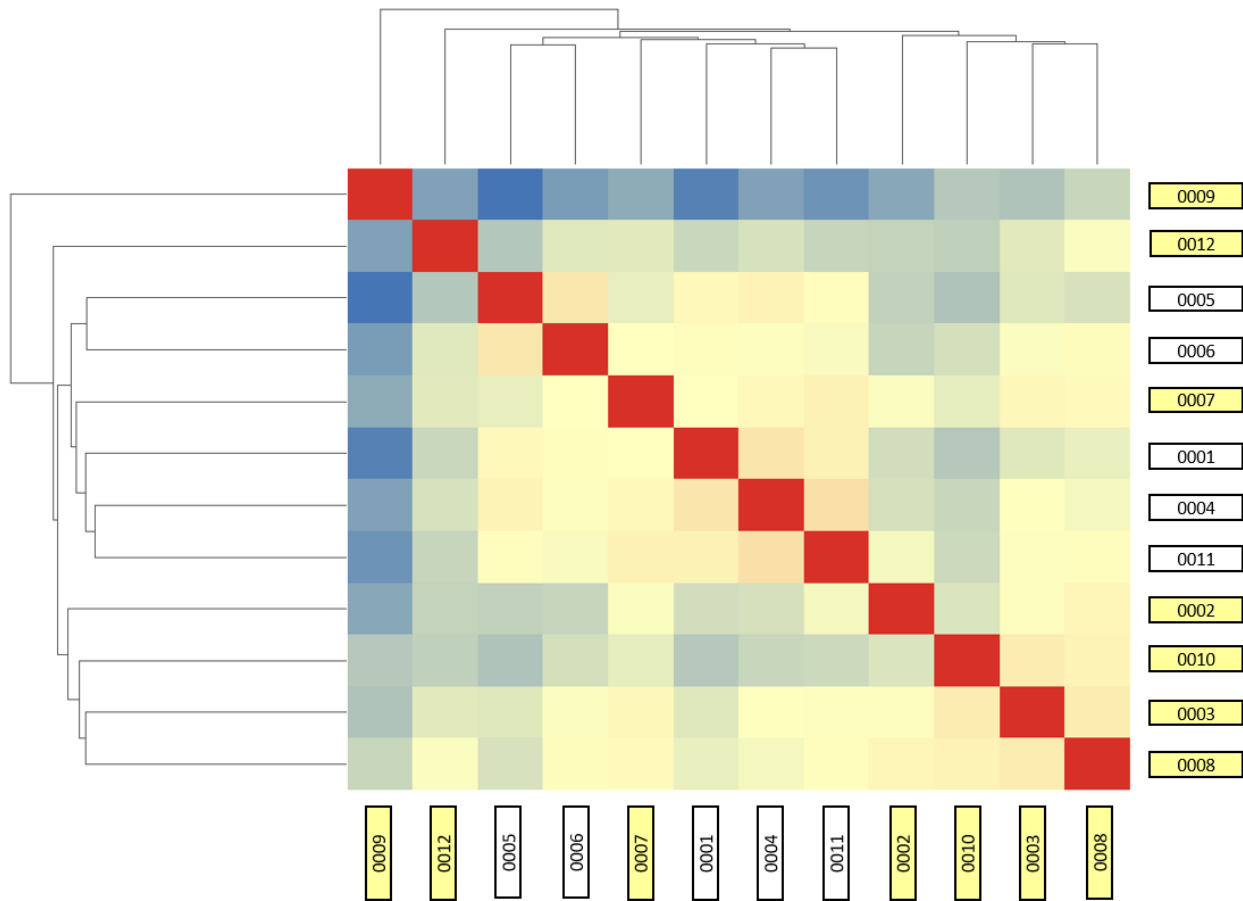


Figure 2. Heat map of Spearman's correlation of the normalized counts as expression levels from all individual samples compared against each other, represented by a colored field ranging from blue (0.95) to red (1). Dystrophin-deficiency is indicated by yellow highlighting of the animal number.

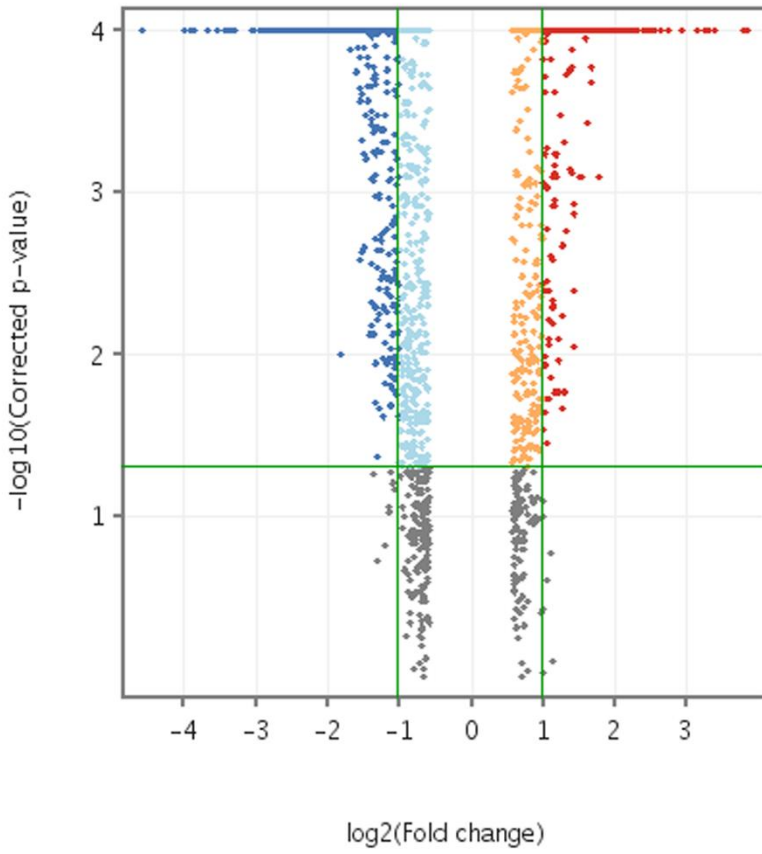


Figure 3. Volcano plot showing DEGs between dystrophin-deficient and littermate control male Australian labradoodles. The x-axis corresponds to the \log_2 fold-change value and the y-axis shows the \log_{10} corrected p-value. Red and dark blue dots represent significant ($p < 0.05$) and remarkable ($FC > 1.5$) DEGs.

Oxidative Stress				Apoptosis		Cardiac Contractility	
	GPX1		TXNRD2		AIF1		ACTC1
	GPX2		TXNRD3		APAF1		BDNF
	GPX3		CYBA		BAD		CACNA1C
	GPX5		FMO2		BAK1		MYBPC3
	GPX6		IL19		BAX		MYH6
	GPX7		IL22		BCL-2		MYL4
	GPX8		NCF2		BID		PLN
	GSTK1		NOX1		BIK		RYR2
	CAT		NOX4		CASP2		S100A1
	CTSB		APOE		CASP3		TNNC1
	MPO		CPA1		CASP4		TNNI3
	PRDX1		CPA2		CASP6		TNNT1
	PRDX2		CPA4		CASP7		TNNT2
	PRDX3		CPA5		CASP8		TPM1
	PRDX4		DNMT1		CASP9		TTN
	PRDX5		DNMT3B		CASP10		
	PRDX6		HIF1A		CASP12		
	SERPIN1		LDLR		E2F1		
	SOD1		NRF1		HAX1		
	SOD2		PINK1		MCL1		
	SOD3		TXNIP		MYC		
	TXN2		TXNRD1				

Fold Change Compared to Controls						
Down-regulated			No Change	Up-regulated		
≥ 2	1.5 > 2	1 > 1.5	1	1 > 1.5	1.5 > 2	≥ 2

Figure 4. Differential expression of genes associated with cardiac oxidative stress, apoptosis, and contractility. The colorimetric scale represents the fold change in the transcripts of dystrophin deficient animals compared to controls.

Chapter 4: Conclusions

Despite early detection and improvements in diagnostic capabilities and treatment modalities, Duchenne muscular dystrophy remains one of the most serious genetic diseases in children worldwide. Fatality is now commonly associated with the development of cardiomyopathy, stemming from early left ventricular strain and myocardial fibrosis. Current DMD research focuses on gene therapy techniques, inhibitors of skeletal muscle hypertrophy, skeletal muscle repair, preventing fibrosis, improving cardiac function, and limiting cardiomyopathy progression. In order to develop cardiac therapeutics, an appropriate animal model is required, and as is typical for animal model research, there is no perfect animal model to evaluate all aspects of the disease. Besides the dystrophin-deficient Australian Labradoodle, numerous other animal models for DMD exist; however, they fail to consistently recapitulate the echocardiographic, electrocardiographic, and cardiac histopathologic changes that occur in DMD-related cardiomyopathy. In order to establish the dystrophin-deficient Australian Labradoodle as a novel model for the study of DMD-associated cardiac changes, we undertook a multi-part study to fully characterize this model.

In the first part, we identified a novel Dystrophin mutation in Australian Labradoodles. We found a C to T transition in exon 21 (at position 2668 of the dystrophin ORF) resulting in a CGA codon (arginine) becoming a stop codon (TGA). Mutations in exon 21 have not been

reported in any other DMD canine model; however, they have been noted in DMD patients. Additionally, G:C>A:T transitions, particularly those due to C>T transitions, are the most common stop mutation class in people with DMD.

In the second part, we examined the clinical and histopathological manifestations of Australian Labradoodle dystrophin deficiency via evaluation of clinical symptomology, clinical pathology parameters (CBC and standard chemistries), echocardiographic and electrocardiographic analyses, cardiac MRI/MRS, and postmortem examination (macroscopic and microscopic). Similar to what is reported in other dogs with dystrophin-deficiency, Labradoodles develop clinical signs shortly after birth; however, unlike other DMD canine models, affected Labradoodles have a very rapid clinical course with weight loss, extensive skeletal muscular atrophy, difficulty ambulating, and moderate to severe dysphagia with ptyalism beginning by 4-months of age, necessitating study termination at 6-months of age. Though occurring at a low incidence, echocardiographic and electrocardiographic findings were similar to what has been reported in people with DMD and included hyperechoic foci in the left ventricular papillary muscles, septal hypokinesis, decreased left ventricular systolic and diastolic volume and internal diameter, and AV block. MRI/MRS analyses failed to reveal statistically significant differences in the mean PCr/ATP between groups; however, due to scheduling and early euthanasias, only two of the study dogs had both the 3- and 6-month MRI/MRS evaluations (one control, one affected). Clinicopathologic abnormalities in affected dogs included significant elevations in ALT, AST, and CK, common findings with myopathies secondary to muscular damage. All affected Labradoodles lacked macroscopic cardiac changes and microscopic changes were limited to a focal area of mineralization adjacent to the SA node in the affected dog with an AV block.

Together, these findings indicate that affected dogs have a rapidly progressive clinical course with echocardiographic and electrocardiographic findings that may be suggestive of early cardiac dysfunction that is similar to what occurs in people with DMD. It is also important to note that these findings are not typical for other DMD animal models and/or occur at a much later age than in the Labradoodle. However, with the exception of SA node mineralization in one affected dog, correlating microscopic cardiac alterations, which are known to occur in DMD patients and other canine models for DMD, were not observed.

In the third part, we performed transcriptome sequencing and analyses on left ventricular myocardial samples. Sequencing found 29,740 gene transcripts expressed in the heart samples with statistically significant differential expression of 1267 transcripts. Expression patterns from affected dogs were generally distinct from controls and similar across affected vs. control dogs with a high correlation between samples. The majority of the genes with the greatest up- and down-regulation had functions associated with cardiac survival, remodeling, contractility, conduction, and immunoregulation. As part of this evaluation, pathway analyses were also sought; however, the HudsonAlpha canine database was not yet robust enough to perform such analyses. Therefore, based on published literature relating to pathways previously evaluated in human cardiac disease differential expression of genes involved in pathways associated with cardiac oxidative stress, apoptosis, and contractility was also evaluated. These findings are significant because similar cardiac transcriptome sequencing has not previously been reported in DMD patients or canine DMD models. Moreover, these findings support the use of the dystrophin-deficient Australian Labradoodle as an appropriate animal model for the study of DMD cardiomyopathy and the results provide insights into pathways and differential gene expression in dystrophinopathic cardiomyopathy. Such findings are important because they aid

researchers in the understanding of potential gene expression patterns involved in the development of DMD cardiomyopathy. Elucidation of differential cardiac gene expression patterns in DMD patients has yet to be completed (primarily because tissue collection would occur postmortem); however, such data would be invaluable for understanding DMD cardiomyopathy and for development of potential targeted gene therapeutics, for which the Australian Labradoodle model could be of benefit, provided similar expression patterns are observed in the human genes and pathways of interest.

As with other DMD animal models, the dystrophin-deficient Australian Labradoodle does not fully recapitulate all aspects of the human disease process, at least not by 6-months of age. Although microscopic cardiac findings may develop in dystrophin-deficient Australian Labradoodles over time, the affected dogs used for this study had difficulty surviving to the 6-month endpoint without supplemental nutrition and fluid therapy, precluding any future attempts at a longer-term study. While the initial echocardiographic and electrocardiographic results are promising, and potentially suggestive of early cardiac changes that are not yet histologically discernible, the incidence of these cardiac findings is low and additional analyses, such as cardiac MRI/MRS, myocardial protein expression, and in-depth pathway analyses, would be necessary to further characterize this animal model and determine its utility for studying DMD cardiomyopathy. In light of the difficulty and expense maintaining an animal model with such a severe skeletal muscle phenotype and early mortality, other means of exploring DMD-related cardiomyopathy may also be warranted, such as developing a novel large animal model using conditional *DMD* gene modification.

References

- AKC. (2019). Dog Breeds. Retrieved from <https://www.akc.org/>
- ALAA. (2018). About Labradoodles. Retrieved from <https://alaa-labradoodles.com/>
- Anderson, J., Head, S., Rae, C., & Morley, J. (2002). Brain function in Duchenne muscular dystrophy. *Brain*, *125*, 4-13.
- Anderson, J., Rogers, R., & Jarrett, H. (1996). Ca²⁺-calmodulin binds to the carboxyl-terminal domain of dystrophin. *J Biol Chem*, *271*, 6605.
- Austin, R., Howard, P., D'Souza, V., Klamut, H., & Ray, P. (1995). Cloning and characterization of alternatively spliced isoforms of Dp71. *Hum Mol Genet*, *4*(9), 1475-1483.
- Bach, J. (1994). Update and perspective on noninvasive respiratory muscle aids, part 2: the expiratory aids. *Chest*, *105*, 1538-1544.
- Bakay, M., Zhao, P., Chen, J., & Hoffman, E. P. (2002). A web-accessible complete transcriptome of normal human and DMD muscle. *Neuromuscular Disorders*, *12*, S125-S141.
- Barber, B., Andrews, J., Lu, Z., West, N., & Meaney, F. (2013). Oral corticosteroids and onset of cardiomyopathy in Duchenne muscular dystrophy. *Journal of Pediatrics*, *163*, 1080-1084.e1081.

- Beggs, A. (1997). Dystrophinopathy, The Expanding Phenotype Dystrophin Abnormalities in X-Linked Dilated Cardiomyopathy. *Circulation*, *95*, 2344-2347.
- Beggs, A., Koenig, M., Boyce, F., & Kunkel, L. (1990). Detection of 98% of DMD/BMD gene deletions by polymerase chain reaction. *Human Genetics*, *86*(1), 45-48.
- Beltran, E., Shelton, G., & Guo, L. (2015). Dystrophin-deficient muscular dystrophy in a Norfolk terrier. *Journal of Small Animal Practice*, *56*, 351-354.
- Benabdesselam, R., Dorbani-Mamine, L., Benmassaoud-Mesbah, O., Rendon, A., Mhaouty-Kodja, S., & Hardin-Pouzet, H. (2012). Dp71 gene disruption alters the composition of the dystrophin-associated protein complex and neuronal nitric oxide synthase expression in the hypothalamic supraoptic and paraventricular nuclei. *J Endocrinol*, *213*(3), 239-249.
- Blake, D., Tinsley, J., & Davies, K. (1996). Utrophin: a structural and functional comparison to dystrophin. *Brain Pathology*, *6*, 37-47.
- Blake, D., Tinsley, J., Davies, K., Knight, A., Winder, S., & Kendrick-Jones, J. (1995). Coiled-coil regions in the carboxy-terminal domains of dystrophin and related proteins: potentials for protein-protein interactions. *Trends Biochem. Sci.*, *20*, 133.
- Blake, D., Weir, A., Newey, W., & Davies, K. (2002). Function and genetics of dystrophin and dystrophin-related proteins in muscle. *Physiol Rev*, *82*, 291.
- Blunden, A., & Gower, S. (2011). Hypertrophic feline muscular dystrophy: diagnostic overview and a novel immunohistochemical diagnostic method using formalin-fixed tissue. *Veterinary Record*, *168*, 510-515.
- Boffi, A., Bozzi, M., Sciandra, F., Woellner, C., Bigotti, M., Ilari, A., & Brancaccio, A. (2001). Plasticity of secondary structure in the N-terminal region of beta dystroglycan. *Biochim. Biophys. Acta*, *1546*, 114.

- Boland, B., Silbert, P., Groover, R., Wollan, P., & Silverstein, M. (1996). Skeletal, Cardiac, and Smooth Muscle Failure in Duchenne Muscular Dystrophy. *Pediatric Neurology, 14*, 7-12.
- Bork, P., & Sudol, M. (1994). The WW domain: a signalling site in dystrophin? *Trends Biochem. Sci., 19*, 531.
- Bouhouch, R., Elhouari, T., Oukerraj, L., Fellat, I., Zarzur, J., Bennani, R., & Arharbi, M. (2008). Management of Cardiac Involvement in NeuroMuscular Diseases: Review. *The Open Cardiovascular Medicine Journal, 2*, 93-96.
- Bovolenta, M., Erriquez, D., Valli, E., Brioschi, S., Scotton, C., & Neri, M. (2012). The DMD locus harbours multiple long non-coding RNAs which orchestrate and control transcription of muscle dystrophin mRNA isoforms. *Plos One, 7*(9), e45328.
- Bresolin, N., Castelli, E., Comi, G., Felisari, G., Bardoni, A., & Perani, D. (1994). Cognitive impairment in Duchenne muscular dystrophy. *Neuromuscular Disorders, 4*, 359-369.
- Brinkmeyer-Langford, C., Chu, C., Balog-Alvarez, C., Yu, X., Cai, J., Nabity, M., & Kornegay, J. (2018). Expression profiling of disease progression in canine model of Duchenne muscular dystrophy. *Plos One, 13*(3), e0194485.
- Brunklaus, E., Parish, E., Muntoni, F., & Scuplak, S. (2015). The value of cardiac MRI versus echocardiography in the pre-operative assessment of patients with Duchenne muscular dystrophy. *European Journal of Paediatric Neurology, 19*, 395-401.
- Bushby, K., Finkel, R., Birnkrant, D., Case, L. E., Clemens, P. R., Cripe, L., Kaul, A., Kinnett, K., McDonald, C., Pandya, S., Poysky, J., Shapiro, F., Tomezsko, J., & Constatin, C. (2010). Diagnosis and management of Duchenne muscular dystrophy, part 2: implementation of multidisciplinary care. *Lancet: Neurology, 9*, 177-189.

- Byers, T., Lidov, H., & Kunkel, L. (1993). An alternative dystrophin transcript specific to peripheral nerve. *Nat Genet*, 4(1), 77-81.
- Campanelli, J., Roberds, S., Campbell, K., & Scheller, R. (1994). A role for dystrophin-associated glycoproteins and utrophin in agrin-induced AChR clustering. *Cell*, 77(5), 663-674.
- Campbell, K., Rodino-Klapac, L., Sahenk, Z., Shilling, C., & Lewis, S. (2010). Revertant muscle fibers expressing dystrophin do not tolerize the immune system in Duchenne muscular dystrophy: lessons learned from a Phase I clinical trial (939). *Journal of Immunology*, 184(Supplement 96.9).
- Carpenter, J., Hoffman, E., & Romanul, F. (1989). Feline Muscular Dystrophy with Dystrophin Deficiency. *American Journal of Pathology*, 135, 909-919.
- Caspers, C., Mathews, K., Paramsothy, P., & Oleszek, J. (2015). Neurobehavioral concerns among males with dystrophinopathy using population-based surveillance data from the Muscular Dystrophy Surveillance, Tracking, and Research Network. *Journal of Developmental Behavioral Pediatrics*, 36, 455-463.
- CDC. (2009). Prevalence of Duchenne/Becker muscular dystrophy among males aged 5-24 years - four states, 2007. *MMWR Morb Mortal Wkly Rep*, 58(40), 1119-1122.
- CDC. (2016). Muscular Dystrophy. Retrieved from <https://www.cdc.gov/ncbddd/musculardystrophy/>. Retrieved Jan 1, 2017, from National Center on Birth Defects and Developmental Disabilities, Centers for Disease Control and Prevention <https://www.cdc.gov/ncbddd/musculardystrophy/>
- Ciafaloni, E., Fox, D., Pandya, S., Westfield, C., Puzhankara, S., Romitti, P., & Matthews, K. (2009). Delayed diagnosis in Duchenne muscular dystrophy: data from the Muscular

- Dystrophy Surveillance, Tracking, and Research Network (MD STARnet). *J Pediatr*, 155, 380-385.
- Collins, C., & Morgan, J. (2003). Duchenne's muscular dystrophy: animal models used to investigate pathogenesis and develop therapeutic strategies. *International Journal of Experimental Pathology*, 84(4), 165-172.
- Constantin, B. (2014). Dystrophin complex functions as a scaffold for signalling proteins. *Biochimica et Biophysica Acta*, 1838, 635-642.
- Cooper, B., Winand, N., Stedman, H., Valentine, B., Hoffman, E., Kunkel, L., Scott, M., Fischbeck, K., Kornegay, J., & Avery, R. (1988). The homologue of the Duchenne locus is defective in X-linked muscular dystrophy of dogs. *Nature*, 334(6178), 154-156.
- Crosbie, R., Heighway, J., Venzke, D., Lee, J., & Campbell, K. (1997). Sarcospan, the 25-kDa transmembrane component of the dystrophin-glycoprotein complex. *J Biol Chem*, 272(50), 31221-31224.
- Crosbie, R., Lebakken, C., Holt, K., Venzke, D., Straub, V., Lee, J., Grady, R., & Chamberlain, J. (1999). Membrane targeting and stabilization of sarcospan is mediated by the sarcoglycan subcomplex. *J Cell Biol*, 145, 153.
- Crosbie, R., Lim, L., Moore, S., Hirano, M., & Hays, A. (2000). Molecular and genetic characterization of sarcospan: insights into sarcoglycan-sarcospan interactions. *Hum Mol Genet*, 9(13), 2019-2027.
- D'Souza, V., Nguyen, T., Morris, G., Karges, W., Pillers, D., & Ray, P. (1995). A novel dystrophin isoform is required for normal retinal electrophysiology. *Hum Mol Genet*, 4(5), 837-842.

- Danko, I., Chapman, V., & Wolff, J. (1992). The frequency of revertants in the mdx mouse genetic models for Duchenne muscular dystrophy. *Pediatric Research*, 32, 128-131.
- Deconinck, A., Rafael, J., & Skinner, J. (1997). Utrophin-Dystrophin-Deficient Mice as a Model for Duchenne Muscular Dystrophy. *Cell*, 90, 717-727.
- Deconinck, N., & Bernard, D. (2007). Pathophysiology of Duchenne Muscular Dystrophy: Current Hypotheses. *Pediatr Neurol*, 36, 1-7.
- deLeon, M. B., Gomez, P., Elizondo, G., Zatarain-Palacios, R., Garcia-Sierra, F., & Cisneros, B. (2006). Beta-naphthoflavone represses dystrophin Dp71 expression in hepatic cells. *Biochim Biophys Acta*, 1759(3-4), 152-158.
- Delfin, D. A., Xu, Y., Schill, K. E., Mays, T. A., Canan, B. D., Zang, K. E., Barnum, J. A., Janssen, P. M., & Rafael-Fortney, J. A. (2012). Sustaining cardiac Claudin-5 levels prevents functional hallmarks of cardiomyopathy in a muscular dystrophy mouse model. *Molecular Therapy*, 20(7), 1378-1383.
- Dent, K., Dunn, D., Niederhausern, A. v., Aoyagi, A., Kerr, L., Bromberg, M., Hart, K., Tuohy, T., White, S., Dunnen, J. d., Weiss, R., & Flanigan, K. (2005). Improved molecular diagnosis of dystrophinopathies in an unselected clinical cohort. *American Journal of Medical Genetics. Part A*, 134(3), 295-298.
- Di, S., Sciandra, F., Maras, B., Di, R., Petrucci, T., Giardina, B., & Brancaccio, A. (1999). Structural and functional analysis of the N-terminal extracellular region of beta-dystroglycan. *Biochem. Biophys. Res. Commun.*, 266, 274.
- Draviam, R., Shand, S., & Watkins, S. (2006). The beta-delta-core of sarcoglycan is essential for deposition at the plasma membrane. *Muscle and Nerve*, 34, 691.

- Duchenne, G. (1868). Recherches sur la paralysie musculaire psuedohypertrophique, ou paralysie myo-sclerosique. *Arch Gen Med*, 11.
- Durbeej, M., Cohn, R., Hrstka, R., & Moore, S. (2000). Disruption of the beta-sarcoglycan gene reveals pathogenetic complexity of limb-girdle muscular dystrophy type 2E. *Molecular Cell*, 5, 141-151.
- Ervasti, J., & Campbell, K. (1991). Membrane organization of the dystrophin-glycoprotein complex. *Cell*, 66, 1121-1131.
- Ervasti, J., & Campbell, K. (1993). A role for the dystrophin-glycoprotein complex as a transmembrane linker between laminin and actin. *Journal of Cell Biology*, 122(4), 809-823.
- Feener, C., Koenig, M., & Kunkel, L. (1989). Alternative splicing of human dystrophin mRNA generates isoforms at the carboxy terminus. *Nature*, 338(6215), 509-511.
- Fine, D. M., Shin, J.-H., Yue, Y., Volkmann, D., Leach, S. B., Smith, B. F., McIntosh, M., & Duan, D. (2011). Age-matched comparison reveals early electrocardiography and echocardiography changes in dystrophin-deficient dogs. *Neuromuscular Disorders*, 21, 453-461.
- Flanigan, K., Dunn, D., Niederhausern, A. v., Soltanzadeh, P., Gappmaier, E., Howard, M., Sampson, J., Mendell, J., Wall, C., King, W., Pestronk, A., Florence, J., Connolly, A., Mathews, K., Stephan, C., Laubenthal, K., Wong, B., Morehart, P., Meyer, A., Finkel, R., Bonnemann, C., Medne, L., Day, J., Dalton, J., Margolis, M., Hinton, V., Consortium, U. D. P., & Weiss, R. (2009). Mutational spectrum of DMD mutations in dystrophinopathy patients: application of modern diagnostic techniques to a large cohort. *Human Mutation*, 30(12), 1657-1666.

- Frankel, K., & Rosser, R. (1976). The pathology of the heart in progressive muscular dystrophy: epimyocardial fibrosis. *Human Pathology*, 7(4), 375-386.
- Gao, Z., Xu, H., DiSilvestre, D., Halperin, V. L., Tunin, R., Tian, Y., Yu, W., Winslow, R. L., & Tomaselli, G. F. (2006). Transcriptomic profiling of the canine tachycardia-induced heart failure model: global comparison to human and murine heart failure. *Journal of Molecular and Cellular Cardiology*, 40(1), 76-86.
- Gaschen, L., Lang, J., & Lin, S. (1999). Cardiomyopathy in dystrophin-deficient hypertrophic feline muscular dystrophy. *Journal of Veterinary Internal Medicine*, 13, 346-356.
- Gorecki, D., Monaco, A., Derry, J., Walker, A., Barnard, E., & Barnard, P. (1992). Expression of four alternative dystrophin transcripts in brain regions regulated by different promoters. *Hum Mol Genet*, 7(7), 505-510.
- Gozal, D. (2000). Pulmonary Manifestations of Neuromuscular Disease With Special Reference to Duchenne Muscular Dystrophy and Spinal Muscular Atrophy. *Pediatric Pulmonology*, 29, 141-150.
- Grilley, J., Boehm, E., Rajagopalan, B., & Blamire, A. (2000). Magnetic Resonance Spectroscopy Evidence of Abnormal Cardiac energetics in Xp21 Muscular Dystrophy. *Journal of the American College of Cardiology*, 36, 1953-1958.
- Grimm, T., Kress, W., Meng, G., & Muller, C. R. (2012). Risk assessment and genetic counseling in families with Duchenne muscular dystrophy. *Acta Myol*, XXXI, 179-183.
- Grimm, T., Meng, G., Liechti-Gallati, S., Bettecken, T., Muller, C., & Muller, B. (1994). On the origin of deletions and point mutations in Duchenne muscular dystrophy: most deletions arise in oogenesis and most point mutations result from events in spermatogenesis. *J Med Genet*, 31(3), 183-186.

- Haenggi, T., Schaub, M., & Fritschy, J. (2005). Molecular heterogeneity of the dystrophin-associated protein complex in the mouse kidney nephron: differential alterations in the absence of utrophin and dystrophin. *Cell Tissue Res*, *319*(2), 299-313.
- Hendriksen, J., & Vles, J. (2008). Neuropsychiatric disorders in males with duchenne muscular dystrophy: frequency rate of attention-deficit hyperactivity disorder (ADHD), autism spectrum disorder, and obsessive-compulsive disorder. *J Child Neurol*, *23*(5), 477-481.
- Hinton, V., Vivo, D. D., Nereo, N., Goldstein, E., & Stern, Y. (2000). Poor verbal working memory across intellectual level in boys with Duchenne dystrophy. *Neurology*, *54*, 2127-2132.
- Hoffman, E., Brown, R., & Kunkel, L. (1987). Dystrophin: the protein product of the Duchenne muscular dystrophy locus. *Cell*, *51*(6), 919-928.
- Hoffman, E., Morgan, J., Watkins, S., & Partridge, T. (1990). Somatic reversion/suppression of the mouse mdx phenotype in vivo. *Journal of Neurological Science*, *99*, 9-25.
- Holland, A., Carberry, S., & Ohlendieck, K. (2013). Proteomics of the Dystrophin-glycoprotein Complex and Dystropinopathy. *Curr Protein Pept Sci*, *14*(8), 680-697.
- Ibraghimov-Beskrovnaya, O., Ervasti, J., Leveille, C., Slaughter, C., Sernett, S., & Campbell, K. (1992). Primary structure of the 43 K and 156 K dystrophin-associated glycoproteins linking dystrophin to the extracellular matrix. *Nature*, *355*, 696-702.
- Ishikawa-Sakurai, M., Yoshida, M., Imamura, M., Davies, K., & Ozawa, E. (2004). ZZ domain is essentially required for the physiological binding of dystrophin and utrophin to beta-dystroglycan. *Hum Mol Genet*, *13*, 693.
- Ito, D., Kitagawa, M., & Jeffrey, N. (2011). Dystrophin-deficient muscular dystrophy in an Alaskan malamute. *Veterinary Record*, *169*, 127.

- Johnson, E. K., Li, B., Yoon, J. H., Flanigan, K. M., Martin, P. T., Ervasti, J., & Montanaro, F. (2013). Identification of New Dystroglycan Complexes in Skeletal Muscle. *Plos One*, 8(8), 1-17.
- Johnson, E. K., Zhang, L., Adams, M. E., Phillips, A., Freitas, M. A., Froehner, S. C., Green-Church, K. B., & Montanaro, F. (2012). Proteomic analysis reveals new cardiac-specific dystrophin-associated proteins. *PLoS One*, 7(8), e43515.
doi:10.1371/journal.pone.0043515
- Jones, B., Brennan, S., & Mooney, C. (2004). Muscular dystrophy with truncated dystrophin in a family of Japanese Spitz dogs. *Journal of Neurological Science*, 217, 413-449.
- Kawamura, J., Kato, S., Ishihara, T., Hiraishi, Y., & Kawashiro, T. (1997). Difference of new mutation rates in dystrophin gene between deletion and duplication mutation in Duchenne and Becker muscular dystrophy. *Rinsho Shinkeigaku*, 37, 212-217.
- Klarenbeek, S., Gerritzen-Bruning, M., & Rozenmuller, A. (2007). Canine X-linked muscular dystrophy in a family of Grand Basset Griffon Vendeen dogs. *Journal of Comparative Pathology*, 137, 249-252.
- Klein, C., Coovert, D., Bulman, D., Ray, P., Mendell, J., & Burghes, A. (1992). Somatic reversion/suppression in Duchenne muscular dystrophy (DMD): evidence supporting a frame-restoring mechanism in rare dystrophin-positive fibers. *American Journal of Human Genetics*, 50, 950-959.
- Klinger, W., Jurkat-Rott, K., Lehmann-Horn, F., & Schleip, R. (2012). The role of fibrosis in Duchenne muscular dystrophy. *Acta Myol*, 31(3), 184-195.
- Klymiuk, N., Blutke, A., Graf, A., Krause, S., Burkhardt, K., Weunsch, A., Krebs, S., Kessler, B., Zakhartchenko, V., Kurome, M., Kemter, E., Nagashima, H., Schoser, B., Herbach,

- N., Blum, H., Wanke, R., Aatsma-Ru, A., Thirion, C., Lochmuller, H., Walter, M., & Wolf, E. (2013). Dystrophin-deficient pigs provide new insights into the hierarchy of physiological derangements of dystrophic muscle. *Hum Mol Genet*, 22(21), 4368-4382.
- Kobayashi, Y., & Campbell, K. (2012). Skeletal Muscle Dystrophin-Glycoprotein Complex and Muscular Dystrophy. In J. A. Hill & E. N. Olson (Eds.), *Muscle, Fundamental Biology and Mechanisms of Disease* (pp. 935-941): Academic Press.
- Koenig, M., & Kunkel, L. (1990). Detailed analysis of the repeat domain of dystrophin reveals four potential hinge segments that may confer flexibility. *J Biol Chem*, 265, 4560.
- Koenig, M., Monaco, A., & Kunkel, L. (1988). The complete sequence of dystrophin predicts a rod-shaped cytoskeletal protein. *Cell*, 53, 219.
- Kohn, B., Guscetti, F., & Waxenberger, M. (1993). Muscular dystrophy in a cat. *Tierarztl Prax*, 21, 451-457.
- Kornegay, J. N., Bogan, J. R., Bogan, D. J., Childers, M. K., Li, J., Nghiem, P., Detwiler, D. A., Larsen, C. A., Grange, R. W., Bhavaraju-Sanka, R. K., Tou, S., Keene, B. P., Jr., J. F. H., Wang, J., Fan, Q., Schatzberg, S. J., Styner, M. A., Flanigan, K. M., Xiao, X., & Hoffman, E. P. (2012). Canine models of Duchenne muscular dystrophy and their use in therapeutic strategies. *Mammalian Genome*, 23, 85-108.
- Kunkel, L., Monaco, A., Middlesworth, W., Ochs, N., & Latt, S. (1985). Specific cloning of DNA fragments absent from the DNA of a male patient with an X-chromosome deletion. *PNAS*, 82, 4778-4782.
- Lefaucheur, J., Pastoret, C., & Sebille, A. (1995). Phenotype of dystrophinopathy in old mdx mice. *The Anatomical Record*, 242(1), 70-76.

- Leibowitz, D., & Dubowitz, V. (1981). Intellect and behaviour in Duchenne muscular dystrophy. *Dev Med Child Neurol*, 23, 577-590.
- Lidov, H., Byers, T., Watkins, S., & Kunkel, L. (1990). Localization of dystrophin to postsynaptic regions of central nervous system cortical neurons. *Nature*, 348(6303), 725-728.
- Lidov, H., Selig, S., & Kunkel, L. (1995). Dp140: a novel 140 kDa CNs transcript from the dystrophin locus. *Hum Mol Genet*, 4(3), 329-335.
- Lim, L., Duclos, F., Broux, O., Bourg, N., Sunada, Y., allamand, V., Meyer, J., Richard, I., Moormaw, C., & Slaughter, C. (1995). Beta-sarcoglycan: characterization and role in limb-girdle muscular dystrophy linked to 4q12. *Nat Genet*, 11, 257.
- Manzur, A., Kuntzer, T., Pike, M., & Swan, A. (2008). Glucocorticoid corticosteroids for Duchenne muscular dystrophy. *Cochrane Database of Systematic Reviews*, 1(CD003725).
- Matsumara, T., Saito, T., Fujimura, H., Shinno, S., & Sakoda, S. (2011). A longitudinal cause-of-death analysis of patients with Duchenne muscular dystrophy. *Rinsho Shinkeigaku*, 51(10), 743-750.
- Mavrogeni, S., Papvasiliou, A., Spargias, K., Constandoulakis, P., Papadopoulos, G., Karanasios, E., Georgakopoulos, D., Kolovou, G., Papandopoulou, E., Markussis, V., & Cokkinos, D. (2010). Myocardial inflammation in Duchenne Muscular Dystrophy as a precipitating factor for heart failure: a prospective study. *BMC Neurol*, 10(33), 1-7.
- Mazur, W., Hor, K. N., Germann, J. T., Fleck, R. J., Al-Khalidi, H. R., Wansapura, J. P., Chung, E. S., Taylor, M. D., Jefferies, J. L., Benson, D. W., & Gottliebson, W. M. (2012). Patterns of left ventricular remodeling in patients with Duchenne Muscular Dystrophy: a

- cardiac MRI study of ventricular geometry, global function, and strain. *International Journal of Cardiovascular Imaging*, 28, 99-107.
- McNally, E. (2007). New approaches in the therapy of cardiomyopathy in muscular dystrophy. *Annu Rev Med*, 58, 75-88.
- MDA. (2014). Duchenne Muscular Dystrophy (DMD). *Signs and Symptoms*. Retrieved from <http://mda.org/disease/duchenne-muscular-dystrophy/signs-and-symptoms>
- Moriuchi, T., Kagawa, N., Mukoyama, M., & Hizawa, K. (1993). Autopsy analyses of the muscular dystrophies. *Tokushima J Exp Med*, 40(1-2), 83-93.
- Muntoni, F., Torelli, S., & Ferlini, A. (2003). Dystrophin an dmutations: one gene, several proteins, multiple phenotypes. *Lancet Neurol*, 2, 731-740.
- NCBI. (2020). DMD dystrophin [Homo sapiens (human)] (Webpage). Retrieved from <http://www.ncbi.nlm.nih.gov/gene/1756>. Retrieved Feb 26, 2020, from National Center for Biotechnology Information, U.S. National Library of Medicine <http://www.ncbi.nlm.nih.gov/gene/1756>
- Nicholson, L., Davison, K., Johnson, M., Slater, C., & Young, C. (1989). Dystrophin in skeletal muscle. II. Immunoreactivity in patients with Xp21 muscular dystrophy. *Journal of Neurological Science*, 94, 137-146.
- NIH. (2012, February 12, 2017). Types of Heart Block. Retrieved from <https://www.nhlbi.nih.gov/health/health-topics/topics/hb/types>
- Nishio, H., Takeshima, Y., Narita, N., Yanagawa, H., Suzuki, Y., Ishikawa, Y., Minami, R., Nakamura, H., & Matsuo, M. (1994). Identification of a novel first exon in the human dystrophin gene and of a new promoter located more than 500 kb upstream of the nearest known promoter. *J Clin Invest*, 94(3), 1037-1042.

- Noguchi, S., McNally, E., Ben, O., Hagiwara, Y., Mizuno, Y., Yoshia, M., Yamamoto, H., Bonnemann, C., Gussoni, E., & Denton, P. (1995). Mutations in the dystrophin-associated protein gamma-sarcoglycan in chromosome 13 muscular dystrophy. *Science*, 270, 819.
- Norwood, R., Harling, C., Chinnery, P., Eagle, M., Bushby, K., & Straub, V. (2009). Prevalence of genetic muscle disease in Northern England: in-depth analysis of muscle clinic population. *Brain*, 132(Pt 11), 3175-3186.
- Nudel, U., Zuk, D., Einat, P., Zeelon, E., Levy, Z., Neuman, S., & Yaffe, D. (1989). Duchenne muscular dystrophy gene product is not identical in muscle and brain. *Nature*, 337(6202), 76-78.
- Oak, S., Zhou, Y., & Jarrett, H. (2003). Skeletal muscle signaling pathway through the dystrophin glycoprotein complex and Rac1. *J Biol Chem*, 278, 39287.
- Oda, T., Shimizu, N., Yonenobu, K., & Nabeshima, T. (1993). Longitudinal study of spinal deformity in Duchenne muscular dystrophy. *Journal of Pediatric Orthopedics*, 13, 478-488.
- Ohlendieck, K., & Campbell, K. (1991). Dystrophin-associated proteins are greatly reduced in skeletal muscle from mdx mice. *Journal of Cell Biology*, 115(6), 1685-1694.
- Ozawa, E., Mizuno, Y., Hagiwara, Y., & Sasaoka, T. (2005). Molecular and cell biology of the sarcoglycan complex. *Muscle and Nerve*, 32, 563.
- Passamano, L., Taglia, A., Palladino, A., Viggiano, E., D'Ambrosio, P., Scutifero, M., Cecio, M. R., Torre, V., Luca, F. D., Picillo, E., Paciello, O., Piluso, G., Nigro, G., & Politano, L. (2012). Improvement of survival in Duchenne Muscular Dystrophy: retrospective analysis of 835 patients. *Acta Myologica*, XXXI, 121-125.

- Perloff, J. (1984). Cardiac rhythm and conduction in Duchenne's muscular dystrophy: a prospective study of 20 patients. *Journal of the American College of Cardiology*, *3*, 1263-1268.
- Philip-Couderc, P., Smih, F., Pelat, M., Vidal, C., Verwaerde, P., Pathak, A., Buys, S., Galinier, M., Senard, J.-M., & Rouet, P. (2003). Cardiac transcriptome analysis in obesity-related hypertension. *Hypertension*, *41*, 414-421.
- Ponting, C., Blake, D., Davies, K., Kendrick-Jones, J., & Winder, S. (1996). ZZ and TAZ: new putative zinc fingers in dystrophin and other proteins. *Trends Biochem. Sci.*, *21*, 11.
- Quinlan, J. G., Han, J. S., Wong, B. L., Lorenz, J. N., Wenisch, A. S., & Levin, L. S. (2004). Evolution of the mdx mouse cardiomyopathy: physiological and morphological findings. *Neuromuscular Disorders*, *14*(8-9), 491-496.
- Renschler, S., Linn, H., Deininger, K., Bedford, M., Espanel, X., & Sudol, M. (1999). The WW domain of dystrophin requires Ef-hands region to interact with beta-dystroglycan. *Biol Chem*, *280*, 431.
- RNA-seqlopedia. Retrieved from <https://rnaseq.uoregon.edu/#analysis-overview>. Retrieved May 15, 2019, from Cresko Laboratory of the University of Oregon <https://rnaseq.uoregon.edu/#analysis-overview>
- Roberds, S., Anderson, R., Ibraghimov-Beskravnaya, O., & Campbell, K. (1993). Primary structure and muscle-specific expression of the 50-kDa dystrophin-associated glycoprotein (adhalin). *Journal of Biological Chemistry*, *268*, 23739-23742.
- Roberds, S., Leturcq, F., Allamand, V., Piccolo, F., Jeanpierre, M., & Anderson, R. (1994). Missense mutations in the adhalin gene linked to autosomal recessive muscular dystrophy. *Cell*, *78*(4), 625-633.

- Romitti, P., Zhu, Y., Puzhankara, S., James, K., Nabukera, S., & Zamba, G. (2015). Prevalence of Duchenne and Becker muscular dystrophies in the United States. *Pediatrics*, *135*(3), 513-521.
- Sander, M., Chavoshan, B., Harris, S., Iannaccone, S., Stull, J., Thomas, G., & Victor, R. (2000). Functional muscle ischemia in neuronal nitric oxide synthase-deficient skeletal muscle of children with Duchenne muscular dystrophy. *PNAS*, *97*(2513818-13823).
- Sanyal, S. K., & Johnson, W. W. (1982). Cardiac Conduction Abnormalities in Children with Duchenne's Progressive Muscular Dystrophy: Electrocardiographic Features and Morphologic Correlates. *Circulation*, *66*, 853-863.
- Schatzberg, S., Anderson, L., & Wilton, S. (1998). Alternative dystrophin gene transcripts in golden retriever muscular dystrophy. *Muscle and Nerve*, *21*, 991-998.
- Schatzberg, S. J., Olby, N. J., Breen, M., Anderson, L. V. B., Langford, C. F., Dickens, H. F., Wilton, S. D., Zeiss, C. J., Binns, M. M., Kornegay, J. N., Morris, G. E., & Sharp, N. J. H. (1999). Molecular analysis of a spontaneous dystrophin 'knockout' dog. *Neuromuscular Disorders*, *9*(5), 289-295.
- Schofield, J., Blake, D., Simmons, C., Morris, G., Tinsley, J., Davies, K., & Edwards, Y. (1994). Apo-dystrophin-1 and apo-dystrophin-2, products of the Duchenne muscular dystrophy locus: expression during mouse embryogenesis and in cultured cell lines. *Hum Mol Genet*, *3*(8), 1309-1316.
- Sharp, N., Kornegay, J., & Camp, S. V. (1991). An error in dystrophin mRNA processing in golden retriever muscular dystrophy, an animal homologue of Duchenne muscular dystrophy. *Genomics*, *13*, 115-121.

- Sharpe, K. M., Premsukh, M. D., & Townsend, D. (2013). Alterations of dystrophin-associated glycoproteins in the heart lacking dystrophin or dystrophin and utrophin. *J Muscle Res Cell Motil*, 34, 395-405.
- Shi, W., Chen, Z., Schottenfeld, J., Stahl, R., Kunkel, L., & Chan, Y. (2004). Specific assembly pathway of sarcoglycans is dependent on beta- and delta-sarcoglycan. *Muscle and Nerve*, 29, 409.
- Shimatsu, Y., Katagiri, K., Furuta, T., Nakura, M., Tanioka, Y., Yuasa, K., Tomohiro, M., Kornegay, J. N., Nonaka, I., & Takeda, S. i. (2003). Canine X-linked muscular dystrophy in Japan (CXMD₁). *Experimental Animals*, 52(2), 93-97.
- Sicinski, P., Geng, Y., & Ryder-Cook, A. (1989). The molecular basis of muscular dystrophy in the mdx mouse: a point mutation. *Science*, 244, 1578-1580.
- Smith, B., Kornegay, J., & Duan, D. (2007). Independent canine models of Duchenne muscular dystrophy due to intronic insertions of repetitive DNA. *Mol Ther*, 15(Suppl 1), S51.
- Smith, B. F., Yue, Y., Woods, P. R., Kornegay, J. N., Shin, J.-H., Williams, R. R., & Duan, D. (2011). An intronic LINE-1 element insertion in the dystrophin gene aborts dystrophin expression and results in Duchenne-like muscular dystrophy in the corgi breed. *Laboratory Investigation*, 91(2), 216-231.
- Sotgia, F., Lee, J., Das, K., Bedford, M., Petrucci, T., Macioce, P., Sargiacomo, M., Bricarelli, F., Minetti, C., Sudol, M., & Lisanti, M. (2000). Caveolin-3 directly interacts with the C-terminal tail fo beta-dystroglycan. Identification of a central WW-like domain within caveolin family members. *J Biol Chem*, 275, 38048.
- Spence, H., Dhillon, A., James, M., & Winder, S. (2004). Dystroglycan, a scaffold for the ERK-MAP kinase cascade. *EMBO Rep*, 5, 484.

- Spurney, C. F., Knoblach, S., Pistilli, E. E., Nagaraju, K., Martin, G. R., & Hoffman, E. P. (2008). Dystrophin-deficient cardiomyopathy in mouse: Expression of Nox4 and Lox are associated with fibrosis and altered functional parameter in the heart. *Neuromuscular Disorders*, 18, 371-381.
- Stedman, H., Sweeney, H., & Shrager, J. (1991). The mdx mouse diaphragm reproduces the degenerative changes of Duchenne muscular dystrophy. *Nature*, 352, 536-539.
- Sunada, Y., Bernier, S., Kozak, C., Yamada, Y., & Campbell, K. (1994). Deficiency of merosin in dystrophic dy mice and genetic linkage of laminin M chain gene to dy locus. *Journal of Biological Chemistry*, 269(19), 13729-13732.
- Sunohara, N., Arahata, K., & Hoffman, E. (1990). Quadriceps myopathy: forme frusta of Becker muscular dystrophy. *Ann Neurol*, 28(5), 634-639.
- Suzuki, A., Yoshida, M., Hayashi, K., Mizuno, Y., Hagiwara, Y., & Ozawa, E. (1994). Molecular organization at the glycoprotein-complex-binding site of dystrophin - Three dystrophin-associated proteins bind directly to teh carboxy-terminal portion of dystrophin. *European Journal of Biochemistry*, 220(2), 283-292.
- Suzuki, A., Yoshida, M., Yamamoto, H., & Ozawa, E. (1992). Glycoprotein-binding site of dystrophin is confined to the cysteine-rich domain and the first half of the carboxy-terminal domain. *FEBS Lett*, 308, 154.
- Sweeney, H. L., & Barton, E. R. (2000). The dystrophin-associated glycoprotein complex: What parts can you do without? *PNAS*, 97(25), 13464-13466.
- Tadayoni, R., Rendon, A., Soria-Jasso, L., & Cisneros, B. (2012). Dystrophin dp71: the smallest but multifunctional product of the Duchenne muscular dystrophy gene. *Mol Neurobiol*, 45(1), 43-60.

- Thanh, L., Man, N., Helliwell, T., & Morris, G. (1995). Characterization of Revertant Muscle Fibers in Duchenne Muscular Dystrophy, Using Exon-Specific Monoclonal Antibodies against Dystrophin. *American Journal of Human Genetics*, *56*, 725-731.
- Tinsley, J., Blake, D., & Davies, K. (1993). Apo-dystrophin-3: a 2.2 kb transcript from the DMD locus encoding the dystrophin glycoprotein binding site. *Hum Mol Genet*, *2*(5), 521-524.
- Tokarz, S., Duncan, N., Rash, S., Sadeghi, A., Dewan, A., & Pillers, D. (1998). Redefinition of dystrophin isoform distribution in mouse tissue by RT-PCR implies role in nonmuscle manifestations of duchenne muscular dystrophy. *Mol Genet Metab*, *65*(4), 272-281.
- Torelli, S., Brown, S., Jimenez-Mallebrera, C., Feng, L., Muntoni, F., & Sewry, C. (2004). Absence of neuronal nitric oxide synthase (nNOS) as a pathological marker for the diagnosis of Becker muscular dystrophy with rod domain deletions. *Neuropathol Appl Neurobiol*, *30*(5), 540-545.
- Tozawa, T., Itoh, K., Yaoi, T., Tando, S., Umekage, M., Dai, H., Hosoi, H., & Fushiki, S. (2012). The shortest isoform of dystrophin (Dp40) interacts with a group of prosynaptic proteins to form a presumptive novel complex in mouse brain. *Mol Neurobiol*, *45*(2), 287-297.
- Velden, V. v. d. (1998). Glucocorticoids: mechanisms of action and anti-inflammatory potential in asthma. *Mediators of Inflammation*, *7*(4), 229-237.
- Verhaert, D., Richards, K., Rafael-Fortney, J. A., & Raman, S. V. (2011). Cardiac involvement in patients with muscular dystrophies: magnetic resonance imaging phenotype and genotypic considerations. *Circulation Cardiovascular Imaging*, *4*, 67-76.
- Wagner, K. R., Lechtzin, N., & Judge, D. P. (2007). Current treatment of adult Duchenne muscular dystrophy. *Biochimica et Biophysica Acta*, *1772*, 229-237.

- Walmsley, G. L., Arechavala-Gomez, V., Fernandez-Fuente, M., Burke, M. M., Nagel, N., Holder, A., Stanley, R., Chandler, K., Marks, S. L., Muntoni, F., Shelton, G. D., & Piercy, r. J. (2010). A Duchenne muscular dystrophy gene hot spot mutation in dystrophin-deficient Cavalier King Charles spaniels is amenable to Exon 51 skipping. *Plos One*, 5(1), 1-9.
- Wang, Z., Gerstein, M., & Snyder, M. (2009). RNA-Seq: a revolutionary tool for transcriptomics. *Nat Rev Genet*, 10(1), 57-63.
- Wheeler, M., Zarnegar, S., & McNally, E. (2002). Zeta-sarcoglycan, a novel component of the sarcoglycan complex, is reduced in muscular dystrophy. *Hum Mol Genet*, 11, 2147.
- Wheway, J., & Roberts, R. (2003). The dystrophin lymphocyte promoter revisited: 4.5-megabase intron, or artifact? *Neuromuscular Disorders*, 13(1), 17-20.
- Wicklund, M. (2013). The Muscular Dystrophies. *Continuum*, 19(6), 1535-1570.
- Wieczorek, L., Garosi, L., & Shelton, G. (2006). Dystrophin-deficient muscular dystrophy in an old English sheepdog. *Veterinary Record*, 158, 270-273.
- Winand, N., Pradham, D., & Cooper, B. (1994). Molecular characterization of severe Duchenne-type muscular dystrophy in a family of Rottweiler dogs. *Proceedings of the Muscular Dystrophy Association: Molecular Mechanisms of Neuromuscular Disease*.
- Winder, S., Gibson, T., & Kendrick-Jones, J. (1995). Dystrophin and utrophin: the missing links! *FEBS Lett*, 169, 27.
- Yamashita, T., Kanaya, K., Kawaguchi, S., & Murakami, T. (2001). Prediction of progression of spinal deformity in Duchenne muscular dystrophy: A preliminary report. *Spine*, 26, E223-226.

- Yanagisawa, A., Miyagawa, M., Yotsukura, M., & Tsuya, T. (1992). The prevalence and prognostic significance of arrhythmias in Duchenne type muscular dystrophy. *American Heart Journal*, *124*, 1244-1250.
- Yanay, N., Elbaz, M., Konikov, J., Elgavish, S., Rabie, M., Mitrani-Rosenbaum, S., & Nevo, Y. (2017). Characterization of molecular pathophysiology in muscular dystrophy by next generation RNA sequencing using DMD and CMD mouse models. *Neuromuscul Disord*, *27*(Supplement 2), S169.
- Yang, B., Jung, D., Motto, D., Meyer, J., Koretzky, G., & Campbell, K. (1995). SH3 domain-mediated interaction of dystroglycan and Grb2. *J Biol Chem*, *270*(20), 11711-11714.
- Yang, B., Jung, D., Rafael, J., Chamberlain, J., & Campbell, K. (1995). Identification of alpha-syntrophin binding to syntrophin triplet, dystrophin and utrophin. *Journal of Biological Chemistry*, *270*(10).
- Zimprich, A., Grabowski, M., & Asmus, F. (2001). Mutations in the gene encoding epsilon-sarcoglycan cause myoclonus-dystonia syndrome. *Nat Genet*, *29*, 66-69.

Appendix I: Supportive Photographs and Figures



Figure 1. Photographs of dystrophin-deficient Labradoodles

(A) Affected dog at 2-months of age with a mild plantigrade stance and minimal lumbar kyphosis. (B) Affected dog at 6-months of age with severe skeletal muscle atrophy, plantigrade stance, and lumbar kyphosis.

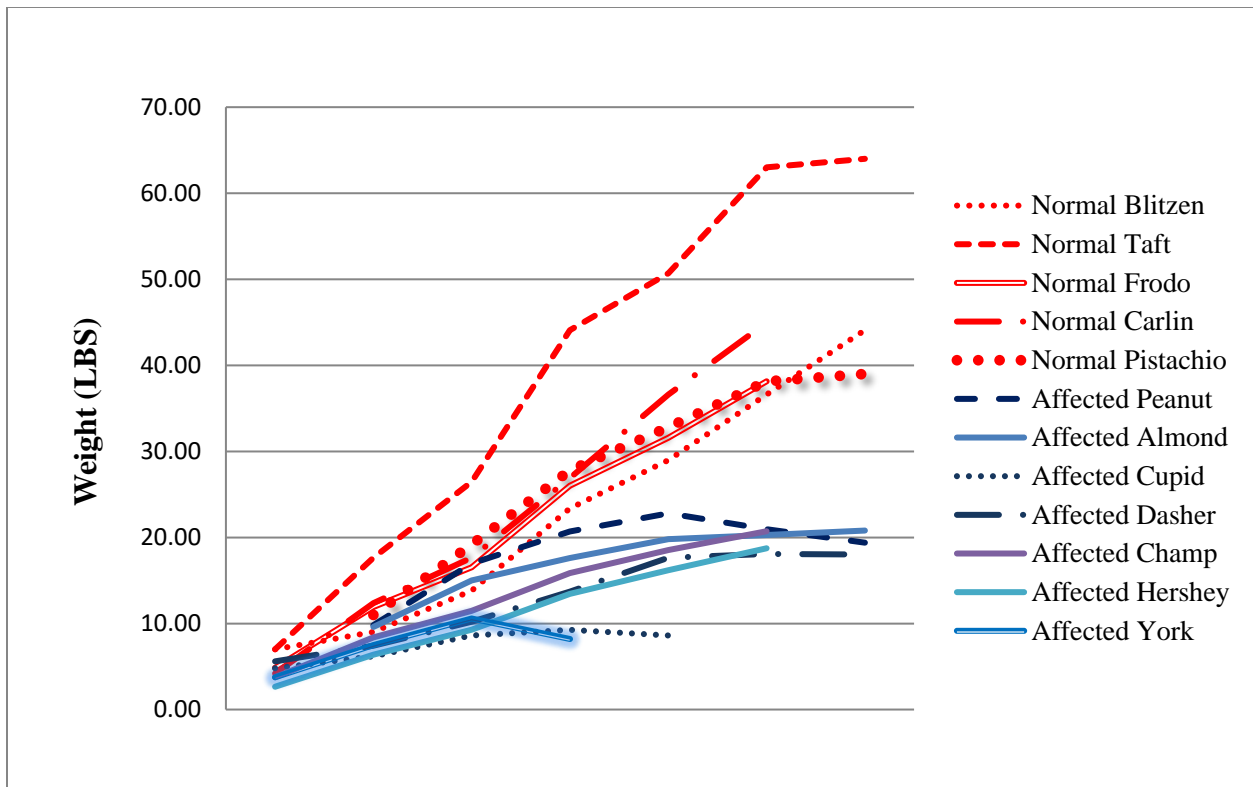


Figure 2. Comparison of weight gains between dystrophin-deficient and control dogs

The dystrophin-deficient dogs had poor weight gains, and in several instances weight losses, compared to their normal (control) littermates. The horizontal axis represents time in months; the initial weights were collected at 1-month of age and the final weights were collected at the time of euthanasia.

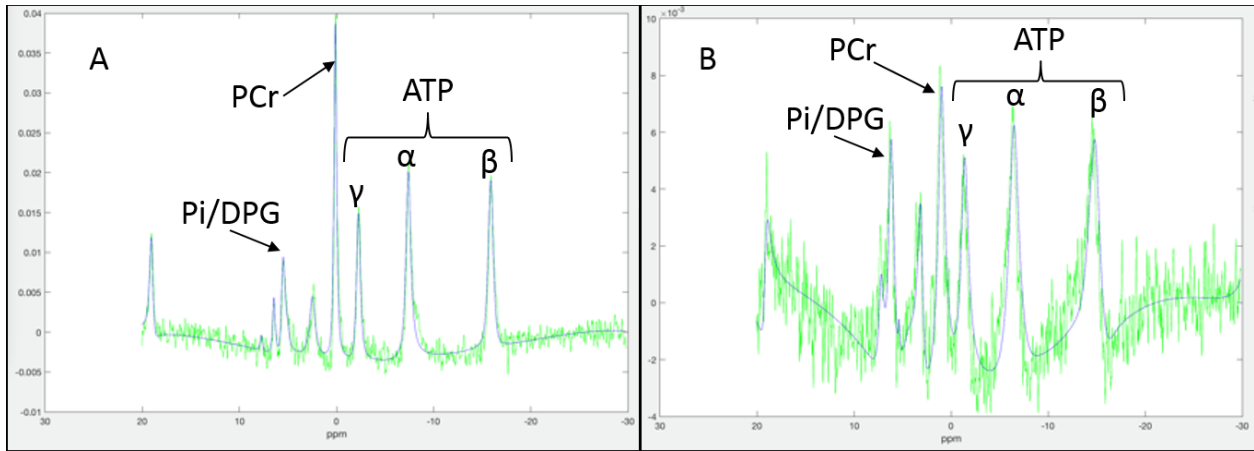


Figure 3. ^{31}P MR spectra

(A) Control dog vs (B) affected dog. The peaks, from left to right, are inorganic phosphate, creatine phosphate, and the $[\gamma\text{-P}]$, $[\alpha\text{-P}]$, and $[\beta\text{-P}]$ of ATP. There were no significant differences in PCr/ATP between affected and control dogs.

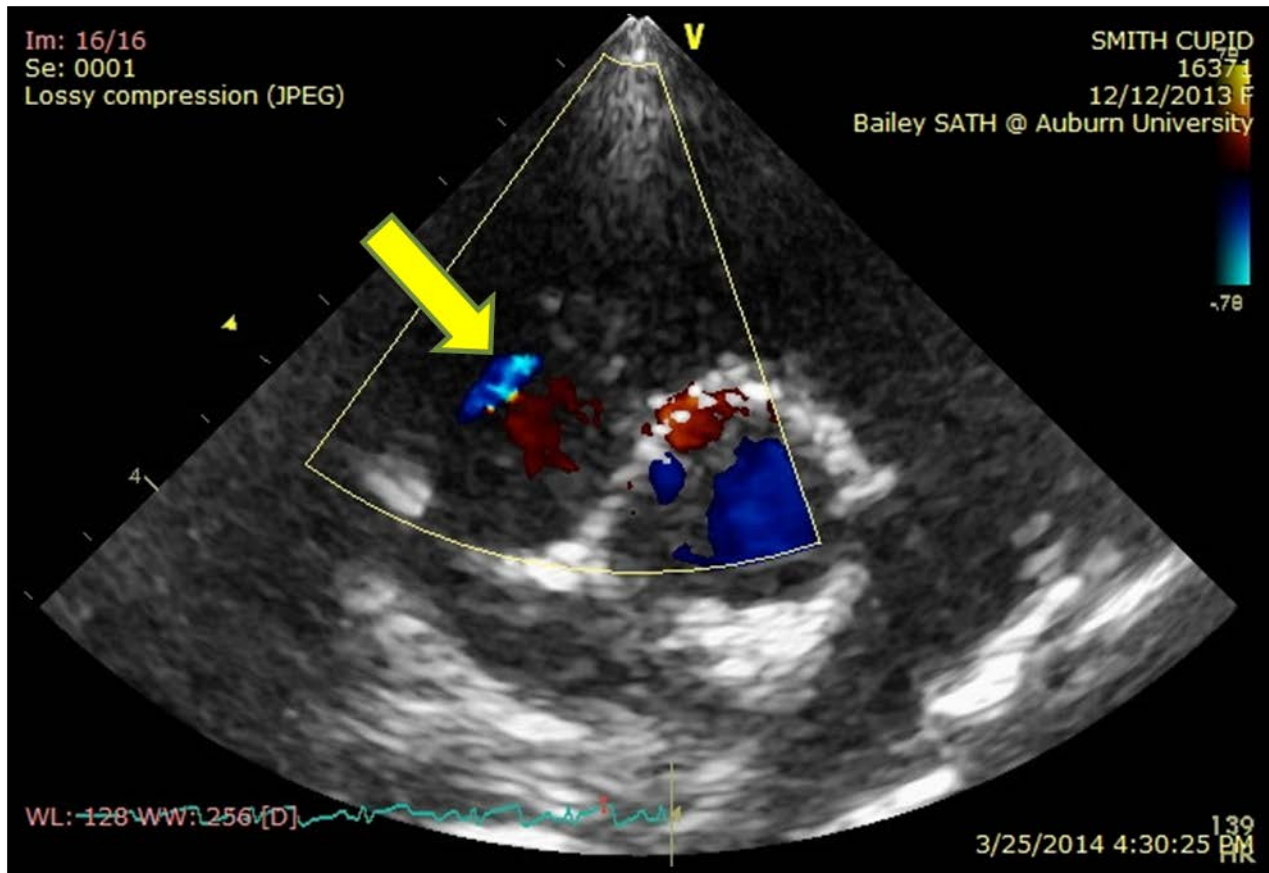


Figure 4. Echocardiographic image of tricuspid valve regurgitation

Mild tricuspid valve regurgitation was consistently present in 3/7 affected dogs (42.9%) throughout the course of the study. The yellow arrow indicates the backward flow of blood into the right atrium (i.e. regurgitant jet).



Figure 5. Gross photograph of the diaphragm from an affected dog

Compared to controls, the dystrophin-deficient dogs had severe skeletal muscle hypertrophy and fibrosis involving the peripheral portions of the diaphragm (resulting in increased thickness and decreased compliance) with severe thinning centrally.